I. NUCLEAR SPIN-INTERNAL-ROTATION COUPLING

II. FLUORINE SPIN-ROTATION INTERACTION AND MAGNETIC SHIELDING IN FLUOROBENZENE

Thesis by

Alan Sander Dubin

In Partial Fulfillment of the Requirements

For the Degree of

Doctor of Philosophy

California Institute of Technology

Pasadena, California

1967

(Submitted March 1, 1967)

To My Mother and Father

ACKNOWLEDGEMENTS

There have been many people who, by example, have considerably influenced my thinking and personality during these years at the Institute.

To Professor Sunney I. Chan, my research adviser, for his never having been too busy to listen, to help, to teach, or to laugh, I express my sincerest gratitude.

Special thanks go to Professors George S. Hammond and G. Wilse Robinson for their encouragement and for exposing me to their very contagious enthusiasm.

A great part of my graduate training came from the impromptu and free-wheeling seminars with other graduate students and research fellows of the Chan and Robinson groups. In particular, it is a pleasure to mention Mr. Thomas E. Burke who shared in the construction of the pulsed NMR spectrometer and who with Mr. Robert T. Iwamasa provided honest criticism and real encouragement throughout the last few years.

I am indebted to Mr. Carver Jewett who built the pulsed transmitter and to Mr. William Schuelke and his staff for the design and construction of the probe support.

The experimental work reported in Part II of this thesis was undertaken by Professor Sunney I. Chan when he was a National Science Foundation Postdoctoral Fellow working in Professor Norman F. Ramsey's molecular beam laboratory at Harvard University.

I would also like to express my appreciation to the staff of the Booth Computing Center here at the California Institute of Technology for their advice and cooperation during the course of this work. Ken Hebert, Steve Caine, and Kiku Matsumoto were particularly helpful.

I am grateful to the Institute for financial support.

I cannot thank enough my bride Joan, who transcribed this thesis from some pretty rough manuscripts and prepared it in such a beautiful form.

ABSTRACT. PART I.

The interaction of a nuclear magnetic moment situated on an internal top with the magnetic fields produced by the internal as well as overall molecular rotation has been derived following the method of Van Vleck for the spin-rotation interaction in rigid molecules. It is shown that the Hamiltonian for this problem may be written

$$\mathcal{H}_{SR} = \vec{I} \cdot \underset{\sim}{M} \cdot \vec{J} + \vec{I} \cdot \underset{\sim}{M}'' \cdot \vec{j}''$$

where the first term is the ordinary spin-rotation interaction and the second term arises from the spin-internal-rotation coupling.

The F^{19} nuclear spin-lattice relaxation time (T_1) of benzotrifluoride and several chemically substituted benzotrifluorides, have been measured both neat and in solution, at room temperature by pulsed nuclear magnetic resonance. From these experimental results it is concluded that in benzotrifluoride the internal rotation is crucial to the spin relaxation of the fluorines and that the dominant relaxation mechanism is the fluctuating spin-internal-rotation interaction.

ABSTRACT. PART II.

The radiofrequency spectrum corresponding to the reorientation of the F^{19} nuclear moment in flurobenzene has been studied by the molecular beam magnetic resonance method. A molecular beam apparatus with an electron bombardment detector was used in the experiments. The F^{19} resonance is a composite spectrum with contributions from many rotational states and is not resolved. A detailed analysis of the resonance line shape and width by the method of moments led to the following diagonal components of the fluorine spin-rotational tensor in the principal inertial axis system of the molecule:

$$C_{aa}^{F} = -1.0 \pm 0.5 \ kHz$$
$$C_{bb}^{F} = -2.7 \pm 0.2 \ kHz$$
$$C_{cc}^{F} = -1.9 \pm 0.1 \ kHz$$

From these interaction constants, the paramagnetic contribution to the F^{19} nuclear shielding in C_6H_5F was determined to be -284 ± ppm. It was further concluded that the F^{19} nucleus in this molecule is more shielded when the applied magnetic field is directed along the C-F bond axis. The anisotropy of the magnetic shielding tensor, $\sigma_{\parallel} - \sigma_{\perp}$, is +160 ± 30 ppm.

TABLE OF CONTENTS

Page

PART II: FLUORINE SPIN-ROTATION INTERACTION AND MAGNETIC SHIELDING IN FLUOROBENZENE

PART I

NUCLEAR SPIN-INTERNAL-ROTATION COUPLING

A. GENERAL INTRODUCTION.

In part I of this thesis we are mainly concerned with the spin-lattice relaxation of F^{19} nuclei which are situated on internal tops and the effect of the internal rotation on the observed relaxation rates. In particular we are interested in the relaxation mechanism arising from the time-dependent interaction of the nuclear moments with the magnetic fields produced by the internal rotation.

The coupling of net electronic spin angular momentum with the rotational angular momentum has long been known to molecular spectroscopists who, very early, observed the phenomenon as spin-doubling, tripling, etc., of the rotational structure of electronic transitions of diatomic molecules. More recently the effect has been observed in pure rotational microwave spectroscopy. With the development of molecular-beam magnetic-resonance spectroscopy the much smaller, analogous interaction of the nuclear moments with the molecular rotation could be accurately evaluated. Due primarily to the effort of N. F. Ramsey and his coworkers the nuclear spin-rotation interaction constants are known for several diatomic and linear molecules and a few

spherical tops and symmetric and asymmetric rotors. In addition to the molecular-beam method these constants have also since been measured by high-resolution microwave spectroscopy and beam maser spectroscopy. Interest in the work is stimulated by the fact that theory indicates the second order part of the nuclear spin-rotation constants is simply related to the second order part of the magnetic shielding which has received considerable attention in nuclear magnetic resonance studies. Nuclear spin-rotation coupling is also of interest in the field of nuclear magnetic relaxation since sufficient evidence has now accumulated to indicate that this may be an important, often dominant, relaxation mechanism, especially for heavier nuclei such as fluorine.

In addition to the spin-rotation coupling one might also expect nuclear magnetic moments to be capable of interacting with magnetic fields produced by groups of atoms undergoing internal molecular reorientation, that is, a nuclear spin-internal-rotation interaction should exist. In view of the discussion in Part II of this thesis concerning the difficulties in evaluating the ordinary spin-rotation constants for large molecules, it is unlikely that the spin-internal-rotation interaction could be studied effec-

tively by molecular beam or microwave techniques with the current state of the art. However, nuclear magnetic relaxation studies do offer the possibility of identifying the presence of this interaction in the event that it turns out to be a major relaxation mechanism.

We begin with a discussion of spin-relaxation and the various known mechanisms and how they may manifest themselves in the absence and presence of internal rotation. Then we derive the rotational Hamiltonian for a molecule containing a single internal top and in the following section, the interaction of a nuclear moment on that top with the rotational motions (including internal) of the molecule. It will also be shown that the total spin-rotation Hamiltonian for such a case may be written as a sum of a spin-overall-rotation interaction and a spin-internal-rotation interaction and that the latter part vanishes in the limit of a high barrier to internal rotation, as one would expect.

We then discuss the experimental method for measuring the nuclear spin relaxation times by pulsed magnetic resonance and the results of our measurements on benzotrifluoride, several of its derivatives and related compounds. Arguments are then presented for the case of F^{19} relaxation in benzotrifluoride occuring primarily by the fluctuations

spin-internal-rotation interaction.

B. NUCLEAR SPIN RELAXATION MECHANISMS AND THE CALCULATION OF RELAXATION TIMES IN MOBILE DIAMAGNETIC LIQUIDS.

1. Introduction

In liquids and gases there exist various random motions of molecules and it is the time-dependent spin perturbations produced by these random motions which are responsible for nuclear spin relaxation. These motions include, for example, overall rotational reorientation of individual molecules, relative translational motion of molecules, chemical exchange of atoms and internal reorientations such as inversion or internal rotation. Bloembergen, Purcell, and Pound (1) proposed that this molecular activity caused fluctuating magnetic or electric fields to appear at the nuclei and that the Fourier spectrum of the fluctuating field contained non-vanishing components at the precise frequencies required to induce transitions between states of the spin-system. This brings the spin system into thermal equilibrium with the rest of the liquid namely, the "lattice". Thus, one of the major purposes of relaxation studies lies in the ability of such experiments to

shed light on the general problem of molecular dynamics.

2. Bloch's Equation

In 1946 Bloch (2) postulated the following linear form for the differential equation describing the nuclear magnetic relaxation of an ensemble of spins.

$$d\vec{M}/dt = \gamma \vec{M} \times \vec{H} - \vec{i}\, M_x/T_2 - \vec{j}\, M_y/T_2 - \vec{k}\,(M_z - M_0)/T_1 \qquad (1)$$

with $$\gamma = \vec{\mu}/\vec{I}\hbar \qquad (2)$$

and $$\vec{H}(t) = \vec{k}\, H_0 + \vec{H}_1(t) \qquad (3)$$

This means that starting with arbitrary magnitude and direction, the z-component of $\vec{M}$ will, in the absence of $\vec{H}_1$, reach the value of M_0 exponentially with a time constant T_1, the <u>longitudinal</u> relaxation time; the x- and y- components will vanish exponentially with a time constant T_2, the <u>transverse</u> relaxation time. The validity of this phenomenological equation has since been verified (3).

3. The Density Matrix Method (4).

In the following paragraphs we outline a scheme for calculating the relaxation times appearing in the Bloch equations.

The equation of motion of the density matrix is

$$\frac{d\rho}{dt} = \frac{i}{\hbar}[\rho, \mathcal{H}] \qquad (4)$$

If the total Hamiltonian is taken as a sum of a large, time-independent interaction $\mathcal{H}_0$ and a smaller time-dependent

part,

$$\mathcal{H} = \mathcal{H}_0 + \mathcal{H}_1(t) \tag{5}$$

then $$\frac{d\rho}{dt} = \frac{i}{\hbar}[\rho, \mathcal{H}_0 + \mathcal{H}_1(t)] \tag{6}$$

In the interaction representation, i.e.

$$X^* \equiv \exp(i\mathcal{H}_0 t/\hbar)\, X\, \exp(-i\mathcal{H}_0 t/\hbar) \tag{7}$$

equation (6) becomes

$$\frac{d\rho^*}{dt} = \frac{i}{\hbar}[\rho^*, \mathcal{H}_1^*(t)] \tag{8}$$

which, to second order in $\mathcal{H}_1^*$, is

$$\frac{d\rho^*(t)}{dt} = \frac{i}{\hbar}[\rho^*(0), \mathcal{H}_1^*(t)] + \left(\frac{i}{\hbar}\right)^2 \int_0^t [[\rho^*(0), \mathcal{H}_1^*(t')], \mathcal{H}_1^*(t)]\, dt' \tag{9}$$

since $$(n|\rho^*|m) = \exp\left(\left(i/\hbar\right)(E_n - E_m)t\right)(n|\rho|m) \tag{10}$$

the diagonal elements of the density matrix are the same in both representations and their respective time derivaties will also be equal.

To derive the probability per unit time for transitions from a state k to a state m we assume

$$(n|\rho^*(0)|m) = (n|\rho(0)|m) = 0 \tag{11}$$

and $$(k|\rho^*(0)|k) = (k|\rho(0)|k) = 1 \tag{12}$$

that is, at t = 0 only state k is occupied. Under these conditions equation (9) becomes

$$\frac{d}{dt}(m|\rho^*(t)|m) = \frac{d}{dt}(m|\rho(t)|m) \equiv W_{km} \tag{13}$$

$$= \frac{1}{\hbar^2}\int_0^t [(m|\mathcal{H}_1^*(t)|k)(k|\mathcal{H}_1^*(t')|m) + (m|\mathcal{H}_1^*(t)|k)(k|\mathcal{H}_1^*(t')|m)]\, dt'$$

Since $\mathcal{H}_1(t)$ varies from ensemble to ensemble within the sample, we average over the ensembles. If we transform to the "original" representation within equation (7)

$$\frac{d}{dt}\overline{(m|\rho|m)} = \frac{1}{\hbar^2}\int_0^t \Big[\overline{(m|\mathcal{H}_1(t')|k)(k|\mathcal{H}_1(t)|m)}\, e^{i(m-k)(t'-t)} + \overline{(m|\mathcal{H}_1(t)|k)(k|\mathcal{H}_1(t')|m)}\, e^{i(m-k)(t-t')}\Big]dt' \tag{14}$$

where $m \equiv E_m/\hbar$, $k \equiv E_k/\hbar$, etc.

For stationary random functions, ensemble averages such as those appearing in equation (14) depend only on

$$-\tau \equiv t'-t \tag{15}$$

The correlation function, $G_{mk}(\tau)$, is defined

$$G_{mk}(\tau) \equiv \overline{(m|\mathcal{H}_1(t-\tau)|k)(k|\mathcal{H}_1(t)|m)} \tag{16}$$

$G_{mk}(\tau)$ has the properties that it is a maximum at $t = 0$, falls off slowly with increasing τ, and goes to zero for $\tau > \tau_c$ where τ_c is known as the "correlation time". The substitution of equation (16) into equation (14) yields

$$\frac{d}{dt}(m|\rho|m) = \frac{1}{\hbar^2}\int_{-t}^{+t} G_{mk}(\tau)\, e^{-(m-k)\tau}\, d\tau \tag{17}$$

If $t \gg \tau_c$, the integration limits may be extended to $\pm\infty$.

$$\frac{d}{dt}(m|\rho|m) = \hbar^{-2}\int_{-\infty}^{+\infty} G_{mk}(\tau)\, e^{-(m-k)\tau}\, d\tau \tag{18}$$

The spectral density of the correlation function is defined

$$J_{mk}(\omega) = \int_{-\infty}^{+\infty} G_{mk}(\tau)\, e^{-i\omega\tau}\, d\tau = \hbar^2 W_{km} \tag{19}$$

For spin $\frac{1}{2}$ systems

$$\frac{1}{T_1} = 2 W_{km} \tag{20}$$

The calculation of T_1 involves the computation of the correlation function of the time dependent part of the perturbing Hamiltonian and the evaluation of its non-vanishing Fourier components.

For lack of detailed information on the nature of the correlation functions, in nuclear relaxation calculations they are ordinarily taken to be exponential.

$$\langle F(t)\, F^*(t+\tau)\rangle = \langle |F(0)|^2\rangle\, e^{-\tau/\tau_c} \tag{21}$$

For certain types of time-dependent perturbations, for example, a field fluctuating between two values $\pm h_0$, at a rate given by

$$\frac{dP_1}{dt} = w(P_2 - P_1) \tag{22}$$

where P_1 (P_2) is the probability that in an ensemble in which the field was $+h_0$ at $\tau_0 = 0$ it will be $+h_0$ ($-h_0$) at time τ , the correlation function is

$$G(\tau) = h_0^2\, e^{-2w\tau} \tag{23}$$

in which $2w \simeq \tau_c^{-1}$. Simple diffusion models also lead to exponentially decaying correlation functions.

At this point the nuclear spin relaxation time is expressed in terms of a correlation time (or times) for the random operator. Although these correlation times are usually not independently known, they often may be estimated to within an order of magnitude. In some cases the correlation time has been related to certain macroscopic properties of the liquid by postulating a reasonable model for the random motion of interest, vide infra.

4. Relaxation in the Absence of Internal Rotation.

The time-dependent perturbation discussed in the last section may arise in several ways. About a half-dozen relaxation mechanisms have been investigated to a greater or lesser degree in mobile diamagnetic liquids. These include the inter- and intramolecular tensor dipolar interactions, the interrupted scalar dipolar interaction, the spin-rotational interaction and the anisotropic chemical shift. In this section the general features of each of these processes will be discussed for the case of a rigid molecule. The particular manifestations each interaction has in the presence of molecular internal rotation will be investigated in the following section.

a. The Inter- and Intramolecular Tensor Dipolar Interactions.

The tensor dipole-dipole interaction between two spins $\vec{I}_1$ and $\vec{I}_2$ separated by a distance $|\vec{r}_{12}|$ is

$$\mathcal{H}_{dd} = (\gamma^2 \hbar^2 r_{12}^{-3})\ \vec{I}_1 \cdot \underset{\sim}{T} \cdot \vec{I}_2 \qquad (25)$$

in which the (fluctuating) traceless coupling dyadic $\underset{\sim}{T}$ is

$$\underset{\sim}{T} = (\underset{\sim}{1} - 3\hat{a}\hat{a}) \qquad (26)$$

In equation (26) $\underset{\sim}{1}$ is the unit dyadic and $\hat{a}\hat{a}$ is the tensor product of two unit vectors directed along $\vec{r}_{12}$.

The Hamiltonian (25) is time dependent due to fluctuations in the magnitude and direction of $\vec{r}_{12}$. For rigid molecules intramolecular relaxation arises from the latter and intermolecular relaxation from both. For two like nuclei, i.e. $I_1 = I_2$

$$T_1^{-1} = \frac{3}{2}\gamma^4\hbar^2 r^{-6}\, I(I+1)\left(J_1(\omega_0) + J_2(2\omega_0)\right) \qquad (27)$$

and

$$T_2^{-1} = \frac{3}{2}\gamma^4\hbar^2 r^{-6}\, I(I+1)\left(\frac{1}{4}J_0(0) + \frac{5}{2}J_1(\omega_0) + \frac{1}{4}J_2(2\omega_0)\right) \qquad (28)$$

where

$$J_i(\omega) = \int_{-\infty}^{+\infty} \langle F_i(t+\tau)\, F_i^*(t)\rangle\, e^{i\omega\tau}\, d\tau \qquad (29)$$

In equation (29) the F_1 are the orientation functions,

$$F_0(t) = (1-3n^2),\quad F_1(t) = (l+im)n,\quad F_2(t) = (l+im)^2 \qquad (30)$$

and the $\underline{l}$, $\underline{m}$, and $\underline{n}$, are the components of $\hat{a}$. The correlation functions are taken to be of the form of (21). Evaluating the functions (29) and substituting the results into (27) and (28) yields for the intramolecular dipolar relaxation

$$\frac{1}{T_1} = \frac{6}{20}\hbar^2\gamma^4 r^{-6}\left(\frac{\tau_c}{1+\omega^2\tau_c^2} + \frac{4\tau_c}{1+4\omega^2\tau_c^2}\right)$$

$$\frac{1}{T_2} = \frac{3}{20}\hbar^2\gamma^4 r^{-6}\left(3\tau_c + \frac{5\tau_c}{1+\omega^2\tau_c^2} + \frac{2\tau_c}{1+4\omega^2\tau_c^2}\right) \qquad (31)$$

In the case of "extreme narrowing" i.e., $\omega^2\tau_c^2 \ll 1$,

$$T_1^{-1} = T_2^{-1} = \frac{3}{2}\hbar^2\gamma^4 r^{-6}\tau_c \qquad (32)$$

For isotropic rotational Browian motion (assuming the molecule to be a rigid sphere in a continuous viscous medium) the correlation time is (10)

$$\tau_c = 2a^2/9D = 1/6D'$$

in which D and D' are the translational and rotational diffusion coefficients respectively, and a is the radius of the molecule.

T_1 and T_2 are the time constants defined by the Bloch equations for the exponential decays of the z- and x- or y-components of the magnetization. This result may be extended to any number of nuclei by pairwise summation of the relations (31) or (32). But this may only be done in the event that the motions of the pairs are not correlated, since non-vanishing correlation functions of the form $\langle F_{ij}(t) F_{kl}^*(t+\tau)\rangle$ must then be taken into consideration. For three nuclei in fixed equivalent positions on an equilateral triangle or four on a regular tetrahedron, Hubbard (5) showed that in each case the decay of the z-component of the magnetization was given in the extreme

narrowing limit by a sum of two exponentials.

$$\frac{M_z(t) - M_0}{M_z(0) - M_0} = a e^{-\alpha t/T_1} + b e^{-\beta t/T_1} \qquad (33)$$

Where, $M_z(t)$, $M_z(0)$, and M_0 are the values of the z-magnetization at the time t, time 0, and at equilibrium, respectively, and where T_1 is the value calculated in the absence of the correlated motion. Hubbard also evaluated the coefficients: for the three spin case, a = .008, b = .992, α = .42, β = 1.005; and similar results for four spins. Hence the relaxation curves in such situations will be experimentally indistinguishable from single exponentials.

For two <u>unlike</u> nuclei ($I_1 \neq I_2$) the longitudinal relaxation is given by two coupled differential equations and Solomom (6) has shown that for extreme narrowing ($\omega_{I_1}^2 \tau_c^2 << 1$ and $\omega_{I_2}^2 \tau_c^2 << 1$)

$$\frac{I_{1z}(t) - I_{1z0}}{I_{1z}(0) - I_{1z0}} = \frac{1}{2}\left(e^{-t/T_1} + e^{-t/D_1}\right) \qquad (34)$$

Where $T_1^{-1} = \frac{3}{2}\delta$ and $D_1^{-1} = \frac{1}{2}\delta$ and $\delta \equiv \hbar^2 \gamma_{I_1}^2 \gamma_{I_2}^2 r^{-6} \tau_c$.

The relaxation appears as the sum of two equally weighted exponentials and if $\gamma_{I_1} \sim \gamma_{I_2}$ one of the exponentials has the "ordinary" T_1 given by (32) and the other has a decay constant three times as large.

The intermolecular dipolar relaxation takes into

account both the relative translational motion of the molecules in the liquid as well as their reorientational behavior. Assuming these motions to be independent, Hubbard (11) has shown that for the short correlation time limit, the relaxation times for spin ½ nuclei in equivalent positions in spherical molecules are given by an infinite series the first three terms of which are

$$T_1^{-1} = T_2^{-1} = \frac{n\pi\gamma^4\hbar^2}{5aD}\left(1 + 0.233\left(\frac{b}{a}\right)^2 + 0.15\left(\frac{b}{a}\right)^4 + \cdots\right)$$

where n is the number of spins per unit volume, a is the radius of the molecule, b is the distance from the magnetic nucleus to the center of the molecule, and D is the translational diffusion coefficient.

b. The Interrupted Scalar Interaction.

The electron-coupled nuclear spin-spin (scalar) interaction is

$$\mathcal{H}_{sc} = A\,\vec{I}_1 \cdot \vec{I}_2 \qquad (35)$$

The coupling constant A may become time-dependent by processes such as chemical exchange. In the event that T_1^{-1} or τ_e^{-1} (the rate of exchange) is much larger than A the scalar interaction can become a relaxation mechanism.

With the assumptions (a) the steady state splitting is completely "wiped out" by exchange and (b) the amount

of time spent by spin I_1 being uncoupled to <u>any</u> spin I_2 is negligible, the relaxation time constants for a two spin $\frac{1}{2}$ system are (7)

$$T_1^{-1} = (3\delta)/2 \tag{36}$$

$$D^{-1} = \delta/2 + A^2\left(\frac{\tau_e}{1+(\omega_{I_1}-\omega_{I_2})^2\tau_e^2}\right) \tag{37}$$

$$T_2^{-1} = \delta + A^2\left(\tau_e + \frac{\tau_e}{1+(\omega_{I_1}-\omega_{I_2})^2\tau_e^2}\right) \tag{38}$$

where the δ's are due to the tensor dipole-dipole part as discussed above and the second terms in (37) and (38) arise from the scalar interaction.

c. <u>The Anisotropic Chemical Shift.</u>

The Zeeman interaction of a nuclear spin in a molecule is

$$\mathcal{H}_z = \vec{H}_0 \cdot (\underset{\sim}{1} - \underset{\sim}{\sigma}) \cdot \vec{I} \tag{39}$$

in which σ is the shielding tensor with definite components in the molecule-fixed axis system. The chemical shift observed in liquids undergoing rapid tumbling is

$$\Delta\omega = \delta_0 \omega_0' \tag{40}$$

where ω_0' is the "bare nucleus" Larmor frequency and

$$\delta_0 = \frac{1}{3} \text{Trace}(\underset{\sim}{\sigma}). \tag{41}$$

The traceless part, $\underset{\sim}{\sigma}'$, of the shielding tensor, under molecular tumbling, can produce nuclear spin relaxation. Defining η as a measure of the asymmetry

$$\eta = (\delta_x - \delta_y)/\delta_z \tag{42}$$

where the δ_i are the diagonal components of the traceless part, the relaxation times, under extreme narrowing, due to this mechanism are (8,9)

$$T_1^{-1} = \frac{6}{40}(\gamma H_0)^2 \delta_z^2 \left(1 + \frac{\eta^2}{3}\right)\tau_c \tag{43}$$

$$T_2^{-1} = \frac{7}{40}(\gamma H_0)^2 \delta_z^2 \left(1 + \frac{\eta}{3}\right)\tau_c \tag{44}$$

This relaxation process has two interesting characteristics. First it is definitely field dependent ($\propto H_0^2$) (as contrasted with the interrupted scalar interaction which is field dependent only in the case that $(\omega_{I_1} - \omega_{I_2})\tau_c$ is not vanishingly small), and second, even in the extreme narrowing limit, $T_1 \neq T_2$.

d. The Spin-Rotational Interaction.

A nuclear spin may also experience a tensor coupling to the molecular rotation,

$$\mathcal{H}_{SR} = \vec{I} \cdot \underset{\sim}{C} \cdot \vec{J} \tag{45}$$

where the spin-rotational tensor $\underset{\sim}{C}$ has fixed components in the molecular frame. The interaction (45) becomes time-dependent through random fluctuations in m_J and J. Generally it is assumed that the changes in angular momentum

and orientation of the molecule are independent. It is expected that this should be a good approximation as long as the correlation times for the respective changes in angular momentum and molecular orientation are very different. The nuclear spin relaxation due to this mechanism is (10),

$$T_1^{-1} = 2\,J(\omega_0) \tag{46}$$

$$T_2^{-1} = J(0) + J(\omega_0) \tag{47}$$

In which

$$J(\omega) = \frac{I k T}{9\hbar^2}\left((2C_\perp + C_{11})^2 \frac{\tau_1}{1+\omega^2\tau_1^2} + 2(C_{11}-C_\perp)^2 \frac{\tau_{12}}{1+\omega^2\tau_{12}^2} \right) \tag{48}$$

Expression (48) is derived on the basis that the angular velocity may be treated classically by assuming it obeys an equation analogous to the Langevin equation often used in treatments of translational Brownian motion and that changes in the orientation of the molecule are due to isotropic rotational Brownian motion. $C_\perp$ and C_{11} are the perpendicular and parallel components of the spin-rotational tensor in equation (45), which is assumed to be axially symmetric. The correlation time for the angular velocity is τ_1 and τ_{12} is defined

$$\frac{1}{\tau_{12}} \equiv \frac{1}{\tau_1} + \frac{1}{\tau_c} \tag{49}$$

where τ_c is the correlation time for the molecular

reorientation and is the same correlation time which appears in the dipolar interaction. The term involving τ_2 is valid only if $\tau_1 \ll \tau_c$ or $\tau_c \ll \tau_1$. For extreme narrowing and in the limit where $\tau_1 \ll \tau_c$

$$T_1^{-1} = T_2^{-1} = \frac{2}{3}\left(\frac{I k T \tau_1}{3\hbar^2}\right)(2C_\perp^2 + C_\parallel^2) \qquad (50)$$

where T is the absolute temperature and I is the moment of inertia of the molecule.

e. Identification of Dominant Mechanisms.

The contributions of the various relaxation mechanisms are expected to act in parallel so that we may write for the total relaxation times

$$\frac{1}{T_1} = \sum_i \left(\frac{1}{T_1}\right)^{(i)} \quad \text{and} \quad \frac{1}{T_2} = \sum_i \left(\frac{1}{T_2}\right)^{(i)} \qquad (51)$$

The summation extends over all the processes just discussed. More than one relaxation process may be in effect at a given time. Luckily, experiments which take advantage of a particular characteristic of a given process may be performed to determine what extent each mechanism is active.

For example, the anisotropic chemical shift mechanism can be identified straight away by its proportionality to the square of the magnetic field strength. Although the anisotropic chemical shift mechanism is theoretically reasonable, reports of bona fide examples are extremely rare (12,13,14). The intermolecular dipolar interaction

may be separated from intramolecular interactions since it is the only one which is dependent upon relative translational diffusion and hence on the concentration of the subject nuclei. Dilution studies in "nonmagnetic" (e.g. carbon disulfide) or deuterated solvents signal intermolecular interactions by an inverse dependence of T_1 on concentration (22,23,24,25). Dipolar interactions can be distinguished from spin-rotational interactions by their opposite temperature behavior (16) in the limit of extreme narrowing. Dipolar relaxation times increase with increasing temperature whereas the spin-rotational relaxation times decrease. Dipolar relaxation between "unlike" nuclei may be verified by Overhauser (multiple irradiation) techniques (6,7,15). The problem of separating the contributions due to the simultaneous presence of dipolar interactions between "unlike" nuclei and spin-rotation interactions can be solved in some circumstances by the measurement of the Ovenhauser effect in addition to relaxation rates (17). One ordinarily knows when to suspect the presence of an interrupted scalar interaction (chemical exchange, internal motion, etc.) and Overhauser experiments here again may be used for identification.

Generally speaking in mobile diamagnetic liquids the

most important mechanisms for proton relaxation are the inter- and intramolecular dipolar interactions (16,23,25). For fluorine relaxation dipolar relaxation dominates at low temperatures but at higher temperatures the spin-rotational process usually takes over (13,18,19,20,21).

5. Relaxation in the Presence of Internal Motion.

The existence of internal motion, specifically internal rotation, causes certain new features to appear in the various relaxation processes just described. Although no new interactions appear there are some interesting manifestations of the ones previously discussed which warrant mention here. Below, it is assumed that the nuclei of interest are located on an internal top which is capable of rotation relative to a "framework", such as in toluene, ethane, etc.

a. The Intramolecular Dipolar Interaction.

There are two new features which appear in the intramolecular dipolar interaction as a result of internal motion. First, the orientation functions (equation (30)) and hence the correlation functions must now be modified to take into consideration the time dependence of the relative azimuthal angle between the interspin vector and internal rotation axis. And second, there may be intramolecular

dipolar interactions in which the length of the internuclear vector as well as its orientation changes, for example, between ring and methyl protons in toluene or between the protons of the two methyl groups in ethane. Disregarding ring-top dipolar interactions the relaxation times for two spin ½ nuclei undergoing stochastic internal reorientation among a very large number of equilibrium positions is given (26) in the extreme narrow limit by

$$T_1^{-1} = T_2^{-1} = \frac{3}{2}\gamma^4\hbar^2 r^{-6}\left(\frac{\tau_c}{4} + \frac{3}{4}\left(\left(\frac{1}{\tau_c}\right) + \left(\frac{4}{\tau_c'}\right)\right)^{-1}\right) \qquad (52)$$

in which τ_c' and τ_c are correlation times for the internal and overall reorientation respectively, and where the angle between the interspin vector and the axis of internal rotation has been taken to be 90°. In the event that the internal motion is better described by random jumps from one of three equilibrium positions, ϕ , $\phi \pm 2\pi/3$, to either of the two adjacent positions at an average rate $(3\tau_c)^{-1}$ the relaxation times are

$$T_1^{-1} = T_2^{-1} = \frac{3}{2}\gamma^4\hbar^2 r^{-6}\left(\frac{\tau_c}{4} + \frac{3}{4}\left(\left(\frac{1}{\tau_c}\right) + \left(\frac{1}{\tau_c'}\right)\right)^{-1}\right) \qquad (53)$$

From equations (52) and (53) it is apparent that the effect of internal motion is an increase in relaxation times. Also note that in the limit of a large barrier to internal reorientation $\tau_c' \to \infty$ and (52,53) reduce to the

ordinary dipolar expressions. Consideration of intragroup (e.g. ring-top) interactions introduces additional correlation times (26) which further reduce the relaxation rate.

b. The Interrupted Scalar Interaction.

The effects of internal rotation on high resolution NMR spectra have been well studied (27,28). For internal rotation occurring at such a rate that the effective chemical shifts and coupling constants are averaged, the expressions for the relaxation times are the same as those given for the case of chemical exchange discussed previously, with τ_c interpreted as the correlation time for internal reorientation.

c. The Spin-Internal-Rotation Interaction.

It will be shown later that when a spin possessing nucleus resides on an internal top the total interaction of that nuclear spin with the magnetic fields produced by the rotation of the molecule may be written as a sum of a spin-overall-rotation interaction and a spin-internal-rotation interaction,

$$\mathcal{H}'_{SR} = \vec{I} \cdot \underset{\sim}{M} \cdot \vec{J} + \vec{I} \cdot \underset{\sim}{M} \cdot \vec{j}'' \qquad (54)$$

where $\vec{j}''$ is the angular momentum of the internal top referenced to the framework. It will also be shown that with the internal angular momentum so defined, the second

term on the RHS of (54) will vanish in the limit of high barrier, i.e. zero internal angular momentum referenced to the frame.

C. THE SPIN-INTERNAL-ROTATION INTERACTION.

1. Introduction.

In $^1\Sigma$ molecules there exist magnetic fields which are produced by the electric currents associated with the motions of the nuclei and of the electrons. The interaction of a nuclear magnetic moment with these fields is the spin-rotation interaction. The currents due to the nuclear motion may be calculated from a knowledge of the equilibrium nuclear distances. However, the contribution due to the electronic motion arises from second-order perturbation theory and therefore its calculation requires a knowledge of ground and excited state electronic wave functions. Hence, ab initio calculations of the excited state term cannot ordinarily be performed.

The spin-rotation Hamiltonian operator has been considered in detail for symmetric rotors by Gunther-Mohr, Townes, and Van Vleck (29,30) and has been extended to asymmetric rotors by Schwartz (31). In order to treat the spin-internal-rotation problem the work of these authors must be modified to include the internal angular momentum. In the following paragraphs the Hamiltonian for

the rotation of the molecule will be derived in a form particularly convenient to the problem. This Hamiltonian will then be used to derive the Hamiltonian for the interaction of a nuclear spin located on an internal top with the magnetic fields produced by both the internal and the overall motions of the molecule. Discussions of the solution of the rotational wave functions in the presence of internal rotation, and the matrix elements of the spin-rotation Hamiltonian are given in Appendices A, B, and C respectively.

2. The Hamiltonian for the Rotation of the Molecule (32, 33).

We imagine the molecule to be composed of two parts: a framework and a symmetric top. The internal top is able to rotate more or less freely with respect to the framework. The three Euler angles θ , ϕ , and χ describe the orientation of the principal axes of the molecule with respect to space-fixed axes and α is the relative orientation of the top and framework. The kinetic energy of the whole molecule is

$$T = \frac{1}{2}\vec{\omega}^{+}\cdot\underset{\sim}{I}\cdot\vec{\omega} + \frac{1}{2}\left(\frac{\vec{\partial\alpha}}{\partial t}\right)^{+}\cdot\underset{\sim}{I_\alpha}\cdot\left(\frac{\vec{\partial\alpha}}{\partial t}\right) + \frac{1}{2}\left(\vec{\omega}^{+}\cdot\underset{\sim}{I_\alpha}\cdot\left(\frac{\vec{\partial\alpha}}{\partial t}\right)\right. \\ \left. + \left(\frac{\vec{\partial\alpha}}{\partial t}\right)^{+}\cdot\underset{\sim}{I_\alpha}\cdot\vec{\omega}\right) \qquad (55)$$

For molecules possessing at least two planes of symmetry a set of coordinate axes (a,b,c) may be defined such that the c-axis is coincident with the top axis and the kinetic energy may be written

$$T = \tfrac{1}{2} I_a \omega_a^2 + \tfrac{1}{2} I_b \omega_b^2 + \tfrac{1}{2} I_c \omega_c^2 + \tfrac{1}{2} I_\alpha \dot{\alpha}^2 + I_\alpha \omega_c \dot{\alpha}$$

$$= \tfrac{1}{2} I_a \omega_a^2 + \tfrac{1}{2} I_b \omega_b^2 + \tfrac{1}{2} (I_c - I_\alpha) \omega_c^2 + \tfrac{1}{2} I_\alpha (\omega_c + \dot{\alpha})^2 \qquad (56)$$

I_a, I_b, and I_c are the three moments of inertia of the whole molecule about the three coordinate axes, I_α is the moment of inertia of the top about its symmetry axis; ω_a, ω_b, and ω_c, are the components of the angular velocity $\vec{\omega}$ of the entire molecule and $\dot{\vec{\alpha}}$ is the angular velocity of the internal rotor relative to the frame. Introducing the momenta

$$P_a = \partial T / \partial \omega_a = I_a \omega_a \qquad (57a)$$

$$P_b = \partial T / \partial \omega_b = I_b \omega_b \qquad (57b)$$

$$P_c = \partial T / \partial \omega_c = I_c \omega_c + I_\alpha \dot{\alpha} \qquad (57c)$$

$$p = \partial T / \partial \dot{\alpha} = I_\alpha (\omega_c + \dot{\alpha}) \qquad (57d)$$

leads to the Hamiltonian

$$\mathcal{H} = \frac{P_a^2}{2I_a} + \frac{P_b^2}{2I_b} + \frac{P_c^2}{2(I_c - I_\alpha)} + \frac{I_c p^2}{2I_\alpha (I_c - I_\alpha)} - \frac{p P_c}{(I_c - I_\alpha)} + V(\alpha) \qquad (58)$$

P_a, P_b, and P_c are the components of the total angular momentum (including the internal motion) about the a, b, and c, axes and p is the <u>total</u> angular momentum of the top

including the overall and internal motions. V (α) is the periodic potential barrier restricting the internal motion. As a differential operator $p = \frac{\hbar}{i}\left(\frac{\partial}{\partial \alpha}\right)_{\theta,\phi,\chi}$ which commutes with P_a, P_b, and P_c. It is often convenient to eliminate the cross term in equation (58). This is accomplished by the Nielsen transformation:

$$p' = p - ((I_\alpha / I_c) P_c) = \left(1 - \frac{I_\alpha}{I_c}\right) I_\alpha \dot{\alpha} \qquad (59a)$$

$$p' = r I_\alpha \dot{\alpha} \qquad (59b)$$

$$P_c' = P_c \qquad (59c)$$

With this substitution the Hamiltonian (58) becomes

$$\mathcal{H} = \frac{P_a^2}{2I_a} + \frac{P_b^2}{2I_b} + \frac{P_c^2}{2I_c} + \frac{I_c}{2I_\alpha(I_c - I_\alpha)}(p')^2 + V(\alpha) \qquad (60)$$

Here p' is dependent only on $\dot{\alpha}$ and in the limit $\dot{\alpha} \longrightarrow 0$, i.e. in the limit of high barriers, equation (60) reduces directly to the ordinary rigid rotor Hamiltonian since the coefficents of the P's are the inertial moments of the entire molecule. However p' is not the angular momentum of the internal motion but is smaller than it by the factor $\underline{r}$. Although p' does not commute with P_a or P_b, viz.,

$$(p', P_{(\substack{a\\b})}) = i\hbar\left(\frac{I_\alpha}{I_c}\right) P_{(\substack{b\\a})} \quad , \qquad (61)$$

it does commute with $(P_a^2 + P_b^2)$. For symmetric molecules ($I_a = I_b$) this allows a separation of the Hamiltonian (60)

into two parts corresponding to the over-all rotation and the internal rotation. Alternatively, one may define

$$p'' = I_\alpha \dot{\alpha} = p'/r \tag{62}$$

and then

$$\mathcal{H} = \frac{P_a^2}{2I_a} + \frac{P_b^2}{2I_b} + \frac{P_c^2}{2I_c} + \left((I_c - I_\alpha)/2 I_\alpha I_c\right)(p'')^2 + V(\alpha) \tag{63}$$

where (p'') is the angular momentum of the internal motion referred to the frame-fixed axis system. Equation (63) is the form of the rotational Hamiltonian which will be used in the derviation of the spin-internal-rotation Hamiltonian.

3. The Spin-Rotation Hamiltonian.

To derive the interaction of a nuclear moment situated on an internal rotor with the magnetic fields produced by the overall and internal rotations of the molecule on which it is located, we begin with the Hamiltonian:

$$\mathcal{H} = A(J_a - L_a)^2 + B(J_b - L_b)^2 + C(J_c - L_c)^2 + F'(j'' - \ell'')^2 + V(\alpha) \tag{64a}$$

$$+ \left(\frac{e\mu_0}{c}\right) \sum_{Ki} n_{Ki}^{-3} (\vec{n}_i - \vec{n}_K) \times (\vec{v}_i - (1 - \frac{z_K M_p}{g_K m_K}) \vec{v}_K) \cdot g_K \vec{I}_K \tag{64b}$$

$$- \left(\frac{e\mu_0}{c}\right) \sum_{K \neq L} z_L n_{KL}^{-3} (\vec{n}_K - \vec{n}_L) \times \left((1 - \frac{z_K M_p}{g_K m_K}) \vec{v}_K - \vec{v}_L\right) \cdot g_K \vec{I}_K \tag{64c}$$

The first term (64a) represents the total rotational energy of the nuclei, including the internal rotation, and the potential energy. The J_i's are the components of the

total angular momentum of the molecule and the L_i are the components of the total orbital electronic angular momentum. The total angular momentum of the internal rotor referenced to the frame and the orbital angular momentum of the electrons on it are designated j" and l". Terms (64b) and (64c) represent respectively the interaction of a magnetic nucleus with the field produced by the motions of the electrons and the other nucei.

Since operators involving electronic velocities or angular momenta are off-diagonal in the electronic quantum numbers in a $^1\Sigma$ molecule, the first order contribution to the spin rotational energy is calculated by setting the electronic velocities and orbital angular momenta to zero in (64). This leaves the rotational energy plus

$$\mathcal{H}' = \left(\frac{e\mu_0}{c}\right) \bar{\Sigma}_{Ki}\, \pi_{Ki}^{-3}\, (\vec{\pi}_i - \vec{\pi}_K) \times \left(-\frac{\vec{v}_K}{\beta}\right) \cdot g_K \vec{I}_K \qquad (65a)$$

$$-\left(\frac{e\mu_0}{c}\right) \bar{\Sigma}_{\substack{KL \\ K\neq L}}\, Z_L\, \pi_{KL}^{-3}\, (\vec{\pi}_K - \vec{\pi}_L) \times \left(\frac{\vec{v}_K}{\beta} - \vec{v}_L\right) \cdot g_K \vec{I}_K \qquad (65b)$$

where

$$\beta = \left(1 - \frac{Z_K M_P}{g_K M_K}\right)^{-1} \qquad (66)$$

$\mathcal{H}'$ may in turn be reduced by the substitutions

$$\vec{v} = \vec{\omega} \times \vec{\rho} \qquad (67)$$

The components of the angular velocity are related to the

angular momenta by equations (57a-d). For the nuclei on the internal rotor

$$\vec{v} = (\vec{\omega} + \dot{\vec{\alpha}}) \times \vec{\pi} \tag{68}$$

which yields on substitution

$$\mathcal{H}' = \left(\frac{e\mu_0}{c}\right) \bar{z}_{Ki}\, \pi_{Ki}^{-3}\, (\vec{\pi}_i - \vec{\pi}_K) \times \left(-\frac{(\omega + \dot{\alpha})}{\beta} \times \vec{\pi}_K\right) \cdot g_K \vec{I}_K \tag{69a}$$

$$-\left(\frac{e\mu_0}{c}\right) \sum_{K \neq L} \bar{z}_{KL}\, z_L\, \pi_{KL}^{-3}\, (\vec{\pi}_K - \vec{\pi}_L) \times \left(\frac{(\vec{\omega} + \vec{\alpha})}{\beta} \times \vec{\pi}_K - \begin{Bmatrix} \vec{\omega} \times \vec{\pi}_L \\ (\vec{\omega} + \vec{\alpha}) \times \vec{\pi}_L \end{Bmatrix}\right) \cdot g_K \vec{I}_K \tag{69b}$$

Since we have assumed the K^{th} nucleus, the nucleus of interest, to be on the internal top in (69b) the upper term in the curly traces is used if the L^{th} nucleus is on the frame, the lower if it is on the top. Each term in $\mathcal{H}'$ may be split into two terms, one corresponding to the overall motion and one to the internal motion.

$$\left(\frac{e\mu_0}{c}\right) \bar{z}_{Ki}\, \pi_{Ki}^{-3}\, (\vec{\pi}_i - \vec{\pi}_K) \times \left(\frac{\vec{\omega}}{\beta} \times \vec{\pi}_K\right) \cdot g_K \vec{I}_K + \left(\frac{e\mu_0}{c}\right) \bar{z}_{Ki}\, \pi_{Ki}^{-3}\, (\vec{\pi}_i - \vec{\pi}_K) \times \left(\frac{\dot{\vec{\alpha}}}{\beta} \times \vec{\pi}_K\right) \cdot g_K \vec{I}_K \tag{70a}$$

and

$$-\left(\frac{e\mu_0}{c}\right) \sum_{K \neq L} \bar{z}_{KL}\, z_L\, \pi_{KL}^{-3}\, (\vec{\pi}_K - \vec{\pi}_L) \times \left(\frac{\vec{\omega} \times \vec{\pi}_K}{\beta} - \vec{\omega} \times \vec{\pi}_L\right) \cdot g_K \vec{I}_K$$

$$-\left(\frac{e\mu_0}{c}\right) \sum_{K \neq L} \bar{z}_{KL}\, z_L\, \pi_{KL}^{-3}\, (\vec{\pi}_K - \vec{\pi}_L) \times \left(\frac{\dot{\vec{\alpha}} \times \vec{\pi}_K}{\beta} - \dot{\vec{\alpha}} \times \vec{\pi}_L\right) \cdot g_K \vec{I}_K \tag{70b}$$

The first terms of (70a) and (70b) represent the ordinary spin-rotation interaction. When $\dot{\vec{\alpha}} \to 0$, i.e. very high barrier, "frozen" internal rotation, the second terms in (70a) and (70b) vanish. It should be apparent that the additional terms due to the internal rotation will be of

the same form as those which arise from the ordinary spin-rotation interaction with $\vec{\omega}$ replaced by $\dot{\vec{\alpha}}$.

From the vector triple product identity

$$\vec{A}\times(\vec{B}\times\vec{C}) = \vec{B}(\vec{A}\cdot\vec{C}) - \vec{C}(\vec{A}\cdot\vec{B}) - [\vec{B},\vec{A}]\cdot\vec{C} \tag{71}$$

the $\dot{\vec{\alpha}}$ dependent part of (70a,b) may be reduced to

$$\left(\frac{e\mu_0}{c}\right)\bar{z}_{K\ell}\,\pi_{Ki}^{-3}\left[-\dot{\vec{\alpha}}(\vec{\pi}_i-\vec{\pi}_K)\cdot\frac{\vec{\pi}_{\ell K}}{\beta} + \frac{\vec{\pi}_{\ell K}}{\beta}(\vec{\pi}_i-\vec{\pi}_K)\cdot\dot{\vec{\alpha}}\right]\cdot g_K\vec{I}_K \tag{72a}$$

$$-\left(\frac{e\mu_0}{c}\right)\sum_{\substack{K\ell\\K\neq\ell}}\bar{z}_{K\ell}\,\pi_{K\ell}^{-3}\left[\dot{\vec{\alpha}}(\vec{\pi}_K-\vec{\pi}_\ell)\cdot\left(\frac{\vec{\pi}_{\ell K}}{\beta}-\vec{\pi}_\ell\right) - \left(\frac{\vec{\pi}_{\ell K}}{\beta}-\vec{\pi}_\ell\right)(\vec{\pi}_K-\vec{\pi}_\ell)\cdot\dot{\vec{\alpha}}\right]\cdot g_K\vec{I}_K \tag{72b}$$

which may be rearranged

$$\left(\frac{e\mu_0}{c}\right)\left[-\sum_{Ki}\pi_{Ki}^{-3}(\vec{\pi}_i-\vec{\pi}_K)\cdot\frac{\vec{\pi}_{\ell K}}{\beta} - \sum_{\substack{K\ell\\K\neq\ell}}\bar{z}_{K\ell}\,z_\ell\,\pi_{K\ell}^{-3}(\vec{\pi}_K-\vec{\pi}_\ell)\cdot\left(\frac{\vec{\pi}_{\ell K}}{\beta}-\vec{\pi}_\ell\right)\right]\cdot g_K\dot{\vec{\alpha}}\vec{I}_K \tag{73a}$$

$$-\left(\frac{e\mu_0}{c}\right)\left[-\sum_{Ki}\pi_{Ki}^{-3}\frac{\vec{\pi}_{\ell K}}{\beta}(\vec{\pi}_i\vec{\pi}_K)\cdot\dot{\vec{\alpha}} - \sum_{\substack{K\ell\\K\neq\ell}}\bar{z}_{K\ell}\,z_\ell\,\pi_{K\ell}^{-3}\left(\frac{\vec{\pi}_{\ell K}}{\beta}-\vec{\pi}_\ell\right)(\vec{\pi}_K-\vec{\pi}_\ell)\dot{\vec{\alpha}}\right]\cdot g_K\vec{I}_K \tag{73b}$$

Averaging over the ground state yields

$$\bar{z}_i\left\langle\psi_0\left|\frac{\vec{\pi}_K-\vec{\pi}_i}{\pi_{Ki}^3}\right|\psi_0\right\rangle = \sum_{\substack{K\ell\\K\neq\ell}}\bar{z}_{K\ell}\,z_\ell\,\pi_{K\ell}^{-3}(\vec{\pi}_K-\vec{\pi}_\ell) \tag{74}$$

If $\dot{\vec{\alpha}}$ is taken along the z-axis,

$$\begin{aligned}\dot{\vec{\alpha}} &= (0,0,\dot{\alpha})\\ &= (0,0,j''/I_\alpha)\end{aligned} \tag{75}$$

where j'' is the internal angular momentum of the top relative to the frame and I_α is the moment of inertia of the top about its symmetry axis, then

$$(\vec{\pi}_K-\vec{\pi}_\ell)\cdot\dot{\vec{\alpha}} = (\vec{\pi}_K-\vec{\pi}_\ell)_z\,j''/I_\alpha \tag{76}$$

and the ground state contribution to the spin-internal-rotation interaction is

$$\left(\frac{e\mu_0}{c}\right)\left[\sum_{\substack{K\ell\\K\neq\ell}}\bar{z}_{K\ell}\,z_\ell\,\pi_{K\ell}^{-3}(\vec{\pi}_K-\vec{\pi}_\ell)\cdot\vec{\pi}_\ell\right]g_K\frac{j''}{I_\alpha}I_{Kz} \tag{77a}$$

$$-\left(\frac{e\mu_0}{c}\right)\left[\sum_{\gamma}\bar{z}_{\gamma}\sum_{K\neq L}\bar{z}_{KL}\, z_L R_{KL}^{-3}(\vec{R}_K-\vec{R}_L)_{\gamma}(\vec{R}_L)_{\gamma}\right] g_K \frac{j''}{I_{\alpha}} I_{K\gamma} \qquad (77b)$$

Inspection of the steps from (69a,b) to (77a,b) reveals that (77a,b) vanish if the L^{th} nucleus is not on the top. Combining (77a,b) with the terms obtained for the overall rotation and noting $\vec{\omega} = (\omega_a, \omega_b, \omega_c) = (\omega_x, \omega_y, \omega_z)$ for type III^r representation and

$$\vec{\omega} = \left(J_a/I_a\ ,\ J_b/I_b\ ,\ (J_c-j'')/I_c\right) \qquad (78)$$

we find the total ground state contribution

$$\begin{aligned}
\mathcal{H}' = \quad & \left(\frac{e\mu_0}{c}\right)\left[\sum_{K\neq L}\bar{z}_{KL}\, z_L R_{KL}^{-3}(\vec{R}_K-\vec{R}_L)\cdot\vec{R}_L\right] g_K \bar{z}_{\gamma}\frac{J_{\gamma}I_{K\gamma}}{I_{\gamma}} \\
& -\left(\frac{e\mu_0}{c}\right)\bar{z}_{\gamma,\gamma'}\left[\bar{z}_{KL}\, z_L R_{KL}^{-3}(\vec{R}_K-\vec{R}_L)_{\gamma}\vec{R}_{L\gamma'}\right] g_K \frac{J_{\gamma}I_{K\gamma'}}{I_{\gamma}} \\
& +\left(\frac{e\mu_0}{c}\right)\sum_{\text{all } L \text{ on top}}\bar{z}_{KL}\left[z_L R_{KL}^{-3}(\vec{R}_K-\vec{R}_L)\cdot\vec{R}_L\right] g_K j''\left(\frac{1}{I_a}-\frac{1}{I_c}\right)I_{Kc} \\
& -\left(\frac{e\mu_0}{c}\right)\sum_{\gamma}\bar{z}_{\gamma}\left[\sum_{\text{all } L \text{ on top}} z_L R_{KL}^{-3}(\vec{R}_K-\vec{R}_L)_c\vec{R}_{L\gamma}\right] g_K j''\left(\frac{1}{I_a}-\frac{1}{I_c}\right)I_{K\gamma} \qquad (79) \\
& +\left(\frac{e\mu_0}{c}\right)\sum_{\text{all } L \text{ not on top}}\bar{z}_{KL}\left[z_L R_{KL}^{-3}(\vec{R}_K-\vec{R}_L)\cdot\vec{R}_L\right] g_K\, j''\left(-\frac{1}{I_c}\right)I_{Kc} \\
& -\left(\frac{e\mu_0}{c}\right)\sum_{\gamma}\bar{z}_{\gamma}\left[\sum_{\text{all } L \text{ not on top}}\bar{z}_{KL}\, z_L R_{KL}^{-3}(\vec{R}_K-\vec{R}_L)\vec{R}_{L\gamma}\right] g_K j''\left(-\frac{1}{I_c}\right)I_{K\gamma}
\end{aligned}$$

The second order contribution is calculated from those terms in the Hamiltonian (64) which are off-diagonal in the electronic orbital quantum number. These may be written

$$\mathcal{H}'' = -2\left[AJ_a L_a + BJ_b L_b + CJ_c L_c + F' j'' \ell''\right] + \left(\frac{e\mu_0}{c}\right) \bar{z}_{\kappa i} \left[r_{\kappa i}^{-3} (\vec{r}_i - \vec{r}_\kappa) \times \vec{v}_i\right] \cdot g_\kappa \vec{I}_\kappa \tag{80}$$

The first term consists of the cross-products in the rotational energy and the second term is that part of interaction of the nuclear moments with the electrons which vanish in the first order calculation. In the perturbation calculation we retain only those terms bilinear in I and J.

If, for convenience we define

$$\xi_{\gamma\gamma'} = \left(\frac{e\mu_0}{c}\right) \bar{z}_{\kappa i} \left[r_{\kappa i}^{-3} (\vec{r}_i - \vec{r}_\kappa) \times \vec{v}_i\right]_\gamma \tag{81}$$

the total second-order contribution may be expressed

$$\mathcal{H}'' = (e\mu_0/c) \bar{z}_{\gamma\gamma'} \bar{z}_{n\neq n_0} (E_{n_0} - E_n)^{-1} \left[\langle n_0 | \xi_{\gamma\gamma'} | n \rangle \langle n | L_\gamma | n_0 \rangle + \text{c.c.}\right] g_\kappa \frac{J_\gamma I_\kappa \mu'}{I_\gamma} + \left(\frac{e\mu_0}{c}\right) \bar{z}_{\gamma\gamma'} \bar{z}_{n\neq n_0} (E_{n_0} - E_n)^{-1} \left[\langle n_0 | \xi_{\gamma\gamma'} | n \rangle \langle n | \ell'' | n_0 \rangle + \text{c.c.}\right] g_\kappa j'' \left(\frac{1}{I_a} - \frac{1}{I_c}\right) I_{k\gamma'} \tag{82}$$

The total spin-rotational interaction is the sum of $\mathcal{H}'$ and $\mathcal{H}''$ and in tensor form is

$$\mathcal{H}_{SR} = \vec{I} \cdot \underset{\sim}{M} \cdot \vec{J} + \vec{I} \cdot \underset{\sim}{M}'' \cdot \vec{j}'' \tag{83}$$

where $\underset{\sim}{M}$ and $\underset{\sim}{M}''$ are the coefficients appearing in equations (79) and (82). $\underset{\sim}{M}$ represents the rotational magnetic field per unit total angular momentum and $\underset{\sim}{M}''$ represents the internal rotational magnetic field per unit internal angular momentum of the top relative to the framework. For very high barriers $\vec{\alpha} \to 0$, $j'' \to 0$ and the second term in (83) vanishes leaving the ordinary spin-rotation interaction. Equation (83) may be recast as

$$\mathcal{H}_{SR} = \vec{I} \cdot \underset{\sim}{M} \cdot \vec{J} + r\, \vec{I} \cdot \underset{\sim}{M'} \cdot \vec{j}'' \tag{84}$$

where the constant r is defined in equation (59a):

$$r = 1 - I_\alpha / I_c \tag{85}$$

From (59a) and the definition of j" in (62)

$$j'' r = j' = j - \frac{I_\alpha}{I_c} J_c \tag{86}$$

in which j is the <u>total</u> angular momentum of the internal top. In terms of $\vec{j}$ the Hamiltonian (84) becomes

$$\mathcal{H}_{SR} = \vec{I} \cdot \underset{\sim}{M} \cdot \vec{J} - M' \left(\frac{I_\alpha}{I_c} \right) J_c + M' \vec{I} \cdot \vec{j} \tag{87}$$

<u>4. Spin-Internal-Rotation Matrix Elements.</u>

The matrix elements of the ordinary spin-rotation Hamiltonian are given for one, two and three spins in Appendix C. In Section 3 it was shown that the spin-internal-rotation Hamiltonian contains terms of the form

$$\mathcal{H}_{SIR} \sim M' j I_c \tag{88}$$

where j is the <u>total</u> angular momentum operator for the internal top whose axis of rotation is along the c-principal axis of the molecule and I_c is the c-component of the nuclear spin angular momentum of the nucleus of interest located on the top. The matrix element of I_c in the $|j J \tau M\rangle$ scheme (in which the rotational energy, including internal, is diagonal) is, as shown in Appendix C,

$$\langle j J \tau | I_c | j J \tau \rangle = \frac{1}{J(J+1)} \langle j J \tau | \vec{I} \cdot \vec{J} | j J \tau \rangle \langle j J \tau | J_c | j J \tau \rangle \tag{89}$$

From equation (88) we then write

$$\langle j J\tau | \mathcal{H}_{SIR} | j J\tau \rangle = M' \theta(I,J) \langle j J\tau | j J_c | j J\tau \rangle \qquad (90)$$

where $$\theta(I,J) = ((J)(J+1) - F(F+1) + I(I+1))/2J(J+1) \qquad (91)$$

But $\vec{j}$ commutes with $\vec{J}$ and for very low barriers it commutes with the total Hamiltonian. This allows equation (90) to be reduced to

$$\langle j J\tau | \mathcal{H}_{SIR} | j J\tau \rangle = m M' \theta(I,J) \langle j J\tau | J_c | j J\tau \rangle \qquad (92)$$

where m is the eigenvalue of $\vec{j}$. In the high field limit:

$$\langle \mathcal{H}_{SIR} \rangle = m m_I m_J M' \langle j J\tau | J_c | j J\tau \rangle \qquad (93)$$

The matrix $\langle J_c \rangle$ which vanishes ordinarily for rigid asymmetric rotors will not necessarily be zero when internal rotation is present. This point is discussed further in Appendix B. The matrix elements involving more than one spin on the internal top are found by the methods given in Appendix C.

For the case of non-vanishing barriers $\vec{j}$ is no longer a constant of the motion since

$$[j, V] \neq 0$$

and the step from (90) to (92) is not valid. In that event the product matrix element $\langle j J_c \rangle$ must be evaluated.

D. EXPERIMENTAL.

1. Introduction

Magnetic resonance experiments may be broadly classified as either pulsed or continuous wave. With respect to the nuclear or electronic spin system under study these two methods yield information analogous to the transient and steady-state responses of an electrical or mechanical device. The two types of experiments are complementary. While continuous wave (CW) equipment is usually employed for energy level determinations, pulsed spectrometers are used for relaxation time measurements. In a CW experiment the spin-containing nuclei are immersed in a magnetic field and in a resonant coil of a radio-frequency radiation source. Either the intensity of the magnetic field or the frequency of the radiation is varied until the spin-system absorbs power from the r.f. source. This is an NMR signal and it corresponds to a transition between spin states of the system in the coil. Instead of continuous irradiation throughout a resonance, in a pulsed experiment intense bursts of r.f. power are applied to the sample. The r.f. is the Larmor frequency and these pulses, on a time scale,

are short compared to the pertinent spin-relaxation times, T_1 and T_2, of the system. The various transient signals observed following the pulses are used to measure T_1 the spin-lattice or longitudinal relaxation time, T_2 the spin-spin or transverse relaxation time and T_2 the free-induction or Bloch decay time. Special sequences of such pulses can also be employed to determine D, the self-diffusion coefficient of pure liquids or gases, J and δ, the spin-spin coupling constant and chemical shift, exchange rates, conformer interconversion rates, line shape moments, and other quantities of interest to those in the field.

The advantage of pulsed NMR over CW are that high magnet resolution and stability are usually not required; J can often be measured with higher accuracy; phenomena such as proton exchange behave differently in such experiments; and, most important, relaxation times are determined in a straightforward manner. Disadvantages include the increased difficulty in interpreting experiments on systems containing several J, δ, or relaxation time values, and the unavailability (until recently) of commercial spectrometers.

2. The Rotating Coordinate Frame.

Since magnetic resonance problems in general and

transient NMR in particular are greatly simplified when viewed in a rotating coordinate system (32), a brief description of this transformation will be given before we discuss the types of pulsed experiments. The results are the same whether we approach the argument on classical or quantum mechanical terms.

In a stationary coordinate system the equation of motion of the nuclear magnetic moment is classically,

$$\hbar \, d\vec{I}/dt = \vec{\mu} \times \vec{H} = \gamma \hbar \vec{I} \times \vec{H} \tag{94}$$

If we define $\partial/\partial t$ as differentiation with respect to a coordinate system rotating with angular velocity $\vec{\omega}$, then

$$\hbar \frac{d\vec{I}}{dt} = \vec{\mu} \times \vec{H} = \frac{\partial \vec{I}}{\partial t} + \vec{\omega} \times \vec{I} \tag{95}$$

Here $\partial \vec{I}/\partial t$ is how an observer rotating at ω would see $\vec{I}$ to develop in time. Equation (95) can be rewritten

$$\hbar \frac{\partial \vec{I}}{\partial t} = \gamma \hbar \vec{I} \times (\vec{H} + \vec{\omega}/\gamma) = \gamma \hbar \vec{I} \times \vec{H}_{eff} \tag{96}$$

where $\vec{H}_{eff}$ is the effective field seen in the rotating coordinate system. Under convential experimental conditions there exists a large constant magnetic field $\vec{H}_o$ with a weaker field $\vec{H}_1$ rotating perpendicular to it with angular velocity $-\omega$. The axes of the rotating coordinate system are then chosen such that $\vec{H}_o = H_o\vec{k}$, and $\vec{H}_1 = H_1\vec{i}$, and $\vec{\omega} = -\omega\vec{k}$. Then the effective field is

$$\vec{H}_{eff} = \left(\vec{H} + \frac{\vec{\omega}}{\gamma}\right) = \left[H_0 - \frac{\omega}{\gamma}\right]\vec{k} + \vec{H}_1 \tag{97}$$

The magnitude of the effective field is

$$\begin{aligned} |H_{eff}| &= \left[\left(H_0 - \frac{\omega}{\gamma}\right)^2 + H_1^2\right]^{1/2} \\ &= \gamma^{-1}\left[(\omega-\omega_0)^2 + \left(\omega_0 H_1/H_0\right)^2\right]^{1/2} \\ &= \gamma^{-1} a \end{aligned} \tag{98}$$

The angle between $\vec{H}$eff and $\vec{H}_0$ is

$$\theta = \cos^{-1}\left(\frac{\omega_0-\omega}{\omega}\right) = \sin^{-1}\left(\omega_0 \frac{H_1}{H_0}/a\right) \tag{99}$$

We now observe that when $\omega=\omega_0$, $\theta=\pi/2$ and a magnetic moment initially parallel to $\vec{H}_0$ can process about $\vec{H}$eff = $\vec{H}_1$ until it is antiparallel to $\vec{H}_0$. Under these circumstances $\vec{H}_0$ does not appear in the rotating frame and the motion of the magnetization is determined by the magnitude of $\vec{H}_1$. This feature renders the interpretation of transient experiments especially easy. Notice also that by going next to a second rotating coordinate system which rotates about $\vec{H}_{eff}$ the effective field in the second system $\vec{H}_{eff}$, can be reduced to zero. There being no effective field in the doubly rotating frame, the state of this system remains constant in time.

Equation (96) can also be obtained relative to the stationary coordinate system. Here,

$$i\hbar\dot{\Psi} = \mathcal{H}\Psi \tag{100}$$

where for our problem

$$\mathcal{H} = -\gamma\hbar\,\vec{I}\cdot\vec{H} \tag{101}$$

The transformation to the rotating coordinate system requires the substitutions

$$\Psi = e^{-i\vec{\omega}\cdot\vec{I}t}\,\Psi_R \tag{102}$$

and

$$\vec{I}\cdot\vec{H}_R = e^{i\vec{\omega}\cdot\vec{I}t}\,\vec{I}\cdot\vec{H}\,e^{-i\vec{\omega}\cdot\vec{I}t} \tag{103}$$

If these substitutions are made in Equation (100) there results

$$\begin{aligned} i\hbar\dot{\Psi}_R &= -\gamma\hbar\,\vec{I}\cdot\vec{H}_{eff}\,\Psi_R \\ &= -\gamma\hbar\,\vec{I}\cdot(\vec{H}_R + \vec{\omega}/\gamma)\Psi_R \end{aligned} \tag{104}$$

as before.

3. Pulsed Magnetic Resonance (33,34,35).

a. Transient Experiments.

If a sample of spin containing nuclei are in a constant magnetic field $\vec{H}_o$, at thermal equilibrium a net magnetization M_o will exist in the sample with $\vec{M}_o = x_o\vec{H}_o$, x_o being the static magnetic susceptibility. In the laboratory frame the individual spins which make up the sample precess about $\vec{H}_o$ with Larmor angular frequency ω_o and although each spin generates a cone in its motion, the random phases cause the ensemble average to be a stationary vector along $\vec{H}_o$.

In a real experiment, however, there will exist in the

sample a distribution of the value of the local fields seen by the nuclei in different locations. This can be due to magnet inhomogeneities over the volume of the sample, as is the usual case in liquids, or it can be due to a dipolar line width as in solids. The distribution in fields results in a distribution of Larmor frequencies, $\Delta\omega$, over the sample and is responsible for the shape of the free induction or Bloch decay, with its characteristic time constant T_2^*.

b. Free-Induction or Bloch Decay, T_2^*.

If a nuclear spin system is in internal thermal equilibrium in a magnetic field H_o and a (smaller) radio-frequency field perpendicular to H_o and of magnitude H_1 is applied precisely at the appropriate Larmor frequency ($\omega_0 = \gamma H_0$) the effective field in the rotating coordinate system is $\vec{H}_1$ and the magnetic moment $\vec{M}_o$ initially parallel to $\vec{H}_o$ will begin to precess in the y'-z plane (where the prime denotes rotating coordinates) of Figure 1a. The frequency of this precession will be $\omega_1 = \gamma H_1$. If the r.f. field is allowed to remain "on" a time t_w the moment $\vec{M}_o$ will precess through an angle $\phi = \gamma H_1 t_w$ (1b). The length of the vector $\vec{M}_o$ will be the same as it was before the field was turned on provided the condition $t_w \ll T_1, T_2, T_2^*$ is met.

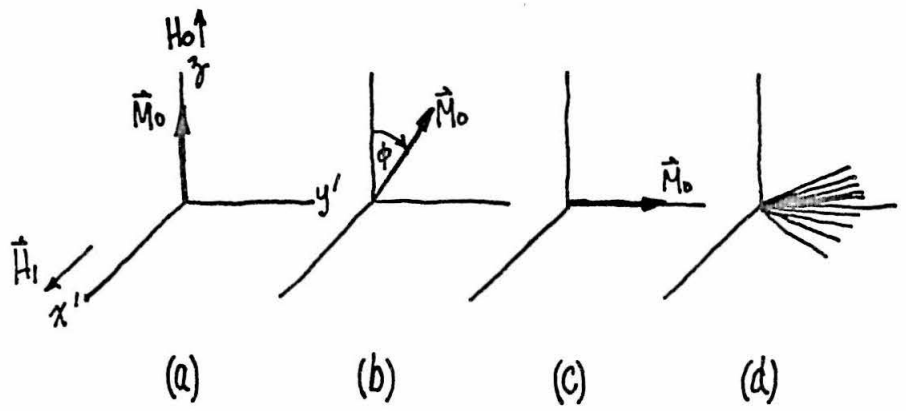

FIGURE 1. 90° PULSE AND BLOCH DECAY.

The two important pulses are the 90 and 180 degree, that is, $\phi = \frac{\pi}{2}$ and π radians respectively. At the end of a 90 degree pulse M_o will be oriented along the y' axis (1c). At this point it is important to recall the component vectors in $\vec{M}_o$ actually span a frequency range about $\omega_o, \Delta\omega$. In the absence of this spread M_o would appear stationary (in the absence also of relaxation processes) and induce a constant r.f. voltage in a receiver coil oriented along y'. But in the presence of this distribution the <u>isochromats</u> comprising $\vec{M}_o$ begin to fan out in the x'-y' plane; those seeing higher (lower) fields than H_o will lead (lag) the y' axis, and in time T_2^*, the free-induction of Bloch decay time, the value of the signal seen in the receiver coil will be reduced by a

factor 1/e. No free-induction decay signal is seen following a 180 degree pulse. T_2^* may also be looked at as the characteristic time required for the macroscopic precessing magnetic moment to have its component vectors lose phase coherency and is therefore often referred to as the spin-phase memory time.

c. Spin-Lattice or Longitudinal Relaxation, T_1.

From the above discussion it is apparent that the maximum amplitude of the Bloch decay signal following a 90 degree pulse is proportional to the magnetization which existed along the z-axis just before the pulse. This feature can be employed to determine T_1, the spin-lattice relaxation time. A 180 degree pulse is applied to a sample at thermal equilbrium inverting the magnetization and giving it the value $Mz = -M_o$ (Figure 2a). If now

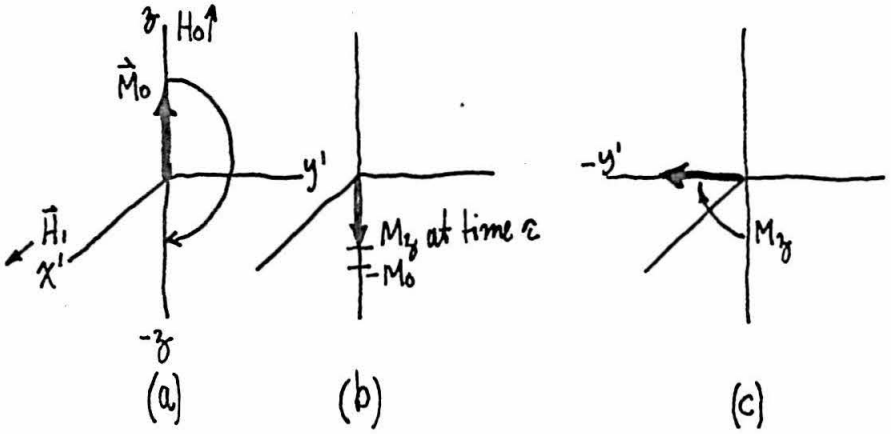

FIGURE 2. MEASUREMENT OF Mz(t) WITH A 180°-90° PULSE PAIR.

some time interval τ is allowed to elapse, the value of the magnetization along the z-axis will change to $Mz > -M_o$ (2b). A 90 degree pulse at this instant will rotate Mz into the -y' axis and a Bloch decay whose signal amplitude is a measure of Mz(t) will be observed (2c). The sample is now allowed to re-equilibrate in several T_1's and the 180-90^o pulse sequence repeated with a different value of τ . If the maximum decay following the 90 degree pulse in several such experiments, wherein τ assumes values from less than T_1 to greater than T_1, is plotted as a function of τ the curve appears as in Figure 3. The time required for the magnetization to go from the value $Mz = -M_o$ to $Mz = 0$ is τ_{NULL} . For this value of τ no free-induction tail is seen following the 90 degree pulse and we have $T_1 = \tau_{NULL} / \ln 2$.

d. Spin-Spin or Transverse Relaxation, T_2.

In pulsed NMR determinations of T_2, the time constant for the decay of the magnetization on the x'-y' plane, are made with the aid of the spin-echo. A spin-echo is formed by first applying a 90 degree pulse establishing a non-equilibrium magnetization along the y'-axis (Figure 4a). In a time greater than the free-induction life the spin isochromats will be uniformly distributed in the x'-y'

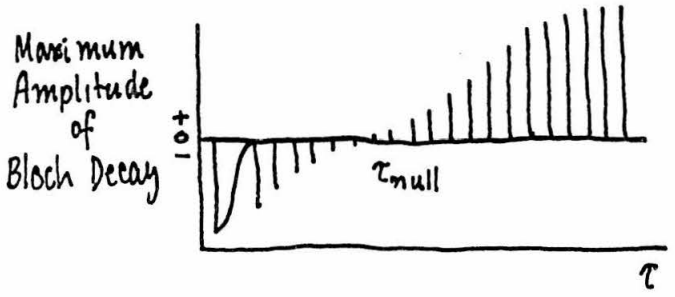

FIGURE 3. T_1 MEASUREMENT BY 180°-90° PULSE PAIR SEQUENCE.

plane (4b,c). If at time $\tau (T_2 > \tau > T_2^*)$ a 180 degree pulse is applied to the system the "pancake" of magnetization will be rotated about the x'-axis resulting in the slower isochromats

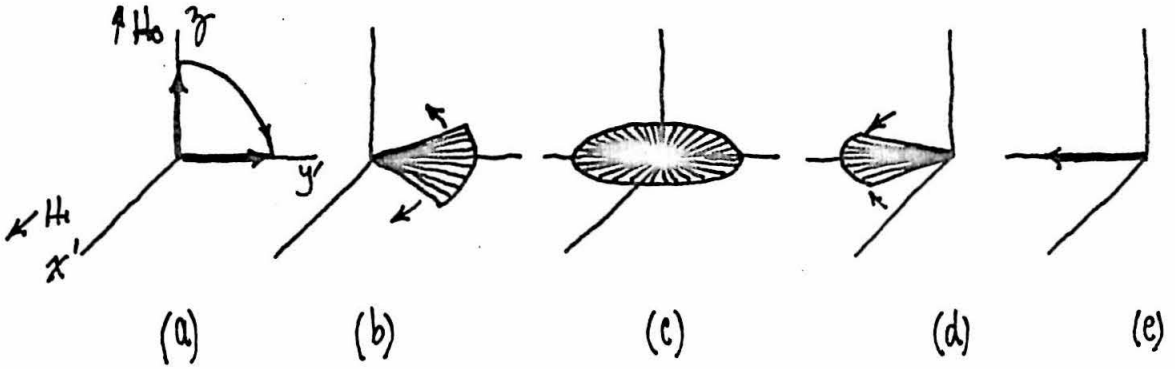

FIGURE 4. FORMATION OF SPIN-ECHO BY 90°-180° PULSE PAIR.

getting ahead of the faster ones (4d) and since the direction of precession is maintained a refocussing occurs at time 2τ. The sequence of events as seen by the receiver coil (demodulated) is shown in Figure 5.

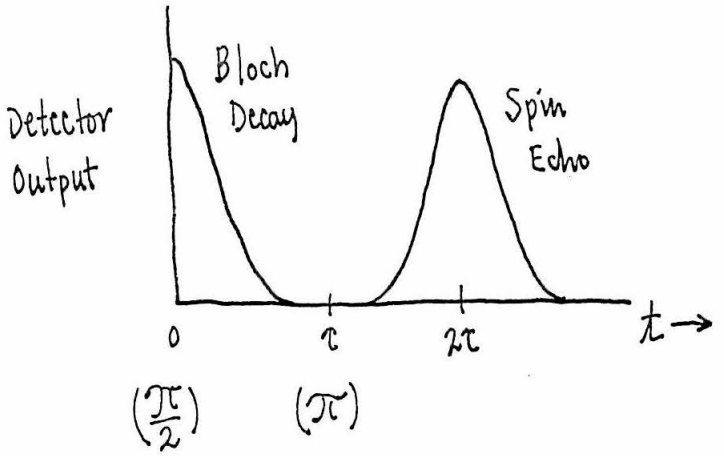

FIGURE 5. FORMATION OF SPIN-ECHO.

The effect of the 180 degree pulse, then, is to integrate the magnetization in the x'-y' plane, that is only those spin isochromats still remaining in the plane. At the instant the echo is formed the status of events is identical to that following a 90 degree pulse, and after the echo reaches its maximum, the regrouped isochromats fan out once again, causing the echo to appear as two Bloch decays back-to-back. No further echoes are expected. If, however, another 180 degree pulse is applied to the system at, say, 3τ (the first echo being formed at 2τ), another echo will be seen at 4τ . Due to the decay of the overall magnetization in the plane, it is apparent that the amplitude of the first echo will be less than that of the first Bloch decay, and the second echo will be less than that of the first echo, etc. By forming several echoes (applying

several 180 degree pulses) we get a picture of the time evolution of the integrated magnetization in the x'-y' plane. For liquids where the Bloch equations have been found to hold, the echo envelope is exponential and provides the value of T_2. In the event that the envelope is not exponential, the inclusion of a diffusion term, describing the diffusion of the spin containing molecule through the magnet inhomogeneities, provides agreement between theory and experiment.

Spin echoes can also be formed after the successive application of two 90 degree pulses. In fact, the first echoes to be observed were so generated. These echoes are not as easily visualized as the 90-180 ones.

The Bloch decay time, T_2^*, and the spin-spin relaxation time, T_2, are measures of different phenomena. The former is due to the distribution of local fields throughout the sample. This is responsible for the finite spectrum of Larmor precession frequencies (each member of this spectrum is an <u>isochromat</u>) and hence the dephasing following a 90° pulse. The transverse relaxation time, T_2, is the decay constant of the <u>integrated</u> magnetization in the x-y plane. It is a measure of the rate at which the individual isochromats in the x-y plane are reduced in amplitude.

4. The Pulsed NMR Spectrometer.

If conventional CW NMR spectrometers are designed primarily for energy level resolution, pulsed spectrometers are concerned with time resolution. In the former, r.f. oscillator and D.C. magnetic field stability are the main technical problems, whereas high power pulse production and receiver overload prevention plague the latter. Pulsed spectrometers, like CW equipment, consist mainly of transmitter and receiver circuitry and a magnet. In addition they have timing and pulse instrumentation. Since the time required to produce a 90 or 180 degree pulse will be inversely proportional to the magnitude of the r.f. field and since it is necessary for t_w to be less than T_1 or T_2 it is desirable to employ relatively large values of H_1. In transient experiments H_1 is typically 20-60 gauss, producing 90 degree pulses for protons in 3-1 microseconds. This is to be compared with CW experiments where H_1 is normally less than one gauss. It is also of interest to investigate (or sample) the spin system as soon as possible after the application of the r.f. pulse which demands that the receiver and demodulator circuits be able to recover quickly from large overloads to which they are subject during the pulse. The timing circuitry must produce

accurate and stable pulse sequences of the types described above. All these features have been accomplished in a r.f. phase coherent spectrometer recently completed in this laboratory. The general layout of this instrument is given in Figure 6. The purpose and features of its components are as follows.

a. Basic Clock.

Although we have previously discussed an experiment as a particular sequence of events (90,180,echo,90,180,echo, etc; or 180,90,180,90, etc.) it is standard operating procedure to repeat the full sequence so the entire echo or Bloch decay envelop may be viewed continuously on a scope while critical adjustments are made. Another reason for wanting to repeat the experiment is to take advantage of signal averaging electronics such as Box-Car integrators or integrating digital voltmeters. Basic Clock in this spectrometer is a Hewlett-Packard Model 202A Low Frequency Function Generator operating in the square wave mode.

b. Pulse Sequence Unit, T_1 Experiment.

When the square wave from the clock goes positive, a sawtooth generator (Tektronix Type 162 Waveform Generator) is triggered causing it to send (a) a positive trigger to the first of three identical pulse generators (all Tektronix

FIGURE 6. General layout of the pulsed nuclear magnetic resonance spectrometer.

LAYOUT OF PULSED NMR SPECTROMETER

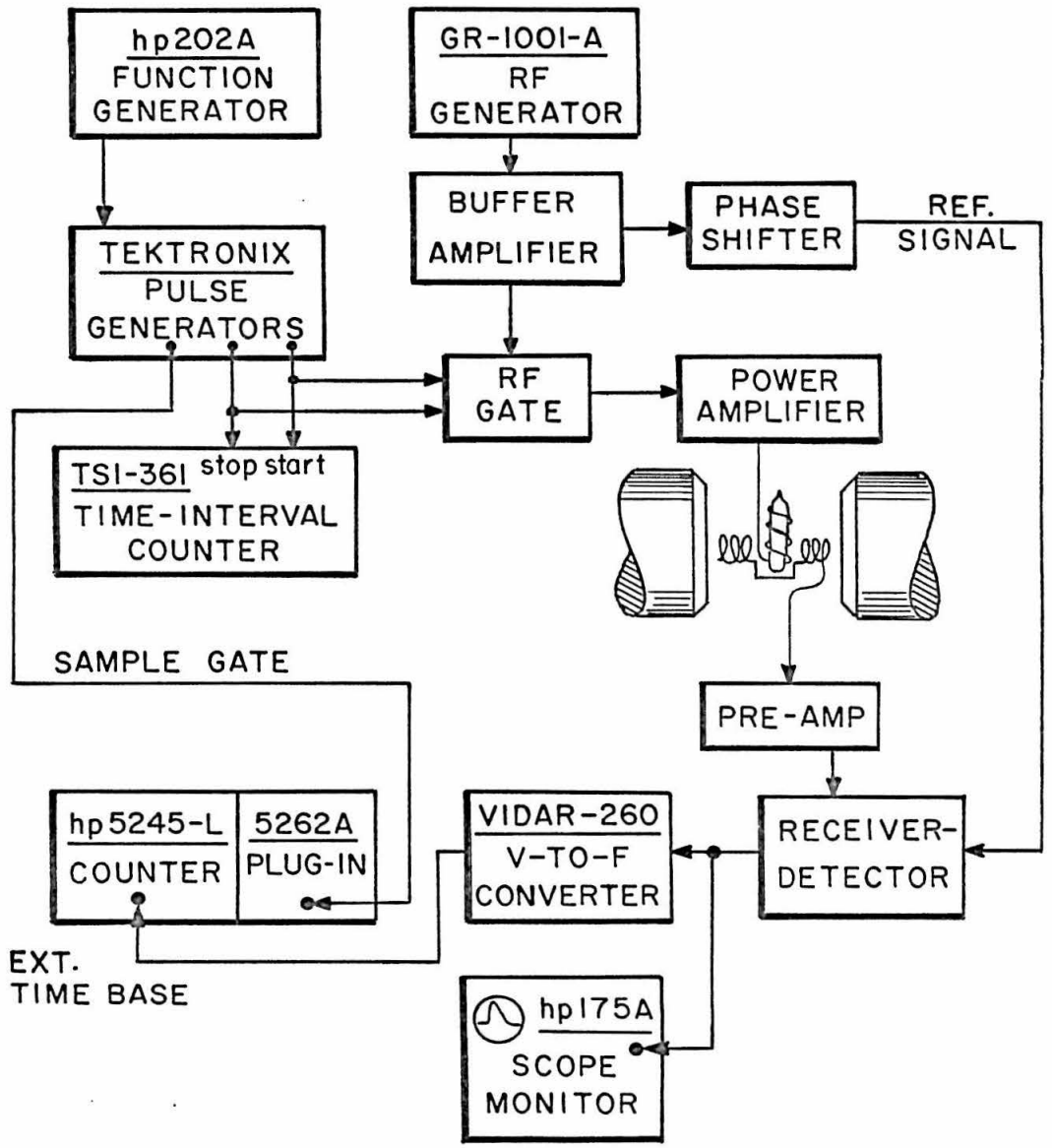

Type 163) and (b) a negative going sawtooth to the second pulse generator. Upon receiving the positive trigger, the first pulse generator immediately produces for the r.f. gate, a control pulse whose width is adjusted to be the 180^{o} pulse. The second pulse generator similarly fires a 90^{o} control pulse when the negative going sawtooth from the 162 reaches some preset value. This delay between the 180^{o} and 90^{o} pulses is adjustable on the second 163. At the same time it produces the 90^{o} pulse it also triggers the third 163 which in turn sends a gating pulse of about three milliseconds to the hp 5245L counter. The counter, operating in conjunction with a voltage-to-frequency converter in a manner to be described below, is used to measure the amplitude of the Bloch decay. The 180^{o}-90^{o} pulse interval is measured digitally by a general purpose counter (Transistor Specialties, Inc., Model 361-R, Mod.26) whose start-stop controls are in parallel with the 180^{o} and 90^{o} r.f. gates.

c. RF Gates.

In the presence of a positive control pulse, the RF gate (Figure 7; designed by J. Owen Maloy, Senior Research Fellow in Physics) allows r.f. from the General Radio Standard Signal Generator Model 1001-A to pass through the

first stage (7077) of the transmitter and to be amplified to levels suitable for our experiments. In the absence of a pulse the cathode of the 7077, operating as a grounded grid amplifier, is biased positive and passes essentially nothing. A positive (~20V) control pulse turns on the 2N2714 causing the 7077 d.c. cathode potential to drop to a few volts negative which allows this tube to conduct. The carrier suppression is of the order of 10^9 or 180 db. The switch in the gate is a 2N2714 giving a r.f. pulse having rise and fall times of about 200 ns as seen on the plate of the 7077.

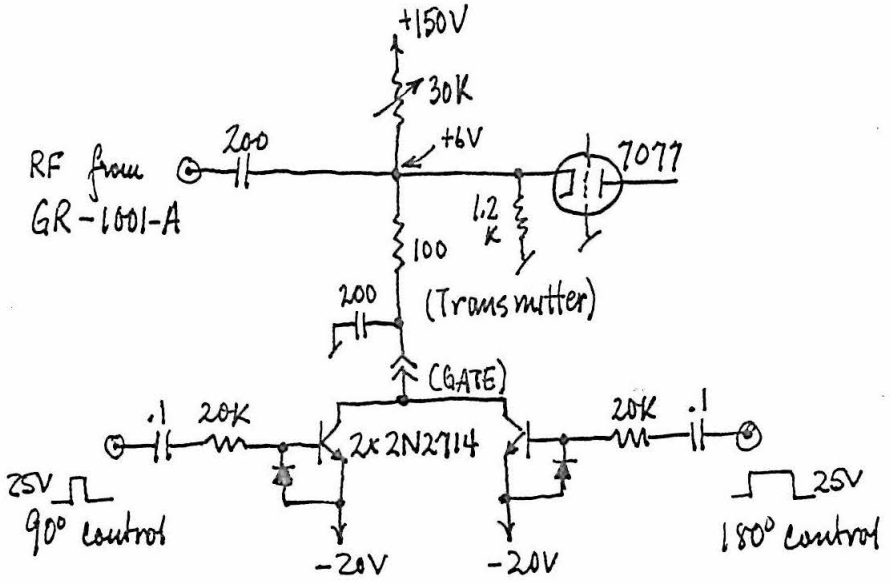

FIGURE 7. RADIO-FREQUENCY GATE.

d. Power Amplifier (Transmitter).

The power amplifier is the design of W.G. Clark (36) and has been constructed by Mr. C. Jewett. It is tunable from 2 to 35 Mc/s and has a pulsed power output of 5 kilowatts yielding a 1200 volt r.f. burst on a Varian wide-line probe at 9 MHz. Our work with this unit shows that a 90 degree pulse for protons is about 3 to 5 microseconds.

The transmitter is powered by five separate supplies of +3000V, +800V, ±150V, and 6V A,DC. The supply system is completely interlocked to turn on sequentially and to turn off the proper high voltage units in the event of component failure.

e. Coils.

The receiver and transmitter coils are those in the Varian 8-16 MHz, wide-line NMR probe with the transmitter coil filtering circuit bypassed by connecting the pin of the UHF connector directly to the transmitter coil. The probe was operated with its aluminum top removed. It was also found necessary to "glyptal" the solder connections to keep them from arcing to the aluminum body of the probe. The

probe is a crossed-coil design having about 40 db isolation between the transmitter and receiver sides. Thus the problem of the transmitter pulse saturating or even damaging the receiver r.f. stages is simplified. Even with the crossed coils, however, about 10V r.f. appears on the receiver coil during a transmitter pulse. This is responsible for about a 25 microsecond blocking or dead time in the receiver which is normally expecting signals in the millivolt to microvolt region. For our measurements in liquids for which the characteristic time constants are $T_2^* \sim 2ms$ and $T_1 \gtrsim 1$ sec. this blocking was not a cause for concern. The working coil diameter is about 17 mm.

f. Preamplifier and Receiver.

Both the preamplifier and receiver designs are those of W.G. Clark (36). The preamplifier was constructed by the author and the receiver by Mr.T.E. Burke. The performance of the transmitter, receiver, and preamplifier is essentially as described by Clark. The reference signal for r.f. phase coherent operation of the receiver is phase shifted by a buffered, variable delay line also constructed by Mr. Burke.

g. Voltage-to-Frequency Converter and Gated Counter.

During the course of this work different methods were

tried for measuring the amplitudes of the Bloch decays. A boxcar integrator (36) (sample, hold and integrate) as well as a slow sawtooth (37) generator for automatic sequencing were constructed by the author. For measuring relaxation curves it was found that this method was only useful for relatively short T_1's ($\lesssim$ 100 ms) and even then one had difficulty in accurately calibrating the time base. We also experimented with a 400 channel "Computer of Average Transients" by gating its input amplifiers and operating in a stepped address advance mode. This method suffered, as did the box car also, from rather large uncertainties in the $M_z = 0$ line, knowledge of which is important for the analysis of the data. In addition, both of these methods yielded relaxation curves which were unexplainably non-exponential for samples (Fe^{+3} doped water) known to have exponential behavior.

The combination of a voltage-to-frequency converter and a externally gatable digital counter was used to obtain all the experimental results in this thesis. The demodulated output of the receiver is converted to an FM signal by a bipolar, Vidar 1 MH_z, V-F converter. The FM signal is then used as a (non-linear) external time-base for a Hewlett-Packard 5245L counter containing a 5262A Time-

Interval plug-in. The start-stop controls of the plug-in are set to trigger on the positive and negative slopes, respectively, of a common signal, namely the gating pulse from the third Tektronix pulser mentioned before. The width of the gating pulse is usually of the order of T_2^*. Thus, both the time interval and amplitude are measured digitally.

5. Analysis of Relaxation Data.

In a typical run T_1 was determined by varying τ, the 180°-90° pulse separation in small increments compared with T_1 until the amplitude of the Bloch decay was a minimum and then $T_1 = \tau_0 / \ln 2$. Ordinarily about five determinations of the Bloch amplitude were averaged for each value of τ. Relaxation curves were calculated for a few compounds and typical results, those for benzotrifluoride and m-hydroxybenzotrifluoride are shown in Figure 8 and 9. The uncertainty of a T_1 determination by the null-method is about $\pm 5\%$ for the neat (undiluted) samples and slightly higher for the diluted ones where the measurements are made much more difficult by the combination of weaker signals and longer relaxation times.

During the preparation of this thesis the author wrote a computer program to fit the relaxation data to an

FIGURE 8. Relaxation curve for benzotrifluoride.

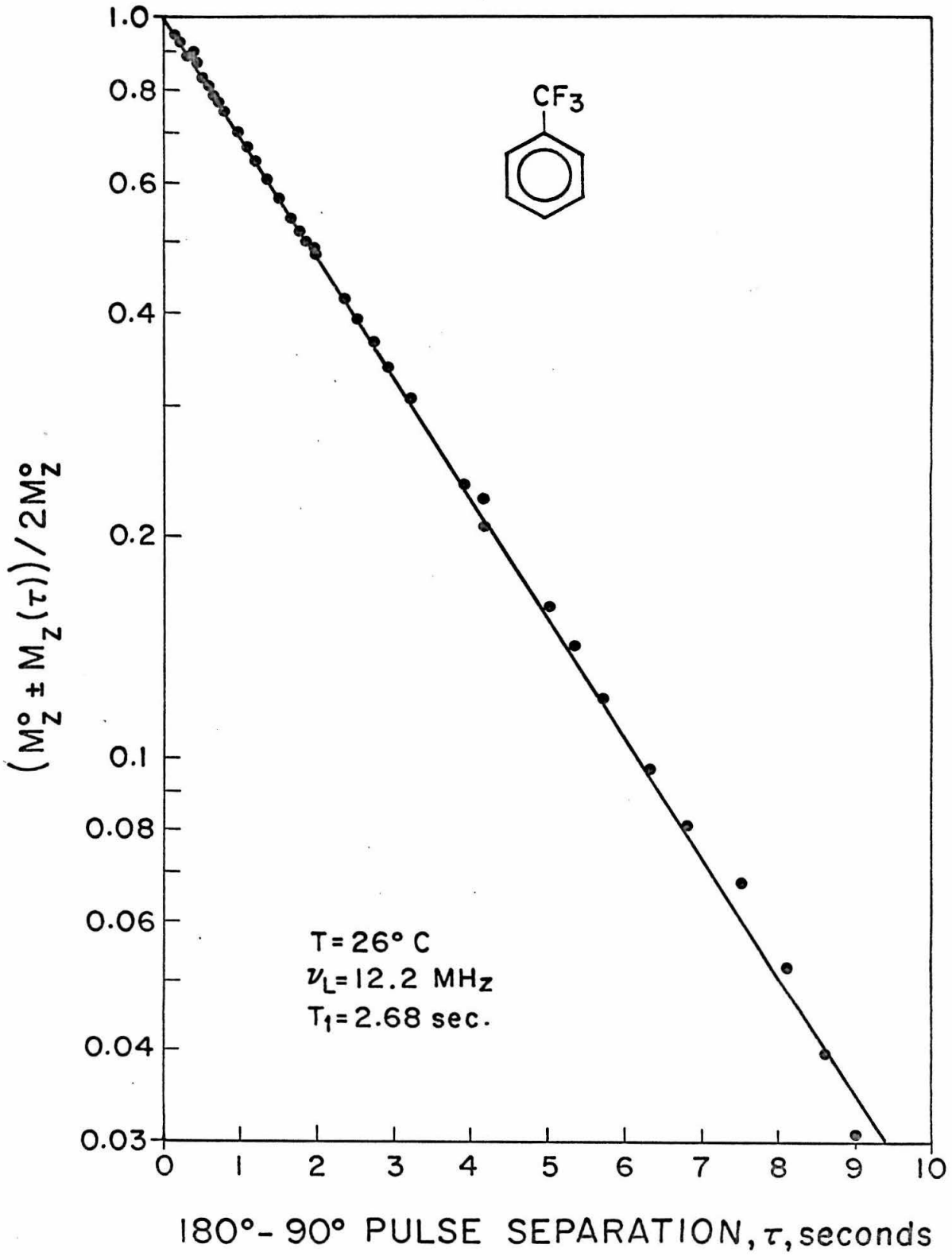
1.0
0.8
0.6
0.4
0.2
0.1
0.08
0.06
0.04
0.03
$(M_z^\circ \pm M_z(\tau))/2M_z^\circ$
CF_3
T = 26° C
ν_L = 12.2 MHz
T_1 = 2.68 sec.
0
1
2
3
4
5
6
7
8
9
10
180°- 90° PULSE SEPARATION, τ, seconds

FIGURE 9. Relaxation curve for meta-hydroxybenzotrifluoride.

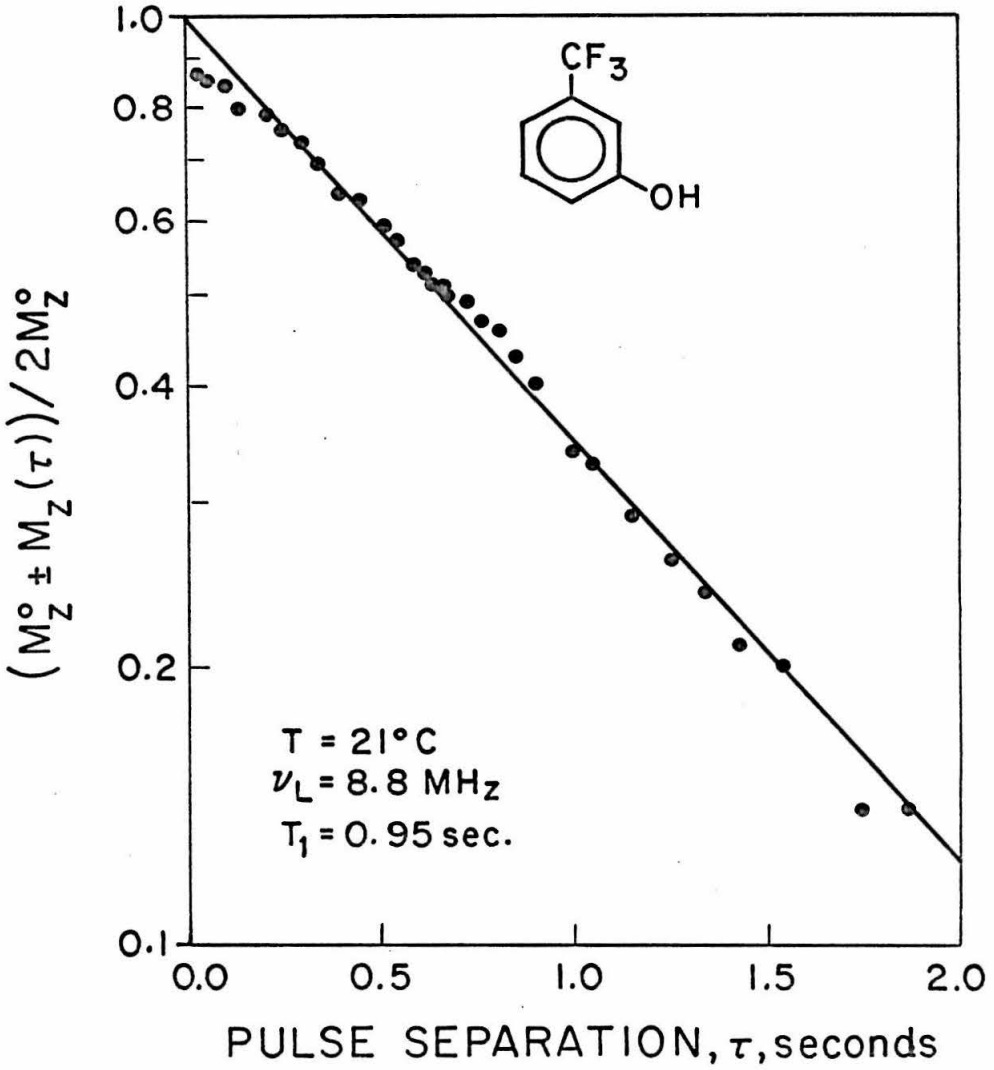
1.0
0.8
0.6
0.4
0.2
0.1
0.0
0.5
1.0
1.5
2.0
$(M_z^\circ \pm M_z(\tau))/2M_z^\circ$
PULSE SEPARATION, τ, seconds
CF_3
OH
T = 21°C
ν_L = 8.8 MHz
T_1 = 0.95 sec.

exponential by the least-squares method. This has been employed extensively by Mr. Burke with a resulting improvement in the accuracy ($\sim\pm 2\%$) of T_1 data now being taken on the spectrometer.

The spectrometer was checked out by measuring several compounds whose relaxation times are in the literature. The proton relaxation in ferric ion doped water as a function of (Fe^{+3}) was determined (38) and found to agree with the known values. Similarly protons in benzene and F^{19} in fluorobenzene yielded T_1's (18 and 12 seconds, respectively, at 21°C) agreement with the literature values. After our experiments were in progress, a temperature study on F^{19} T_1 in benzotrifluoride came to our attention (16). The value of T_1 that these authors obtain at about 20°C is in agreement with our value.

E. RESULTS.

1. Introduction.

We have studied the F^{19} nuclear spin lattice relaxation in benzotrifluoride (α,α,α -trifluorotoluene) and several chemically substituted benzotrifluorides, particularly the halosubstituted ones. These compounds have

been studied both neat and in solution. We will also discuss experiments performed on the amino, hydroxy, and certain di-substituted compounds. In addition, results of experiments on benzyl fluoride (ϕ-CH_2F) will be given to support arguments to be presented on the nature of the dominant relaxation mechanism in the benzotrifluorides. Unless otherwise indicated all measurements were at $\nu = 8.8\ MHz$ and 21°C using a 180°-90° pulse sequence.

Bloch's equation for the longitudinal magnetization may be written

$$\frac{M_z^0 - M_z(t)}{M_z^0 - M_z(0)} = e^{-t/T_1} \tag{105}$$

in which $M_z(t)$, $M_z(0)$ and M_z^0 are the values of the magnetization at time t, time 0, and at thermal equilibrium respectively. In measuring T_1's by a 180°-90° pulse sequence the initial conditions are

$$M_z^0 = -M_z(0) \tag{106}$$

Since with the present experimental configuration we measure only $|M_z(t)|$, in plotting the relaxation curve the ordinate is computed as

$$(M_z^0 \pm M_z(t))/2M_z^0 \tag{107}$$

where the upper sign is used for $t < \tau_0$ and the lower for $t > \tau_0$ and τ_0 is taken as the value of t for which

$|M_z(t)|$ is a minimum.

2. Preparation of Samples.

All the benzotrifluorides used in these experiments were obtained from the commercial suppliers: Pierce Chemical Co., Rockford, Illinois; Aldrich Chemical Co., Milwaukee, Wisconsin; and J.T. Baker Chemical Co., Phillipsburg, New Jersey. The benzotrifluoride was dried and distilled before it was used, but all the other compounds were used as received. The carbon disulfide and other solvents used for the dilution studies were of reagent grade.

Since dissolved (paramagnetic) oxygen is known to promote nuclear spin relaxation by the electron spin-nuclear spin dipolar interaction all samples were outgassed by several freeze-pump-thaw cycles and then sealed under vacuum. The freezing was accomplished with liquid nitrogen. The sample tubes were Pyrex, 17 mm. O.D. and typically $4\frac{1}{2}$" in length when sealed off.

3. Benzotrifluoride.

The spin-lattice relaxation curve for benzotrifluoride has been carefully measured for a time period of five half-lives and has been found to be exponential. Each point in the relaxation curve Figure 9 is an average of five

determinations. The relaxation time for benzotrifluoride determined either from the slope of the relaxation curve or from τ_o /ln2, where τ_o is the pulse separation for $M_z(t) = 0$, is 2.68 seconds at 26°C and 8.8 MH_z T_1 was found to be 2.61 seconds. The difference between these values is well within the reproducibility (±5%) of the experiment at a given temperature and frequency and hence these two values can be considered equal. The expected effect of dissolved oxygen on T_1 was verified by measuring the relaxation time of a sample which had not been outgassed. The result was $T_1 = 1.16 \pm 0.04$ seconds.

In order to determine to what extent the relaxation in benzotrifluoride is determined (a) by intermolecular and (b) by intramolecular interaction T_1 was measured for samples dissolved in various solvents. The results of such experiments are interpreted with the relation

$$T_{1,TOTAL}^{-1} = T_{1,INTRA}^{-1} + \alpha T_{1,INTER}^{-1} + (1-\alpha)(T_{1,INTER}^{-1}) \quad (108)$$

where α is the mole fraction solute and $(T_{1,INTER}^{-1})'$ is the intermolecular T_1 contribution produced by the solvent on the subject nuclei.

First, toluene was chosen as a solvent for its geometric similarity to benzotrifluoride. Although solutions in toluene will have reduced intramolecular fluorine-

fluorine dipolar interactions, they will have fluorine-hydrogen dipolar interactions at least as large as the pure sample, if not larger. A one-to-one by volume solution of ϕCF_3 in toluene yielded a T_1 of 2.7 seconds. Within experimental error, identical results were obtained for one-to-one by volume solutions of benzotrifluoride in ortho-xylene, para-xylene and mesitylene. These results indicate that either (a) the methyl protons have about the same contribution to intermolecular dipolar relaxation as fluorined they "replace" or (b) the contribution of the intermolecular fluorine-fluorine dipolar relaxation to the total relaxation time is small compared to the sum of intramolecular contributions. An intermolecular relaxation time greater than about 10 seconds would account for such behavior. Solutions of benzotrifluoride in carbon disulfide and bromoform were also prepared and investigated. Carbon disulfide is often used in studies such as these due to the facts that C^{12} and S^{32} have nuclear spins 0 and C^{13} ($I = \frac{1}{2}$) and S^{33} ($I = 3/2$) have natural abundances of 1.6% and 0.22% respectively. Hence, it is a "magnetically dilute" solvent and can induce no intermolecular relaxation on its own part. There exists a considerable literature on proton relaxation in carbon disulfide solutions of organic

compounds.) The T_1 results for ϕCF_3 in CS_2 are shown in Figure 10. If we take the extrapolated value at infinite dilution to be approximately equal to T_1,intra we have for benzotrifluoride

T_1,total (neat) = 2.6; T_1,intra. = 3.1; T_1,inter. $\sim$ 20 sec.

The results for ϕCF_3 in $CHBr_3$ are

T_1,intra = 3.5; T_1,inter $\sim$ 11 seconds.

Even though the estimated error in an individual measurement is about $\pm 5\%$ the error in the extrapolated values for T_1,intra and the values of T_1,inter calculated from them is of the order of 10-15%. The dilution studies in CS_2 and $CHBr_3$ confirm the results of the solutions in the aromatic hydrocarbons (toluene, etc.). The dominant spin-lattice relaxation mechanism in benzotrifluoride lies in the intramolecular interactions.

In another experiment an equimolar solution was prepared from phenol (C_6H_5OH) and benzotrifluoride. The relaxation time was T_1 = 2.72 seconds.

Several attempts were made to prepare a solid solution of benzotrifluoride in durene (1,2,4,5-tetramethylbenzene), M.P., 80°C, with which it was hoped one might be able to

FIGURE 10. Spin-lattice relaxation times of benzotrifluoride and benzyl fluoride as a function of concentration in carbon disulfide.

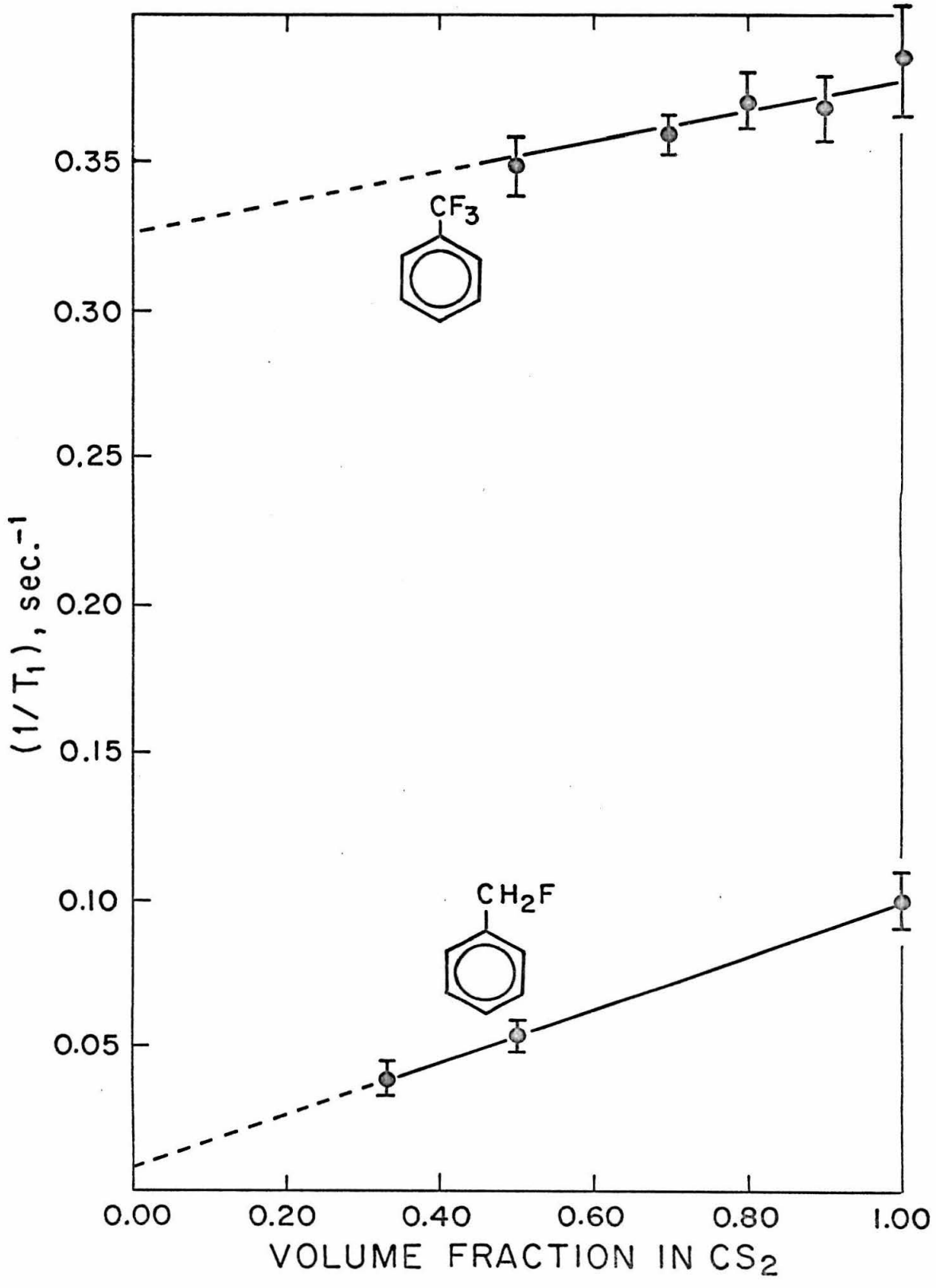
0.35
0.30
0.25
0.20
0.15
0.10
0.05
$(1/T_1)$, sec.$^{-1}$
CF_3
CH_2F
0.00
0.20
0.40
0.60
0.80
1.00
VOLUME FRACTION IN CS_2

study the F^{19} relaxation at room temperature under conditions where it is expected that the phenyl ring is stationary but the $-CF_3$ group is freely rotating. However the solubility of ϕCF_3 in durene is apparently not large enough to permit the preparation of samples having an F^{19} concentration within the sensitivity of our instrument.

It was found possible to prepare a waxy solid "solution" of 1 cc. ϕCF_3 in 6 grams of paraffin. Two samples having this composition were prepared and both possessed T_1's of 1.0 ± 0.2 seconds.

4. Halo-Benzotrifluorides.

We have measured the T_1 values of F^{19} in ortho-, meta-, and para-, chloro-, bromo-, and iodobenzotrifluoride. Although it would have been interesting, we did not study any benzotrifluoride substituted with fluorine on the ring since the pulse technique is essentially low resolution and would not have been able to distinguish between the ring fluorine and the top fluorines. The relaxation times of the pure samples for all the mono- halo-substituted benzotrifluorides are given in Table I. It is observed that the meta- and para- substituted compounds have T_1's very close to that of the unsubstituted ϕ-CF_3 and that the ortho- substituted compounds have T_1's longer than

TABLE I

F^{19} SPIN-LATTICE RELAXATION OF

MONO-HALO-BENZOTRIFLUORIDES

	ORTHO	META	PARA
Chlorobenzotrifluoride	5.54	2.86	2.82
Bromobenzotrifluoride	4.67	2.62	2.75
Iodobenzotrifluoride	3.25	2.52	2.39

the parent compound.

Dilution experiments were also performed on the three ortho-, the meta- and para- chloro, and meta-bromo-benzotrifluorides. These results are plotted in Figures 11-13. The intra- and intermolecular contributions obtained by extrapolating these curves to infinite dilution are given in Table II.

INTRA- AND INTERMOLECULAR CONTRIBUTIONS TO THE F^{19} SPIN-LATTICE RELAXATION TIME IN HALO-BENZOTRIFLUORIDES

	T_1, intra, sec.	T_1, inter, sec.
ortho-Chlorobenzotrifluoride	14	9
ortho-Bromobenzotrifluoride	15	7
ortho-Iodobenzotrifluoride	10	5
meta-Chlorobenzotrifluoride	3.8	12
meta-Bromobenzotrifluoride	3.9	8
para-Chlorobenzotrifluoride	3.2	27

FIGURE 11. Spin-lattice relaxation times of ortho-, meta-, and para- chlorobenzotrifluoride as a function of concentration in carbon disulfide.

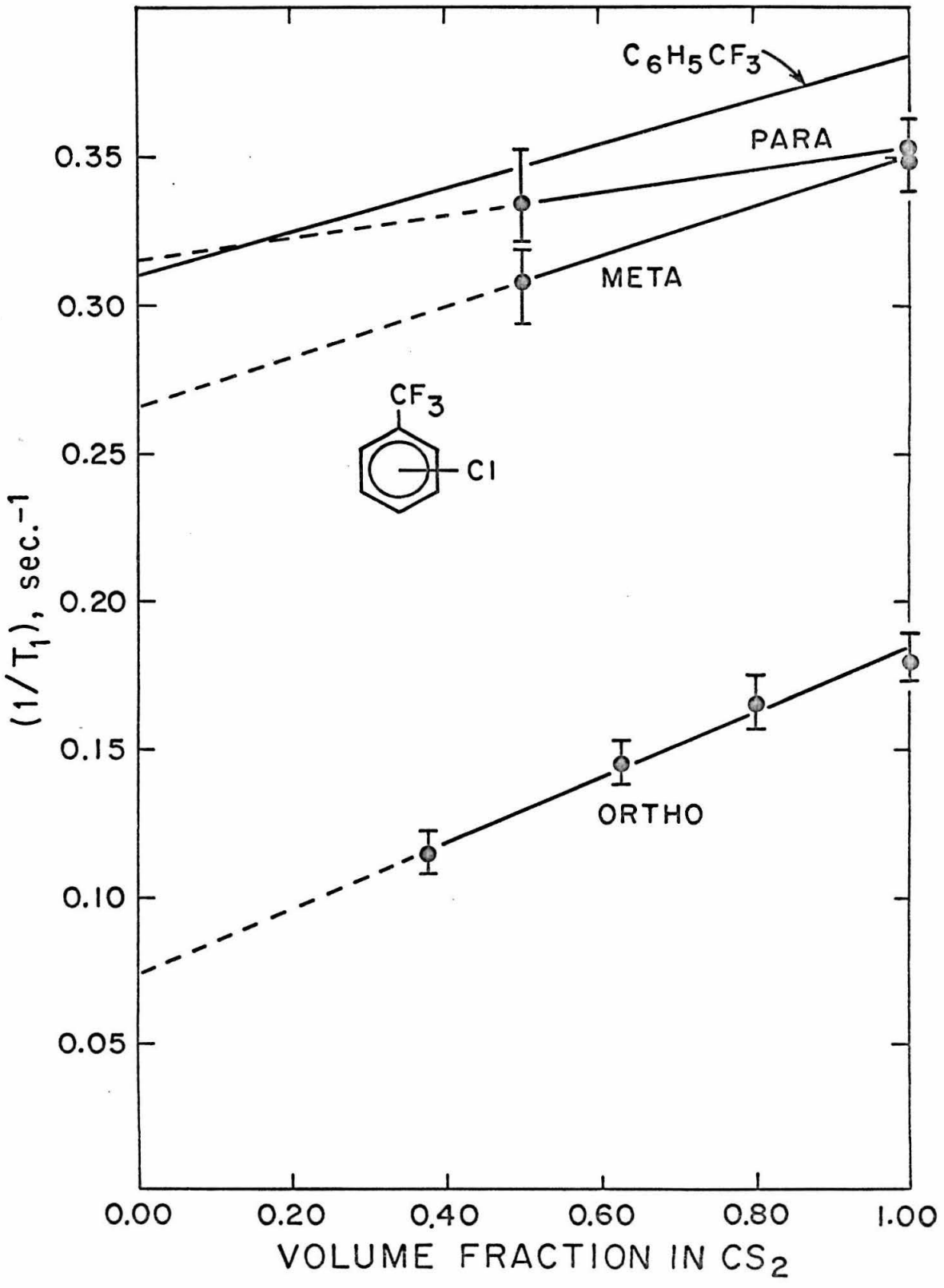
$C_6H_5CF_3$
PARA
META
ORTHO
CF_3
Cl
0.35
0.30
0.25
0.20
0.15
0.10
0.05
$(1/T_1)$, sec.$^{-1}$
0.00
0.20
0.40
0.60
0.80
1.00
VOLUME FRACTION IN CS_2

FIGURE 12. Spin-lattice relaxation times of ortho- and meta- bromobenzotrifluoride as a function of concentration in carbon disulfide.

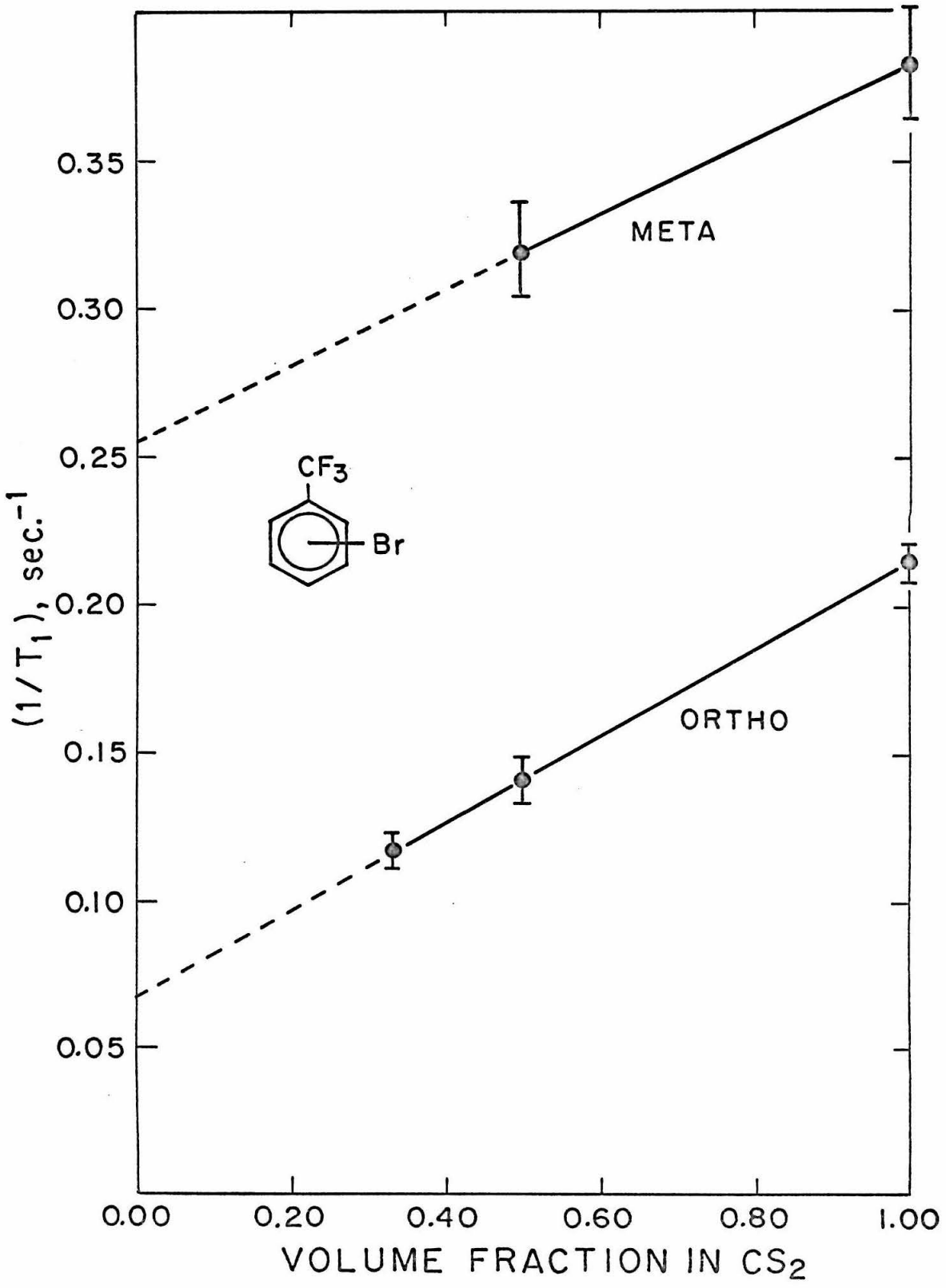
0.35
0.30
0.25
0.20
0.15
0.10
0.05
$(1/T_1)$, sec.$^{-1}$
META
ORTHO
CF_3
Br
0.00
0.20
0.40
0.60
0.80
1.00
VOLUME FRACTION IN CS_2

FIGURE 13. Spin-lattice relaxation times of ortho-aminobenzotrifluoride and ortho- iodo-benzotrifluoride.

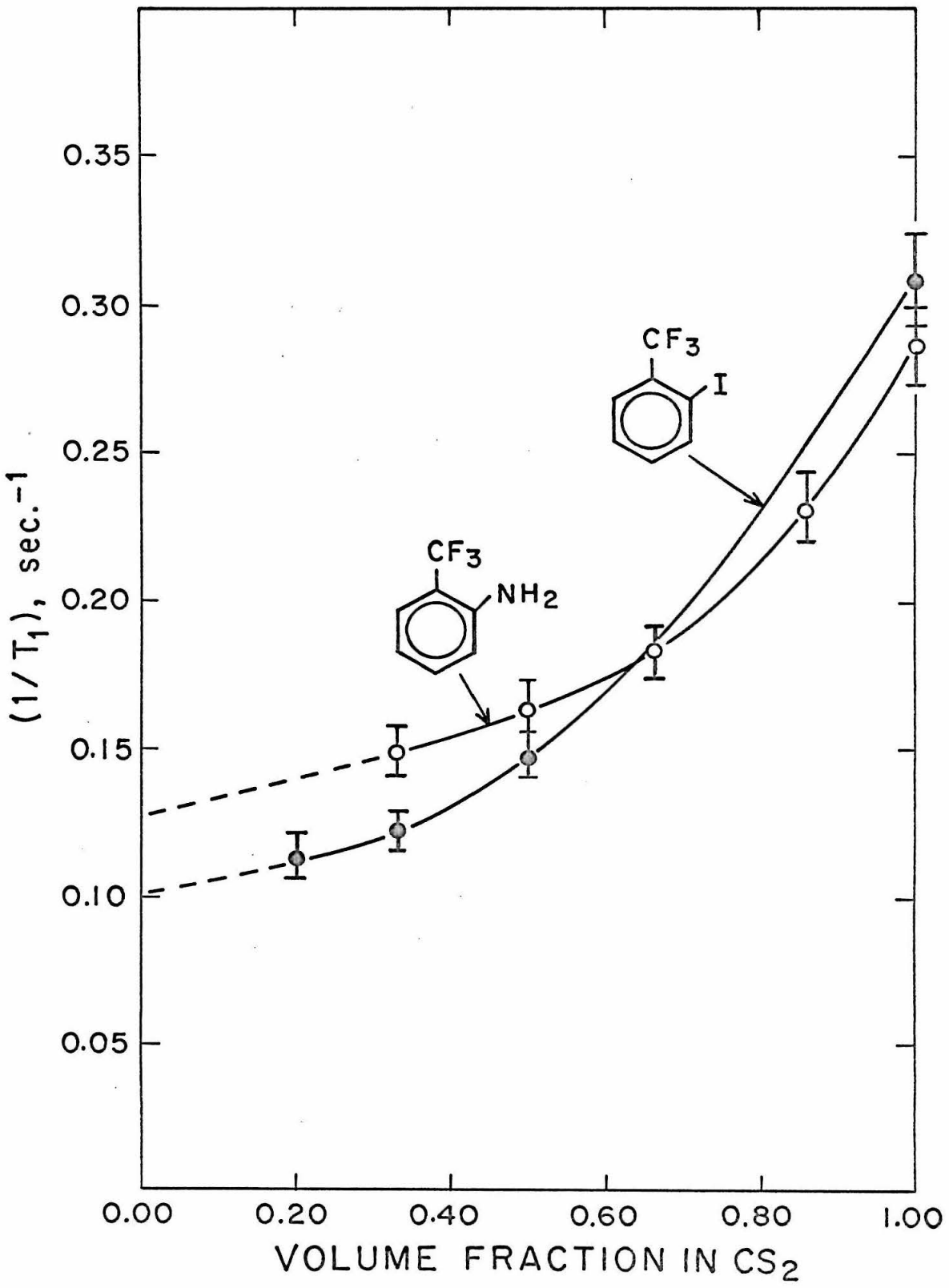
0.35
0.30
0.25
0.20
0.15
0.10
0.05
$(1/T_1)$, sec.$^{-1}$
CF_3
I
CF_3
NH_2
0.00
0.20
0.40
0.60
0.80
1.00
VOLUME FRACTION IN CS_2

There is considerable uncertainty in extracting the values presented in Table II and care must be exercised in assigning significance to apparent trends in the data. However, one thing is clear: The intramolecular relaxation time for the ortho-halo-substituted compounds is much longer than for the compounds substituted in either of the other two positions or for the parent molecule. Hence intramolecular relaxation is much less efficient in the case of the ortho substituted molecules than for the others.

The small T_1 trends for the neat meta- and para-compounds (Cl > Br > I) are probably attributable to chemical or inertial effects and will be discussed later.

5. Amino-Benzotrifluoride.

Neat samples of the amino-benzotrifluorides yielded the T_1 values: ortho 3.5 ± 0.1, meta 2.4 ± 0.15, and para 2.4 ± 0.15 seconds. The ortho value is for a clear sample from Aldrich Chemical Co.. A second sample of the same compound from Pierce Chemical Co. was dark amber and possessed a T_1 of about 3.2 seconds. Carbon disulfide solutions of the ortho compounds were also measured and the results shown in Figure 13. The dilution curve is similar to that for ortho- iodo- ϕCF_3 and here again, ortho substitution causes the intramolecular contribution to the

relaxation to be less effective than in the parent compound. For ortho-$NH_2\phi CF_3$ T_1,intra in CS_2 is about 8 seconds.

One-to-one by volume solutions of both the ortho- and meta- compounds were also prepared in glacial acetic acid and methanol. In methanol solution the meta compound had a T_1 of 2.2 $\pm$ 0.15 seconds and the ortho 4.1 $\pm$ 0.1 seconds. The meta result is expected from the results of the meta halo compounds in CS_2 but the ortho NH_2 T_1 in CH_3OH is 2 seconds shorter than for the same compound at the same volume fraction in CS_2 indicating the probable importance of solvent effects in these studies. The results from the solutions in glacial acetic acid are even more interesting. The T_1's are, for the ortho: 3.2 $\pm$ .16, and for the meta: 1.3 $\pm$ 0.14 seconds. The comparatively short T_1 for the meta is probably due to the reaction of the amine with the glacial acetic acid to form the acetanilide or some precursor to it. This would severely alter the moment of inertia of the molecule and hence its rate of reorientation in the liquid. After several weeks at room temperature (21°C) the sample tube was filled with a yellow precipitate. The ortho result may be due to a combination of dilution effect making T_1 longer and a partial reaction tending to shorten it. Only a very few

precipitated crystals are observed in the tube after several months but this does not preclude the possibility of a considerable degree of reaction if the acetanilide formed is very soluble in glacial acetic acid. To pursue this point, samples of ortho- and meta-benzotrifluoride-acetanilide were obtained and solutions of these were prepared in methanol and glacial acetic acid. The acetic acid solutions were 4 grams of acetanilide to 5 cc. acid. The T_1's were 1.1 ± .14 and 0.78 ± .14 seconds for the ortho- and meta- compounds respectively. The results in methanol for solutions of about 4 grams acetanilide to 8 cc. methanol were 2.7 ± .14 and 1.7 ± 0.14 seconds respectively. These observations on the benzotrifluorideacetanilide confirm the conclusions on the anines in glacial acetic acid.

6. Hydroxy-Benzotrifluoride.

Both ortho- and meta-hydroxybenzotrifluoride were studied. The relaxation curve for the meta substituted compound is shown in Figure 8 and is seen to be exponential. The relaxation time for the meta compound, neat, is T_1 = 0.95 ± .05 seconds. On the basis of our experience with the molecules already discussed this value is unexpectedly low. Solutions of the meta-OH in CS_2 in the ratio 1:1 and 1:2 by volume were prepared. At about 25°C these liquids

are completely soluble but at 21°C, the usual temperature of the spectrometer laboratory, they separate into two layers. The OH-benzotrifluoride-rich layers for both the 1:1 and 1:2 mixtures had a relaxation times of 2.47 ± 0.14 seconds which is reasonable for a small meta substituent. The 1:2 mixture was also run at 24.5°C at which temperature it was a clear solution. The T_1 value was 2.69 ± 0.21 seconds.

These observations lead one to suspect that intermolecular hydrogen bonds may exist in the neat meta compound and that a very small amount of dissolved CS_2 is able to disrupt this structure. The formation of dimers or polymers would result in longer effective correlation times for molecular reorientation and shorter relaxation times. The infrared spectrum of meta-hydroxybenzotrifluoride in carbon tetrachloride solution in the region of the O-H stretch (2800-3800 cm^{-1}) was measured on the Beckmann IR-7 operating in the double-beam mode with the pure solvent in the reference cell. A sharp ($\sim 50\ cm^{-1}$) peak at about 3600 cm^{-1} and a broad ($\sim 200\ cm^{-1}$) asymmetric band centered about 3400 cm^{-1} are observed. The relative intensities of these two features is a function of concentration. The more dilute the solution, the more intense

the sharp peak; the more concentrated, the more intense the broad band. We attribute the 3600 cm^{-1} feature to the monomer O-H stretch and the band at 3400 cm^{-1} to dimers and polymers formed by intermolecular hydrogen bonds.

The ortho hydroxy compound is a solid at room temperature. The relaxation time of a solution of 5 gms. in 8 cc. CS_2 is 5.1 ± 0.4 seconds. The infrared spectrum of this compound in CCl_4 possessed the same features as the meta compound but the dimer-poymer band was less intense.

7. Nitro-Benzotrifluoride.

Two solutions of 4.5 gms. ortho-nitro-ϕCF_3 in 5 cc. CS_2 had T_1's of 6.2 ± 0.6 and 6.6 ± 0.6 seconds. The relaxation time of a neat sample of the meta-nitro-ϕCF_3 (dark brown; labelled "88%") was 2.2 ± 0.2 seconds. These observations are consistent with the previous results on the halo- and amino- substituted molecules.

8. Di-Substituted Benzotrifluorides.

Several 2,5- and 3,4- disubstituted compounds were investigated. No 2,6- disubstituted compounds were commercially available. The results of measurements on solutions of these compounds were as one would have expected from a knowledge of the T_1's of the mono-substituted compounds. The results for four 2-X-5-X'- disubstituted compounds are

given in Table III along with the T_1's for the corresponding monosubstituted compounds at approximately the same concentration. In the case of compounds a) and b) T_1 is approximately midway between $T_1^{(2)}$ and $T_1^{(5)}$ but for c) and d) $T_1 \sim T_1^{(2)}$.

TABLE III

F^{19} SPIN-LATTICE RELAXATION OF DI-SUBSTITUTED BENZOTRIFLUORIDES

Compound	Solvent	Concentration (solute + solvent)	T_1, sec.	$T_1^{(2)}$, sec.	$T_2^{(5)}$, sec.
a) 2-Nitro-5-Bromo-	Ether	5gm + 5cc	5.1 ± 0.3	6.4 ± 0.6	3.1 ± 0.2
b) 2-Chloro-5-Amino-	CS_2	5gm + 5cc	5.5 ± 0.5	7.7 ± 0.4	~3
c) 2,5-Dibromo-	CS_2	5gm + 5cc	6.8 ± 0.7	7.1 ± 0.4	3.1 ± 0.2
d) 2,5-Dichloro-	CS_2	3cc + 3cc	7.0 ± 0.5	7.7 ± 0.5	3.2 ± 0.2

Measurements on neat samples of the di-substituted molecules, however, yielded consistently shorter relaxation times than either of the two mono-substituted from which they could have been derived. This is illustrated by the data in Table IV.

Although the results of Table IV suggest the probable importance of inertial effects, a proper assessment of the

TABLE IV

SPIN-LATTICE RELAXATION TIMES OF NEAT DI-SUBSTITUTED BENZOTRIFLUORIDES

COMPOUND	T_1, sec.	$T_1^{(2)}$, sec.	$T_1^{(3)}$, sec.	$T_1^{(4)}$, sec.	$T_1^{(5)}$, sec.
3-Amino-4-Chloro-	1.5± 0.1	-	2.4± 0.1	2.8± 0.1	-
2-Chloro-5-Nitro-	1.5± 0.1	5.5± 0.3	-	-	2.2± 0.2
3-Nitro-4-Chloro-	1.9± 0.1	-	2.2± 0.2	2.8± 0.1	-
2-Nitro-5-Chloro-	2.0± 0.1	*	-	-	2.9± 0.2
2-Amino-5-Chloro-	2.3± 0.1	3.5± 0.1	-	-	2.9± 0.2
2,5-Dichloro-	3.9± 0.1	5.5± 0.3	-	-	2.9± 0.2

* Solid at room temperature.

situation cannot be made without the aid of information from dilution studies to separate the inter- and intramolecular contributions. Such information is not presently available.

9. Di-(trifluoromethyl)-Benzene and Derivatives.

The 1,3- and 1,4- di-(trifluoromethyl)-benzenes ($\alpha,\alpha,\alpha,\alpha',\alpha',\alpha'$ -hexafluoro-m- and p-xylenes respectively) both have T_1 = 2.6 ± 0.2 seconds (neat). Cyano-, hydroxy-, and nitro- derivatives of the 1,3-$\phi(CF_3)_2$ all

gave relaxation times (neat) shorter than the corresponding molecule with only one $-CF_3$ group. These results are shown in Table V.

TABLE V

F^{19} T_1 OF 1,3-DI-(TRIFLUOROMETHYL)-BENZENE, DERIVATIVES, AND RELATED COMPOUNDS

COMPOUND	T_1, seconds (neat)
3,5-Ditrifluoromethyl-Phenol	0.90 ± 0.04 (0.95 ± 0.05)*
3,5-Ditrifluoromethyl-Benzonitrile	1.59 ± 0.07 (2.11 ± 0.10)
3,5-Ditrifluoromethyl-Nitrobenzene	1.74 ± 0.08 (2.2 ± 0.2)
3,5-Ditrifluoromethyl-Benzene	2.6 ± 0.2 (2.65 ± 0.13)

*(The values given in parentheses are the T_1's for the corresponding compounds with one less $-CF_3$ group.)

As in the previous section on the disubstituted molecules, dilution studies have not been made on these compounds either. Therefore one cannot ascribe the T_1 changes to inter- or intramolecular effects. However, one would imagine that the T_1, inter values for the ditrifluoromethyl compounds would be shorter than for the corresponding mono-fluoromethyl-benzenes due the

possibility of an increased intermolecular fluorine-fluorine dipolar interaction. From the results of this Section and of Section 8 it is apparent that for neat samples T_1 generally decreases with increased substitution.

10. Benzyl Fluoride.

The relaxation time of F^{19} in benzye fluoride (ϕCH_2F) has been measured neat and in carbon disulfide solution. The results are given in Figure 10. From the extrapolated value we have $T_{1,intra} \sim 100$ seconds. Because of the long relaxation times involved and the low concentration of F^{19} in these samples this T_1 data is difficult to acquire. The 180^o-90^o pulse time interval was measured with a stopwatch.

Since, in this compound, dipolar interactions between the hydrogen and fluorine nuclei may be a significant relaxation mechanism the relaxation curve for neat ϕCH_2F was measured over a period of one half-life (about 7 seconds). Although there is considerable scatter in the data, the curve appeared to possess a slight deviation from exponential behavior as would occur if there were "unlike" dipolar relaxation. In the event that the relaxation was due only to the H-F dipolar interaction the relaxation curve would be given by a sum of two equally weight exponentials, one with a time constant three times the other,

and it would be improper to speak of a single relaxation time. In such a case it would be more convenient to speak in terms of τ_0, the pulse separation when the null signal is obtained. The T_1's plotted in Figure (10) are calculated from measured values of τ_0. If a more detailed investigation of ϕCH_2F revealed that the dominant relaxation mechanism were indeed heteronuclear in nature, then the T_1 values given in Figure (10) would not be valid. However, the corresponding τ_0 values could still be profitably interpreted as follows. In the discussion on intermolecular dipolar relaxation between "unlike" nuclei the relaxation curve was given by

$$\frac{M_z(\tau) - M_z^0}{M_z(0) - M_z^0} = \frac{1}{2}\left(e^{-\tau/T_1} + e^{-\tau/3T_1}\right) \qquad (34)$$

For the pulse separation τ_0, $M_z(\tau_0) = 0$. Since the initial condition is $M_z(0) = -M_z^0$, at τ_0 we have

$$\frac{1}{2} = \frac{1}{2}\left(e^{-\tau_0/T_1} + e^{-\tau_0/3T_1}\right) \qquad (109)$$

Numerical solution of equation (35) yields

$$\frac{\tau_0}{3T_1} = 0.384 \quad \text{or} \quad T_1 = \tau_0/1.152 \qquad (110)$$

The T_1's calculated from (36) are shorter than those calculated from $\tau_0/\ln 2$ by about three-fifths. When these shorter values were plotted instead of those shown

in Figure (10), the extrapolated value of T_1,intra was about 70 seconds.

The T_1^u appearing in (34) and the homonuclear dipolar T_1^l are

$$(T_1^u)^{-1} = \frac{3}{2}\hbar^2\gamma_{I_1}^2\gamma_{I_2}^2 r^{-6}\tau_c, \quad (T_1^l)^{-1} = \frac{3}{2}\hbar^2\gamma^4 r^{-6}\tau_c \qquad (111)$$

The gyromagnetic ratios for hydrogen and fluorine are very similar in magnitude $\gamma_H/\gamma_F \sim 1.05$ and therefore $(T_1^{H-F})^{-1}$ should equal approximately $0.9(T_1^{F-F})^{-1}$.

F. INTERPRETATION AND CONCLUSIONS.

1. Introduction.

Three reports (16,41,42) have recently appeared regarding measurements of the fluorine spin-relaxation time in benzotrifluoride. In the pure liquid (16,41) it was found that the F^{19} relaxation time decreases slowly from 3.2 seconds at -20°C to about 0.5 seconds at 300°C, just below the critical temperature. Green and Powles (16) concluded that the relaxation in the liquid arises mainly from the motion of the $-CF_3$ group, the rate of which they add, is probably not very different from that of the phenyl ring. On the other hand, Faulk and Eisner (41) more recently interpreted their results with the assumption that either the molecule is rigid or the "such rotation as does occur does not greatly affect the correlation time." In solid benzotrifluoride, second moment and T_1 measurements (42) indicate that while the phenyl ring is stationary, the $-CF_3$ group is freely rotating and, in fact, serves as a spin sink for the protons.

Powles (16,43) has studied the temperature dependence of the proton relaxation time of both the ring and side-

group protons in toulene, p-xylene, mesitylene, p-fluoro-toulene, and ethylbenzene. From the melting point to the critical temperature the ring protons in all the compounds exhibit increasing T_1 with increasing temperature characteristic of pure dipolar relaxation. However the side-group protons in all the compounds except ethylbenzene show increasing T_1's from the melting point to about 100°C where they have a maximum of about 8-10 seconds and then decrease with increasing temperature. In ethylbenzene the T_1's of both the $-CH_2-$ and $-CH_3$ protons increase continuously up to about 200°C where they are about 20 seconds. These observations are ascribed by Powles to the operation of the spin-rotation mechanism in the methyl group relaxation at high temperatures. He concludes that the spin-rotation magnetic field experienced by the methyl group is determined by its intrinsic angular velocity but he does not pursue a more detailed analysis of the problem.

Although not mentioned by Powles, the temperature dependence of the ethyl protons in ethylbenzene is probably due to the fact that the relatively bulky ethyl group cannot exercize the same sort of internal rotation possible in the methyl benzenes.

Pendred, Pritchard, and Richards (23,24) have made an

extensive series of measurements of proton T_1's of organic compounds in carbon disulfide solution at 25°C. For ring protons in aromatic compounds the dominant relaxation mechanism is the intermolecular dipolar interaction. Typically $T_{1,total}$ is about 10-20 seconds and the infinite dilution $T_{1,intra}$ about 60-100 seconds. But the importance of intermolecular interactions is greatly reduced for protons in methyl groups attached to aromatic rings for which $T_{1,total}$ is approximately 5-10 seconds and $T_{1,intra}$ about 10-15 seconds. In trying to account for these observations on the basis of dipolar interactions Richards (23) calculates relaxation times for the $-CH_3$ groups which are consistently shorter than those observed and is forced to conclude that "while the methyl group must tumble with the rest of the molecule, when there is rotation about the C_3 axis this is largely ineffective in causing relaxation." These conclusions would, of course, be consistent with our previous discussion (Section B.5.a) concerning the effect of internal rotation on the intramolecular T_1, but they are invalid in that he has neglected the spin-internal-rotation mechanism which even for protons at room temperature must present a non-negligible contribution to the relaxation.

The experimental results presented in Section E give

strong evidence that in the benzotrifluorides the internal rotation is crucial to the spin-relaxation of the fluorines and that the dominant relaxation mechanism is the fluctuating spin-internal-rotation interaction.

2. The Spin-Internal-Rotation Relaxation Time.

If the internal rotation in benzotrifluoride may be described by rotational Brownian motion then the results of Hubbard (10) on spin-rotation relaxation are applicable to the spin-internal-rotation problem with appropriate modifications. Equation (50) given above in Section B.4.d for T_1 due to the spin-rotation mechanism is

$$T_1^{-1} = \frac{2}{3} \frac{I k T \tau_1}{\hbar^2} (2C_\perp^2 + C_\parallel^2) \qquad (50)$$

For spin-internal-rotation relaxation moment of inertia, the correlation time and the spin-rotation constants must be replaced by those applicable to the motion of the top.

$$T_1^{-1} = \frac{2}{3} \frac{I_\alpha k T}{\hbar^2} \tau_{SR} C_\alpha^2 \qquad (112)$$

Hubbard (10) gives the rotational correlation time in (50) in terms of the diffusion coefficient as

$$\tau_{SR} = (3ID/4a^2kT) \qquad (113)$$

From (113) it is seen that $(T\tau_{SR})$ is proportional to the diffusion coefficient. Since D ordinarily increases with temperature, $T\tau_{SR}$ also increases with temperature and hence from (50) or (112) T_1 must decrease with temperature. This

accounts for the decrease in T_1 with increasing temperature observed in molecules known, or expected, to possess large spin-rotational interaction.

C_α in (112) is defined as the internal rotational magnetic field per unit internal angular momentum, as discussed previously. The contribution of (112) to the total relaxation time will decrease as the barrier to internal rotation increases, because the internal angular momentum decreases.

The spin-overall-rotation mechanism is, of course simultaneously present. Its contribution to the total measured relaxation time is given in equation (50) with the appropriate constants being those associated with the overall motion.

3. Barrier Effects.

We attribute the increase in T_1 observed on ortho-substitution of benzotrifluoride to an alteration in the height and symmetry of the barrier to internal rotation produced by the substituent. With the increased barrier height $\langle j'' \rangle$ decreases and the effect of the internal rotation as a relaxation mechanism is decreased, leaving the less effective spin-overall-rotation and dipolar mechanisms.

4. Inertial Effects.

That meta- and para- substitution often decrease the relaxation time is most likely due to a lengthening of τ_{SR} produced by the increased mass of the entire molecule. Since the top changes its internal orientation primarily by intermolecular collisions, the correlation time for the internal rotation must be intimately connected with the correlation time for the overall molecular motion. Intermolecular association as apparently occurs in the m-hydroxybenzotrifluoride also acts to increase τ_{SR} and decrease T_1 by increasing the effective moment of inertia.

5. Chemical Effects.

The effects of ring substitution on the pK_a and pK_b of phenols, aromatic carboxylic acids and aromatic amines have been extensively investigated and catalogued. There are well-known resonance, inductive, and steric effects. The first two are qualitiative discriptions of the perturbations in the electronic structure of the molecule produced by the substitution.

It would be naive to think that the substituted benzotrifluorides investigated in this thesis were not electronically perturbed. The electronic perturbations which certainly exist have the effect of altering the $-CF_3$

spin-rotation tensor components and of giving rise to a "chemical effect" in the relaxation time. Although the chemical effect may be extremely important in accounting for the fine details of the T_1 variations it is not as important as the barrier effect. However, it may be as important as the inertial effect.

6. Benzyl Fluoride.

The F^{19} $T_{1,intra}$ observed in benzyl fluoride, ϕCH_2F, is too long to allow one to interpret the T_1 value in benzotrifluoride as dipolar in origin. The benzyl fluoride result is most likely due a much smaller spin-rotation interaction in this molecule.

7. Other.

The anisotropic chemical shift must be ruled out as a significant relaxation mechanism in ϕCF_3 since the value of the F^{19} T_1 at 25°C and 60 MHz Green and Powles (16) report is equal to our value at the same temperature.

The interrupted scalar interaction may also be neglected for benzotrifluoride since the geminal coupling constants are only about 150 Hz.

When dissolved in paraffin the correlation time for the reorientation of the internal top relative to the frame in benzotrifluoride is no longer governed by the inter-

molecular collisions. Since it is known from the second moment measurements in solid ϕCF_3 that the internal top is freely rotating, it is fair to conclude that even in the solid the spin-internal-rotation interaction is responsible for the nuclear spin relaxation. Our very short T_1 for ϕCF_3 in paraffin at room temperature must be due to a correlation time long compared to that in the liquid.

APPENDIX A LIMITING CASES AND SOLUTION OF THE ENERGY MATRIX.

The rotational wave functions and energies of molecules with hindered internal rotation are usually determined for certain limiting cases. For molecules possessing a barrier between about 0.7 and 5.0 kcal/mole "high barrier" approximations are employed. Here, products of the symmetric rotor and torsional functions form a basis, and the asymmetry and cross terms in the angular momenta are evaluated as a perturbation. In the "low barrier" approximation ($V \lesssim 500$cal/mole) the free internal rotation is solved exactly and the barrier added as a perturbation. For calculations of rotational-torsional states the barrier is expanded in a Fourier series and usually only the first symmetry required term is used.

1. Free Rotation.

For symmetric molecules $I_x = I_y$ and the Hamiltonian is:

$$\mathcal{H} = A(P_x^2 + P_y^2) + CP_z^2 + F(p - (I_\alpha / I_z)P_z)^2 \qquad \text{(A1)}$$

The eigenfunctions are:

$$S_{JKm}(\theta, \phi) e^{iK\chi} e^{im\alpha} \qquad \text{(A2)}$$

where $S_{JKm}(\theta,\phi)\, e^{iK\chi}$ are the symmetric rotor wave functions

and m is the quantum number characterizing the internal angular momentum. The eigenenergies are:

$$E = AJ(J+1) + (C-A)K^2 + F(m - (I_\alpha/I_z)K)^2 \qquad \text{(A3)}$$

where

$$F = \hbar^2 I_z/(2I_\alpha(I_z-I_\alpha))$$

For microwave transitions the selection rules are

$$\Delta J = \pm 1, \quad \Delta K = 0, \quad \Delta m = 0$$

Thus the effect of a completely free internal rotor in a symmetric top cannot be detected in the microwave spectrum.

For an (over-all) asymmetric rotor the Hamiltonian is written:

$$\mathcal{H} = \mathcal{H}_0 + \mathcal{H}_1$$

$$\mathcal{H}_0 = \tfrac{1}{2}(A+B)(P_x^2+P_y^2) + C_z P_z^2 + F p^2 - 2C_z p P_z \qquad \text{(A4)}$$

$$\mathcal{H}_1 = \tfrac{1}{2}(A-B)(P_x^2-P_y^2)$$

Using the functions (A2) as a basis set the Hamiltonian is diagonal in J, M, and m and off-diagonal in K by K±2. As for rigid asymmetric rotors, the K degeneracy is lifted but a ± m degeneracy appears as the matrix elements are

$$\langle JKm|\mathcal{H}|JKm\rangle = \tfrac{1}{2}(A+B)J(J+1) + (C_z - \tfrac{A+B}{2})K^2 + Fm^2 - 2C_z Km \qquad \text{(A5a)}$$

$$\langle JKm|\mathcal{H}|JK\pm 2m\rangle = -\tfrac{1}{4}(A-B)(J(J+1)-K(K\pm 1))^{\frac{1}{2}}(J(J+1)-K(K\pm 1)(K\pm 2))^{1/2} \qquad \text{(A5b)}$$

For large values of m the energy matrix may be solved by second order perturbation theory. The selection rules are the same as for rigid asymmetric tops with the additional rule Δ m=0.

2. Low Barriers.

The only really low barriers accurately known are those in nitromethane and methyldifluoroboron. Both of these molecules have sixfold barriers and it is argued that sixfold barriers will generally be low. In which case

$$V(\alpha) = (V_6/2)(1 - \cos 6\alpha) \tag{A6}$$

The rotational states for an asymmetric rotor with a "low" 6-fold barrier will then be found from matrix elements identical to those given in (A5a,b) with the exception that the energy will be off-diagonal in m,

$$\langle JKm|\mathcal{H}|JKm\pm 6\rangle = -V_6/4 \tag{A7}$$

For V_6 small the non-diagonality in m may be removed. To second order this transformation results in an additional diagonal term:

$$FV_6^2/32\,((C_z K - Fm)^2 - 9F^2) \tag{A8}$$

This is not valid for the $|m| = 3$ levels because of the near degeneracy. When m is not a multiple of three, the levels are inherently degenerate for all barriers. For m equal to multiple of three the degeneracy is removed at high barriers. However, for these splittings to be calculated a higher order perturbation than that given by (A8) must be used. The selection rules are still approximately

$$\Delta J = \pm 1, \quad \Delta K = 0, \quad \Delta m = 0.$$

3. High Barriers.

For "high barriers" the Hamiltonian is written

$$\mathcal{H} = \mathcal{H}_0 + \mathcal{H}_1 \tag{A9a}$$

with

$$\mathcal{H}_0 = DP^2 + (C-D)P_z^2 + Fp^2 + V(\alpha) \tag{A9b}$$

$$\mathcal{H}_1 = \tfrac{1}{2}(A-B)(P_x^2 - P_y^2) - 2C_p P_z \tag{A9c}$$

where $D = \frac{1}{2}(A + B)$ and where for symmetric rotors the first term in (A9c) vanishes. $\mathcal{H}_0$ is diagonal in the representation

$$S_{JKM}(\theta,\phi)\, e^{iK\chi}\, U_{\nu\kappa}(\alpha) \tag{A10}$$

where the symmetric rotor functions are as before and the U's are solutions of

$$(Fp^2 + V(\alpha))\, U_{\nu\kappa} = E_{r\kappa}\, U_{\nu\kappa} \tag{A11}$$

which is related to the Mathieu equation for which solutions are tabulated. The perturbation is then evaluated in the above basis. In the limit of a very high barrier the problem reduces approximately to a rigid rotor with moments of inertia Ix, Iy, Iz, (not I_z-I_α) plus a harmonic torsional oscillator with a reduced moment of inertia I_α (Iz-I_α) /Iz.

In conclusion then, we can assume the rotational energies and wave functions of molecules with internal rotors as known or at least calculable.

APPENDIX B THE ASYMMETRIC ROTOR WAVE-FUNCTIONS WITH INTERNAL MOTION AND THE OPERATOR P_z.

The wave functions of the symmetric rotor are

$$\psi_{JKM}(\theta\phi\chi) = e^{i(M+K)\frac{\pi}{2}} N_{JKM} e^{i(M\phi+K\chi)} P_{JKM}(\theta) \tag{B1}$$

where

$$N_{JKM} = \left(\frac{(2J+1)(J+\frac{d}{2}+\frac{s}{2})!(J-\frac{s}{2}+\frac{d}{2})!^{1/2}}{8\pi^2 (J-\frac{s}{2}+\frac{d}{2})!\, d!\, (J+\frac{s}{2}-\frac{d}{2})!^{1/2}} \right)^{1/2}$$

$$P_{JKM}(\theta) = t^{-d/2}(1-t)^{-s/2} \frac{d!}{(d+p)!} \frac{d^p}{dt^p} \left(t^{d+p} + (1-t)^{s+p} \right)$$

$$d = |M-K|\,, \quad s = |M+K|\,, \quad t = (1-\cos\theta)/2\,, \quad 2p = 2J-(d+s)$$

Using the Van Vleck phase convention,

$$\psi^{x}_{JKM} = (-1)^{\beta} \psi_{JKM} \tag{B2}$$

where β is the larger of the K and M, and following Wang and Mulliken, we construct the symmetrized zero order wave functions

$$S(JKM\mu) = 2^{-\frac{1}{2}} \left(\psi^{x}_{JKM} + (-1)^{\mu} \psi_{J-KM} \right) \quad K = 1,2 \cdots J;\ \mu = 0,1$$

$$S(J0M0) = \psi^{x}_{J0M} \tag{B3}$$

The asymmetric rotor problem is usually solved in the symmetric rotor representation using these symmetrized functions as a basis. This is done because the S's are eigenstates of the covering operators E, C_2^x, C_2^y, and C_2^z of

the four group V(x,y,z) whereas the ψ_S' are not.

$$\begin{aligned} E\,S(JK\tau\gamma) &= S(JK\tau\gamma) \\ C_2^x S &= -1^K S \\ C_2^y S &= -1^{J+\tau} S \\ C_2^z S &= -1^{J+K+\gamma} S \\ C_2^y \psi_{JK\tau} &= \psi_{J-K\tau} \end{aligned} \tag{B4}$$

Thus the asymmetric rotor functions A are expanded in terms of the S functions. Where the a's are the expansion coefficients

$$A(J\tau M) = \bar{\Sigma}_{K\gamma}\, a(J\tau M, K\gamma) S(JKM\gamma) \tag{B5}$$

In this basis the energy matrix for the asymmetric rotor is diagonal in J and M and factors twice: Once for even and odd K since the only off-diagonal elements in K are between states differing by $\Delta K = \pm 2$. And second due to the parity of γ since asymmetric rotor Hamiltonian can only connect states of the same Kroning-Wang symmetry. Thus there are four submatrices designated E^+, E^-, O^+, and O^- with the notation $E^+ \rightarrow K$ even, γ positive, etc. Each submatrix corresponds to one of the species of V(x,y,z) namely A, Bx, By, or Bz. For a given asymmetric rotor function the summation in (B5) extends only over those K's contained in the factoring submatrix in which A appears and hence will be only for γ positive or negative, enabling one to write

$$A(J\tau M\gamma) = \bar{\Sigma}_K\, a(J\tau M, K\gamma) S(JKM\gamma) \tag{B6}$$

The diagonal elements of the operator P_z in the S representation are all zero.

$$\langle S_{JKm\sigma} | P_z | S_{JKm\sigma} \rangle \propto \langle \psi^{A}_{JKm} | P_z | \psi^{S}_{JKm} \rangle + \langle \psi^{S}_{J-Km} | P_z | \psi^{A}_{J-Km} \rangle + \text{cross terms} \tag{B7}$$

$$= +K - K = 0$$

Furthermore, the diagonal matrix elements of the same operator will be zero for any expansion of the type (B6) hence the expectation value for P_z will be zero for any asymmetric rotor level.

With the presence of an internal rotor the second factoring is not possible. The symmetrized Wang (or Mulliken) functions are no longer the appropriate zero order functions because of the linear term in K on the diagonal of the energy matrix. For the low barrier case inspection of the matrix elements in (A5a,b) predicts the wave functions will have the form

$$\Psi^{evenK}_{m} = e^{im\alpha} \sum_{evenK} a_K \psi^{S}_{JKm}$$

$$\text{or} \quad \Psi^{oddK}_{m} = e^{im\alpha} \sum_{oddK} a_K \psi^{S}_{JKm} \tag{B8}$$

The value of $\langle \Psi | P_z | \Psi \rangle$ does not necessarily vanish as before.

APPENDIX C MATRIX ELEMENTS OF THE SPIN-ROTATION INTERACTION.

The matrix elements of the spin-rotation interaction Hamiltonian in the coupled and uncoupled cases have been obtained following the methods outlined by Van Vleck (29,30), and Condon and Shortley (39) and as elaborated for the nuclear spin rotation case by Poesener (40). For the calculations in the coupled scheme the nuclear spin angular momenta are reversed so they will have the same commutation relations as the molecular rotation (39).

1. Single Spin.

The spin-rotation Hamiltonian derived in the previous section may be written as a tensor coupling of the nuclear spin and molecular rotational angular momenta.

$$\mathcal{H}_{SR} = \vec{I} \cdot \underset{\sim}{M} \cdot \vec{J} \qquad \text{(C1)}$$

To evaluate the matrix elements we use the coupling scheme $\vec{F} = \vec{I} + \vec{J}$ or, with the reversed spin angular momentum $\vec{\bar{I}} = -\vec{I}$, $\vec{J} = \vec{\bar{I}} + \vec{F}$. The elements diagonal in $\vec{J}$ are found with the aid of the identity

$$\langle \alpha JM | \vec{T} | \alpha JM \rangle = \frac{\langle \alpha JM' | \vec{J} \cdot \vec{T} | \alpha' JM' \rangle}{J(J+1)} \langle \alpha JM | \vec{J} | \alpha JM \rangle \qquad \text{(C2)}$$

which is true for any operator $\vec{T}$ satisfying the com-

mutation relation

$$[\vec{J}, \vec{T}] = i\hbar\, \vec{T} \times \underset{\sim}{1} \tag{C3}$$

where $\underset{\sim}{1}$ is the unit dyadic (39).

Hence equation (C1) becomes (all angular momenta in units of $\hbar$)

$$\mathcal{H}_{SR} = \frac{\vec{I}\cdot\vec{J}}{J(J+1)}\ \vec{J}\cdot\underset{\sim}{M}\cdot\vec{J} \tag{C4}$$

whose diagonal matrix elements in the coupled $|J\tau\rangle$ scheme are

$$\langle J\tau|\mathcal{H}|J\tau\rangle = \frac{J(J+1)-F(F+1)+I(I+1)}{2J(J+1)}\ \Sigma_g M_g \langle J\tau|J_g^2|J\tau\rangle \tag{C5}$$

provided M is diagonal in the molecular inertial frame. Here $|J\tau\rangle$ indicates the <u>asymmetric rotor</u> basis. In the "high field" or decoupled $|J I M_J M_I\rangle$ scheme

$$\langle J\tau|\mathcal{H}|J\tau\rangle = \frac{M_I M_J}{J(J+1)}\ \Sigma_g M_g \langle J_g^2\rangle \tag{C6}$$

<u>2. Matrix Elements for the General Case.</u>

Before proceeding to cases involving more than one spin it will be useful to review some of the results of Condon and Shortley.

If we consider adding n + 1 commuting angular momenta each of which satisfies equation (C3) with respect to $\vec{J}$,

$$\sum_{k=0}^{n} \vec{J}_k = \vec{J} \tag{C7}$$

we can envision adding them together one at a time

$$\begin{array}{lll} \vec{J}_n + \vec{J}_{n-1} & = & \vec{J}_{n-1,n} \\ \vec{J}_{n-1,n} + \vec{J}_{n-2} & = & \vec{J}_{n-2,n} \\ \hline \vec{J}_{k+1,n} + \vec{J}_k & = & \vec{J}_{k,n} \\ \vec{J}_{k,n} + \vec{J}_{k-1} & = & \vec{J}_{k-1,n} \\ \hline \vec{J}_{1,n} + \vec{J}_0 & = & \vec{J}_{0,n} \equiv \vec{J} \end{array} \qquad \text{(C8)}$$

where there are n-1 intermediate angular momenta and $\vec{J}_{0,n} \equiv \vec{J}$ is the total angular momentum. The reduced matrix elements of the constituent angular momenta are

$$\begin{aligned} &\langle j_{k,n}, j_{k-1,n} \cdots j_{1,n} j_{0,n} \| \vec{J}_k \| j'_{k,n} j'_{k-1,n} \cdots j'_{1,n} j'_{0,n} \rangle \\ &= \langle j_{k,n} \| \vec{J}_k \| j'_{k,n} \rangle \langle j_{k,n} j_{k-1,n} | j'_{k,n} j'_{k-1,n} \rangle \cdots \langle j_{1,n} j | j'_{1,n} j' \rangle \end{aligned} \qquad \text{(C9)}$$

The factors $\langle j_{k,n} \| \vec{J}_k \| j'_{k,n} \rangle$ and $\langle j_{k,n} j_{k-1,n} | j'_{k,n} j'_{k-1,n} \rangle$ etc. are given in Tables I and II respectively and the functions symbolized in these tables are defined in Table III. The matrix elements of the scalar product $\vec{J}_k \cdot \vec{J}$ are diagonal in j and are

$$\begin{aligned} &\langle j_{k,n} \cdots j_{1,n} j m | \vec{J}_k \cdot \vec{J} | j'_{k,n} \cdots j'_{1,n} j' m' \rangle \\ &= \langle j_{k,n} \| \vec{J}_k \| j'_{k,n} \rangle \langle j_{k,n} j_{k-1,n} | j'_{k,n} j'_{k-1,n} \rangle \cdots \langle j_{1,n} j | j'_{1,n} j' \rangle \\ &\quad \times j(j+1) \delta_{jj'} \delta_{mm'} \end{aligned} \qquad \text{(C10)}$$

3. Two Spins.

For the case of two nuclear spins I_1 and I_2 with slightly different spin-rotation coupling we write as before

$$\mathcal{H}_{SR} = \vec{I}_1 \cdot \underline{M}^{(1)} \cdot \vec{J} + \vec{I}_2 \cdot \underline{M}^{(2)} \cdot \vec{J} \qquad \text{(C11a)}$$

TABLE I. The Matrices of $\langle j|J_k|j'\rangle$

$$\langle j_{k,n}||J_k||j_{k,n}+1\rangle = \mp\tfrac{1}{2}\varphi(j_k, j_{k,n}+1)$$

$$\langle j_{k,n}||J_k||j_{k,n}\rangle = \theta(j_k, j_{k,n})$$

$$\langle j_{k,n}||J_k||j_{k,n}-1\rangle, = \mp\tfrac{1}{2}\varphi(j_k, j_{k,n})$$

For $k \neq n$ the upper sign is used on the $j, j \pm 1$ element; for $k = n$ the lower.

TABLE II. The Matrix $(st|s't')$

s' \ t'	$t+1$	t	$t-1$
$s+1$	$\frac{1}{2}\xi(s+1, t+1)$	$\eta(s+1, t)/2t(t+1)$	$\frac{1}{2}\zeta(s+1, t-1)$
s	$\frac{1}{2}\varphi(s, t+1)$	$\theta(s,t)$	$\frac{1}{2}\varphi(s,t)$
$s-1$	$\frac{1}{2}\zeta(s,t)$	$\eta(s,t)/2t(t+1)$	$\frac{1}{2}\xi(s,t)$

TABLE III. Definitions of Special Functions

$$\varphi(j_1, j) = \frac{-\sqrt{\{P(j_1, j)Q(j_1, j-1)\}}}{j\sqrt{\{(2j-1)(2j+1)\}}} = \varphi(j_2, j)$$

$$\theta(j_1, j) = \frac{R(j_1, j)}{2j(j+1)}$$

$$P(j_1, j) = (j - j_2 + j_1)(j + j_2 + j_1 + 1)$$

$$Q(j_1, j) = (j_2 + j_1 - 1)(j + j_2 - j_1 + 1)$$

$$R(j_1, j) = j(j+1) - j_2(j_2+1) + j_1(j_1+1)$$

$$\xi(s, t) = \frac{\sqrt{\{P(s, t)P(s, t-1)\}}}{t\sqrt{(2t-1)(2t+1)}}$$

$$\eta(s, t) = \sqrt{\{P(s, t)Q(s, t)\}}$$

$$\zeta(s, t) = \frac{-\sqrt{\{Q(s, t)Q(s, t+1)\}}}{(t+1)\sqrt{(2t+1)(2t+3)}}$$

Here the notation is $\vec{J}_1 + \vec{J}_2 = \vec{J}$; where $\vec{J}$ corresponds to an intermediate or total angular momentum.

$$\text{or} \quad \mathcal{H}_{SR} = \frac{\vec{I}_1 \cdot \vec{J}}{J(J+1)} \vec{J} \cdot \underset{\sim}{M}^{(1)} \cdot \vec{J} + \frac{\vec{I}_2 \cdot \vec{J}}{J(J+1)} \vec{J} \cdot \underset{\sim}{M}^{(2)} \cdot \vec{J} \qquad \text{(C11b)}$$

The coupling scheme is:

Normal $\quad \vec{I}_1 + \vec{I}_2 = \vec{I} \qquad \vec{I} + \vec{J} = \vec{F}$ (C12a)

Reversed $\quad \vec{\vec{I}}_1 + \vec{\vec{I}}_2 = \vec{\vec{I}} \qquad \vec{\vec{I}} + \vec{F} = \vec{J}$ (C12b)

where $\vec{\vec{I}}$ may assume the values I_1+I_2, I_1+I_2-1, . . . $|I_1-I_2|$. With equation (C10) and Tables I-III we may write the matrix elements of (C11b) diagonal in $|J\tau\rangle$ as

$$\langle IJ\tau|\mathcal{H}|IJ\tau\rangle = (\theta(I,J)\bar{\zeta}'\theta(I_1,I) + \theta(I_2,I)\theta(I,J)\bar{\zeta}^2) \qquad \text{(C13a)}$$

$$\langle IJ\tau|\mathcal{H}|I-1J\tau\rangle = -(\bar{\zeta}'-\bar{\zeta}^2)\varphi(I_1,I)\eta(I,J)/4J(J+1) \qquad \text{(C13b)}$$

$$\langle IJ\tau|\mathcal{H}|I+1J\tau\rangle = -(\bar{\zeta}'-\bar{\zeta}^2)\varphi(I_1,I+1)\eta(I+1,J)/4J(J+1) \qquad \text{(C13c)}$$

in which we introduce the notation

$$\bar{\zeta}^i = \zeta_g M_g^{(i)} \langle J_g^2 \rangle \qquad \text{(C14)}$$

In the event that the two spins are similar (i.e. $I_1 = I_2$), are symmetrically situated in the molecule, and have equal spin-rotational couplings then the elements off-diagonal in I vanish and

$$\langle IJ\tau|\mathcal{H}|IJ\tau\rangle = \theta(I,J)\bar{\zeta} \qquad \text{(C15)}$$

as for the case of the single spin since $\theta(I_1,I)+\theta(I_2,I)=1$.

For the high field matrix elements (complete decoupling)

$$\langle \mathcal{H} \rangle = \frac{m_{I_1} m_J}{J(J+1)} \bar{\zeta}' + \frac{m_{I_2} m_J}{J(J+1)} \bar{\zeta}^2 \quad \text{unequal coupling} \qquad \text{(C16a)}$$

$$\langle \mathcal{H} \rangle = (m_{I_1}+m_{I_2}) m_J \bar{\zeta}/J(J+1) \qquad \text{(C16b)}$$

For grossly dissimilar coupling it is more convenient to use the alternate coupling scheme

Normal: $\vec{J}+\vec{I}_1=\vec{F}_1 \qquad \vec{F}_1+\vec{I}_2=\vec{F}$ (C17a)

Reversed: $\vec{\vec{I}}_2+\vec{F}=\vec{F}_1 \qquad \vec{\vec{I}}_1+\vec{F}_1=\vec{J}$ (C17b)

in which the matrix elements of (C11b) are

$$\langle F_1 J\tau|\mathcal{H}|F_1 J\tau\rangle = \theta(I_1,J)\bar{\zeta}' + \theta(I_2,F_1)\left(\theta(F_1,J)\right)\bar{\zeta}^2 \tag{C18a}$$

$$\langle F_1 J\tau|\mathcal{H}|F_1-1\,J\tau\rangle = -\varphi(I_2,F_1)\eta(F_1,J)\Sigma^2/4J(J+1) \tag{C18b}$$

3. Three Spins.

For three spins the following results obtain

$$\mathcal{H}=\sum_{i=1}^{3}\vec{I}_i\cdot\underset{\sim}{M}^{(i)}\cdot\vec{J} \tag{C19a}$$

$$\text{or}\quad \mathcal{H}=\sum_{i=1}^{3}\frac{\vec{I}_i\cdot\vec{J}}{J(J+1)}\,\vec{J}\cdot\underset{\sim}{M}^{(i)}\cdot\vec{J} \tag{C19b}$$

Coupling scheme.

Normal: $\vec{I}_1+\vec{I}_2=\vec{I}_{12}\ ;\ \vec{I}_{12}+\vec{I}_3=\vec{I}\ ;\ \vec{I}+\vec{J}=\vec{F}$ (C20a)

Reversed: $\vec{\vec{I}}_1+\vec{\vec{I}}_2=\vec{\vec{I}}_{12}\ ;\ \vec{\vec{I}}_{12}+\vec{\vec{I}}_3=\vec{\vec{I}}\ ;\ \vec{\vec{I}}+\vec{F}=\vec{J}$ (C20b)

$$\langle \bar{I}_{12}\bar{I}J\tau|\mathcal{H}|\bar{I}_{12}\bar{I}J\tau\rangle = \left(\left(\theta(I_1,I_{12})\bar{\zeta}' + \theta(I_2,I_{12})\bar{\zeta}^2\right)\theta(I_{12},I)+\theta(I_3,I)\bar{\zeta}^3\right)\theta(I,J) \tag{C21a}$$

$$\langle \bar{I}_{12}\bar{I}J\tau|\mathcal{H}|\bar{I}_{12}\bar{I}-1\,J\tau\rangle = \left(\theta(I_1,I_{12})\bar{\zeta}' + \theta(I_2,I_{12})\bar{\zeta}^2\right)\theta(I_{12},I)\frac{\eta(I,J)}{4J(J+1)} - \frac{\varphi(I_3,I)\eta(I,J)}{4J(J+1)}\bar{\zeta}^3 \tag{C21b}$$

vanishes for $\bar{\zeta}'=\bar{\zeta}^2=\bar{\zeta}^3$ since $\theta(I_1,I_{12})+\theta(I_2,I_{12})=1$ and $\varphi(I_{12},I)=\varphi(I_3,I)$ (C21c)

$$\langle \bar{I}_{12}\bar{I}J\tau|\mathcal{H}|\bar{I}_{12}-1\,\bar{I}J\tau\rangle = \left(\left(\varphi(I_{12},I)\bar{\zeta}' - \varphi(I_2,I_{12})\bar{\zeta}^2\right)\frac{\eta(I_{12},I)}{4I(I+1)} + \theta(I_3,I)\bar{\zeta}^3\right)\theta(I,J)$$

$$= \theta(I_3,I)\,\theta(I,J)\,\bar{\zeta}^3 \quad \text{for } \bar{\zeta}'=\bar{\zeta}^2$$

$$\langle \bar{I}_{12}\bar{I}J\tau|\mathcal{H}|\bar{I}_{12}\pm\bar{I}\mp 1J\tau\rangle = \left(\left(\tfrac{1}{2}\varphi(I_1,I_{12})\bar{\varepsilon}^1+\tfrac{1}{2}\varphi(I_2,I_{12})\bar{\varepsilon}^2\right)\tfrac{1}{2}\xi(I_{12},I)-\tfrac{1}{2}\varphi(I_3,I)\bar{\varepsilon}^3\right) \quad \text{(C21d)}$$
$$\times\, \eta(I,J)/2J(J+1)$$
$$= \varphi(I_3,I)\,\eta(I,J)/4J(J+1) \qquad \text{for } \bar{\varepsilon}'=\bar{\varepsilon}^2$$

In the event that two of the three spins are more strongly coupled to the rotation then the third we employ the alternate coupling scheme,

Normal: $\vec{I}_1+\vec{I}_2=\vec{I}_{12}\,;\ \vec{I}_3+\vec{J}=\vec{F}_1\,;\ \vec{F}_1+\vec{I}_{12}=\vec{F}$ (C22a)

Reversed: $\vec{I}_1+\vec{I}_2=\vec{I}_{12}\,;\ \vec{I}_{12}+\vec{F}=\vec{F}_1\,;\ \vec{F}_1+\vec{I}_3=\vec{J}$ (C22b)

in which the matrix elements of (19b) are found to be.

$$\langle \bar{I}_{12}F_1J\tau|\mathcal{H}|\bar{I}_{12}F_1J\tau\rangle = \left(\theta(I_{12},I)\bar{\varepsilon}^1+\theta(I_2,I_{12})\bar{\varepsilon}^2\right)\theta(I_{12},F_1)\theta(F_1,J)+\theta(I_3,J)\bar{\varepsilon}^3 \quad \text{(C23a)}$$

$$\langle \bar{I}_{12}F_1J\tau|\mathcal{H}|\bar{I}_{12}F_1-1J\tau\rangle = \left(\theta(I_{12},I)\bar{\varepsilon}^1+\theta(I_2,I_{12})\bar{\varepsilon}^2\right)\theta(I_{12},F)\,\frac{\eta(F_1,J)}{4J(J+1)} \quad \text{(C23b)}$$

$$\langle \bar{I}_{12}F_1J\tau|\mathcal{H}|\bar{I}_{12}\pm 1F_1J\tau\rangle = \left(\varphi(I_1,I_{12})\bar{\varepsilon}^1-\varphi(I_2,I_{12})\bar{\varepsilon}^2\right)\frac{\eta(I_{12},F_1)}{4F_1(F_1+1)}\theta(F_1,J)+\theta(I_3,J)\bar{\varepsilon}^3 \quad \text{(C23c)}$$

$$\langle \bar{I}_{12}F_1J\tau|\mathcal{H}|\bar{I}_{12}-1F_1-1J\tau\rangle = \left(\varphi(I_1,I_{12})\bar{\varepsilon}^1-\varphi(I_2,I_{12})\bar{\varepsilon}^2\right)\xi(I_{12},F_1)\,\frac{\eta(F_1,J)}{4J(J+1)} \quad \text{(C23d)}$$

G. REFERENCES

1. N. Bloembergen, E. M. Purcell, and R. V. Pound, Phys. Rev. 73, 679 (1948).

2. F. Bloch, Phys. Rev. 70, 460 (1946).

3. E. L. Hahn, Phys. Rev. 80, 580 (1950).

4. C. P. Slichter, Principles of Magnetic Resonance, Harper and Row, New York, 1963, Chapter 5.

5. P. S. Hubbard, Phys. Rev. 109, 1153 (1958); 111, 1746 (E) (1958).

6. I. Solomon, Phys. Rev. 99, 559 (1955).

7. I. Solomon and N. Bloembergen, J. Chem. Phys. 25, 261 (1956).

8. H. M. McConnell and C. H. Holm, J. Chem. Phys. 25, 1289 (1956).

9. A. Abragam, The Principles of Nuclear Magnetism, (Oxford University Press, London, 1961).

10. P. S. Hubbard, Phys. Rev. 131, 1155 (1963).

11. P. S. Hubbard, Phys. Rev. 131, 275 (1963).

12. H. S. Gutowsky and D. E. Woessner, Phys. Rev. 104, 843 (1956).

13. R. J. C. Brown, H. S. Gutowsky, and K. Shimomura, J. Chem. Phys. 38, 76 (1963). See especially footnote 19.

14. E. L. Mackor and C. MacLean, J. Chem. Phys. 42, 4254 (1965). Footnote 3a.

15. K. F. Kuhlman and J. D. Baldeschwieler, J. Chem. Phys. 43, 572 (1965).

16. D. K. Green and J. G. Powles, Proc. Phys. Soc. (London) 85, 87 (1965).

17. P. S. Hubbard, J. Chem. Phys. 42, 3546 (1965).

18. C. S. Johnson, J. S. Waugh, and J. N. Pinkerton, J. Chem. Phys. 35, 1128 (1961).

19. H. S. Gutowsky, I. J. Lawerson and K. Shimomura, Phys. Rev. Letters 6, 349 (1961).

20. J. H. Rugheimer and P. S. Hubbard, J. Chem. Phys. 39, 552 (1963).

21. W. R. Hackelman and P. S. Hubbard, J. Chem. Phys. 39, 2688 (1963).

22. R. W. Mitchell and M. Eisner, J. Chem. Phys. 33, 86 (1960); 34, 651 (1961).

23. A. M. Pritchard and R. E. Richards, Trans. Farad. Soc. 62, 1388 (1965); 62, 2014 (1966).

24. T. L. Pendred, A. M. Pritchard, and R. E. Richards, J. Chem. Soc., (A) 1009 (1966).

25. J. G. Powles and R. Figgins, Mol. Phys., 10, 155 (1966).

26. D. E. Woessner, J. Chem. Phys. 36, 1 (1962); 37, 647 (1962); 42, 1 (1965).

27. J. A. Pople, W. G. Schneider, and H. J. Bernstein, High-Resolution Nuclear Magnetic Resonance, McGraw-Hill Book Co., Inc., New York, 1959, Chapter 13.

28. J. W. Emsley, J. Feeney, and L. H. Sutcliffe, High Resolution Nuclear Magnetic Resonance Spectroscopy, Pergamom Press, Oxford, 1966, Volume 1, p. 551.

29. J. H. Van Vleck, Revs. Mod. Phys. 23, 213 (1951).

30. G. R. Gunther-Mohr, C. H. Townes, and J. H. Van Vleck, Phys. Rev. 94, 1191 (1954).

31. R. Schwartz, Ph.D. Thesis, Harvard University, 1953, (unpublished).

32. I. I. Rabi, N. F. Ramsey, and J. Schwinger, Revs. Mod. Phys. 26, 167 (1954).

32a. E. B. Wilson, Jr., C. C. Lin, and D. R. Lide, Jr., J. Chem. Phys. 23, 136 (1955).

33. E. L. Hahn, Phys. Rev. 80, 580 (1950).

33a. C. C. Lin and J. D. Swalen, Revs. Mod. Phys. 31, 841 (1959).

34. E. L. Hahn, Physics Today, November, 1953, p. 4.

35. H. Y. Carr and E. M. Purcell, Phys. Rev. 94, 630 (1954).

36. W. G. Clark, Rev. Sci. Instr. 35, 316 (1964).

37. J. Owen Maloy, Private Communication.

38. J. Gibson, Unpublished Results.

39. E. U. Condon and G. H. Shortley, The Theory of Atomic Spectra, Cambridge University Press, London, 1963, Chapter III.

40. D. W. Posener, Aust. J. Phys. 11, 1 (1958).

41. R. H. Faulk and M. Eisner, J. Chem. Phys. 44, 2926 (1966).

42. J. E. Anderson and W. P. Slichter, J. Chem. Phys. 43, 433 (1965).

43. J. G. Powles, Ber. Bunsen. Ges. f. Phys. Chem. 67, 328 (1963).

PART II

FLUORINE SPIN-ROTATION INTERACTION

AND

MAGNETIC SHIELDING IN FLUOROBENZENE

(Verbatim from: Sunney I. Chan and Alan S. Dubin, Journal of Chemical Physics, March 1, 1967).

A. INTRODUCTION.

In molecular beam magnetic resonance spectroscopy, the nuclear resonance of a magnetic nucleus frequently exhibits fine structure or is broadened due to the interaction of the magnetic nucleus with the magnetic field produced by end-over-end rotation of the molecule. This interaction, which is commonly referred to as spin-rotation, is described by the following Hamiltonian

$$\mathcal{H} = - \vec{I} \cdot \underset{\sim}{C} \cdot \vec{J} \qquad (1)$$

where $\underset{\sim}{C}$ is the spin-rotational tensor.

The importance of these spin-rotational constants lies in their intimate relationship with the high frequency part of the nuclear magnetic shielding constant. The absolute shielding constant, σ_N , for a nucleus N is related to the diagonal components of the spin-rotational tensor in the principal inertial axis system by (1)

$$\sigma_N = \frac{e^2}{3mc^2} \left\{ \langle \psi_0 | \sum_k \pi_{Nk}^{-1} | \psi_0 \rangle - \sum_{N' \neq N} Z_{N'} R_{NN'}^{-1} + \frac{h}{4M g_N \mu_N^2} \sum_{\alpha=a,b,c} C_{\alpha\alpha} I_\alpha \right\} \qquad (2)$$

Here π_{Nk} , $R_{NN'}$, denote, respectively the distance of this nucleus from the kth electron and the N'th nucleus in the molecule. e is the electron charge; m, the electron mass; c, the velocity of light; h, Planck's constant; M, the proton mass; μ_N , the nuclear magneton; and

g_N, the g-value of the nucleus whose shielding is under consideration. The $I_{\alpha\alpha}$'s are the principal moments of inertia of the molecule and the $C_{\alpha\alpha}$'s are the diagonal components of the spin-rotational tensor about these principal axes. The first term in equation (2) represents the diamagnetic contribution to the nuclear magnetic shielding. The sum of the remaining two terms is then the commonly referred to high frequency or paramagnetic contribution to the shielding. Since this paramagnetic contribution is a second order quantity, its accurate evaluation has encountered considerable difficulties despite several recent successful attempts for proton and fluorine chemical shifts employing variational procedures (2) and the perturbed Hartree-Fock method (3). Consequently, where feasible, a direct experimental determination of these molecular constants is clearly of interest.

As is well known, nuclear magnetic shielding provides an important probe for monitoring electron charge distributions within molecules. Consequently, magnetic shielding constants, together with other molecular properties, are of considerable fundamental importance towards the understanding of the electronic structures of molecules.

Thus, the use of these molecular constants as a check on the accuracy of approximate electronic wave functions is frequently invoked. Since most of these interactions are weak, they represent only small perturbations to the unperturbed electronic Hamiltonian and ab initio calculations of these interaction constants can therefore be made using perturbation and variational methods. A comparison of the calculated results with experimental values therefore not only serves to check the accuracy of approximate wave functions, but also tests the validity of certain approximations inherent in the various perturbation and variational schemes currently employed.

In this paper, we wish to report an experimental determination of the diagonal components of the fluorine spin-rotational tensor in fluorobenzene by the molecular beam magnetic resonance method. From these data and the known structure of the molecule, the high frequency part of the fluorine nuclear shielding, the absolute fluorine shielding, and the anisotrophy of the magnetic shielding tensor are determined. Fluorobenzene is a molecule of fundamental importance in any effort towards understanding the electronic structures of substituted aromatic systems. Unlike the chlorine and bromine nuclei in

chlorobenzene and bromobenzene, however, the F^{19} nucleus does not possess a nuclear quadrupole moment which can interact with electric field gradients at the point of substitution to yield a nuclear quadrupole interaction whereby the charge distribution may be monitored. Nevertheless, the F^{19} magnetic shielding in fluorobenzene can play an equally important role as the nuclear quadrupole interaction in the other halogenated benzenes. In fact, Karplus and Das (4) have attempted to relate the fluorine chemical shifts in fluorobenzene to such familiar localized bond parameters as ionic character, hybridization, and double-bond character.

B. EXPERIMENTAL.

The molecular beam apparatus used in the present experiments has been previously described (5). Beam detection was accomplished by means of an electron bombardment ionizer with an overall efficiency of 10^{-3} to 10^{-4}. For our present experiments, the mass spectrometer was tuned for mass 96, corresponding to the fluorobenzene positive ion. Under optimum operating conditions, the beam intensity was estimated to be 10^{9}

molecules per second and the beam to background ratio was about two to one.

Resonances were observed by phase-sensitive detection and on-off modulation of the r.f. current. The F^{19} resonance was taken at a frequency of about 7.14 Mc/s. The transition region was 3/4 inch in length. A r.f. current of 0.8 amp. was employed. This energizing current is approximately twice the theoretical optimum value. The proton resonance was observed at 7.59 Mc/s. The proton spectrum was more confined and intense. Here the r.f. current was 0.32 amp., which is close to optimum. The transition region was also 3/4 inch in length.

Reagent grade fluorobenzene was obtained from the Eastman Kodak Co. and was used without further purification. Both the fluorine and proton resonances were taken at room temperature.

C. SPECTRA.

The radiofrequency spectrum corresponding to the reorientation of the F^{19} nuclear moment is given in Figure 1a. The spectrum is not resolved and has a full width at half height of about 150 kc/s.

FIGURE 1a. Fluorine resonance spectrum in C_6H_5F at room temperature.

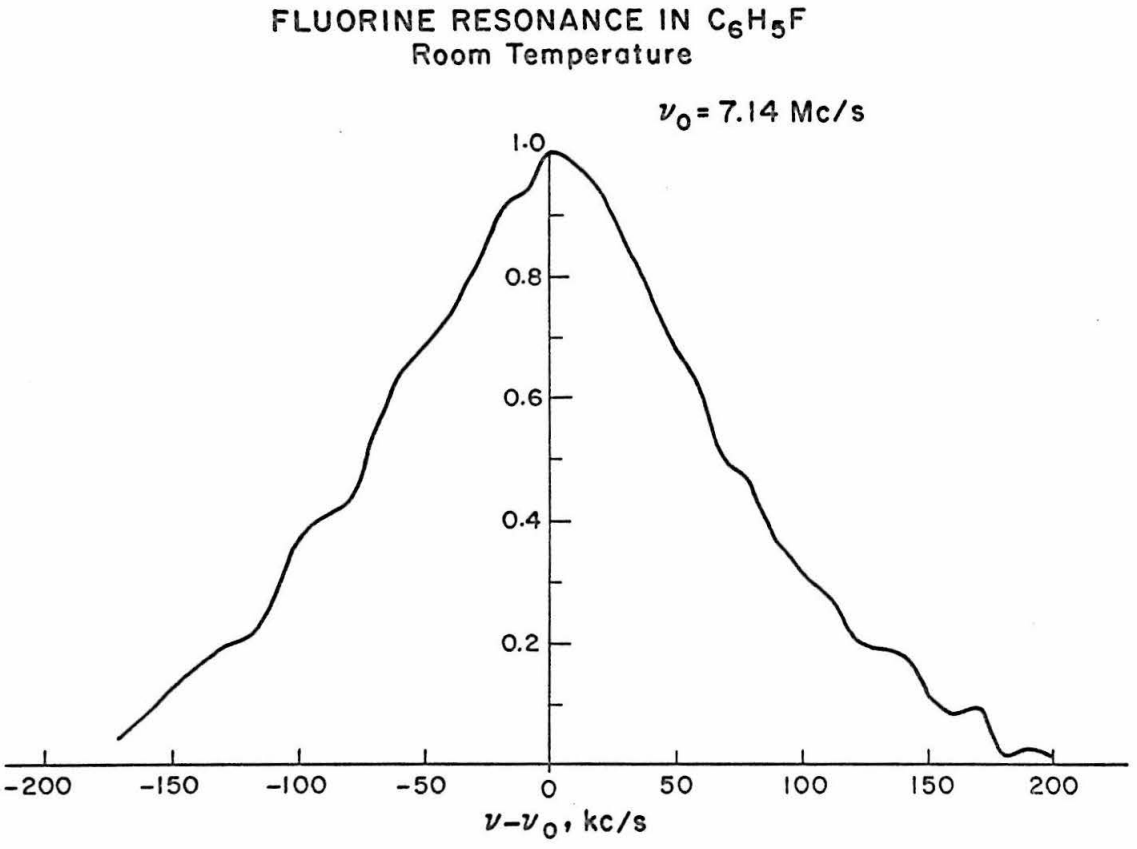
FLUORINE RESONANCE IN C_6H_5F
Room Temperature
ν_0 = 7.14 Mc/s
1.0
0.8
0.6
0.4
0.2
-200
-150
-100
-50
0
50
100
150
200
$\nu-\nu_0$, kc/s

The spectrum corresponding to the reorientation of the H^1 nuclear moment is shown in Figure 1b. This spectrum is also unresolved. However, in contrast to the width of the fluorine resonance, the proton resonance is only 20 kc/s broad.

D. INTERPRETATION.

The Hamiltonian for the fluorobenzene molecule in an external magnetic field can be written as

$$\mathcal{H} = \mathcal{H}_Z + \mathcal{H}_{SR} + \mathcal{H}_{SS} + \mathcal{H}_{DH} \qquad (3)$$

$\mathcal{H}_Z$ is the Zeeman part of the Hamiltonian and includes in addition to the interactions of the various magnetic nuclei in the molecule (fluorine and protons) with the applied field, a similar interaction for the molecular rotational moment. $\mathcal{H}_{SR}$ is the spin-rotational energy and represents the magnetic coupling of the various magnetic nuclei to the rotational magnetic field produced by end-over-end rotation of the molecule. $\mathcal{H}_{SS}$ expresses the spin-spin interaction between pairs of magnetic nuclei and includes both the direct dipole-dipole and the electron-coupled interactions. $\mathcal{H}_{DH}$ represents the orientation-dependent part of the molecular

FIGURE 1b. Proton resonance spectrum in C_6H_5F at room temperature.

PROTON RESONANCE IN C_6H_5F
Room Temperature

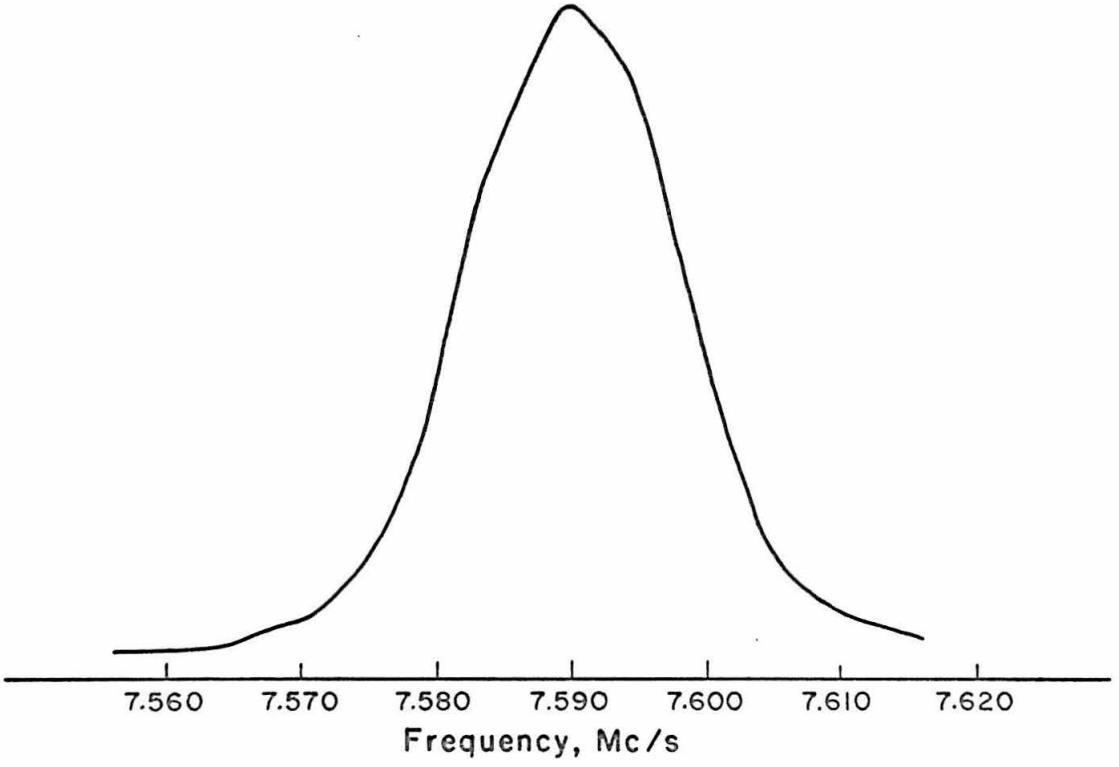

diamagnetic interaction with the external field.

Any Hamiltonian which contains terms involving the mutual interaction of seven angular momenta in an asymmetric rotor is complex. However, our present analysis of the problem is greatly simplified in that the experiments were carried out in an external field under conditions where the Zeeman interactions predominate over the remaining coupling terms in the Hamiltonian. Not only is it then reasonable to construct the Hamiltonian matrix in the uncoupled representation in which all the angular momenta are decoupled from one another, but the energy levels are also well approximated by the diagonal elements of this matrix. Furthermore, in this first order theory, $\mathcal{H}_{DH}$ will not contribute to the nuclear transition frequencies $(\Delta J=0, \Delta M_J=0, \Delta M_I=\pm 1 \quad \Delta M_{I'}=0 \quad I\neq I'$; neither will those terms in $\mathcal{H}_Z$, $\mathcal{H}_{SR}$, and $\mathcal{H}_{SS}$ which do not involve directly the nuclear moment under consideration. This, of course, includes that term in $\mathcal{H}_Z$ which describes the interaction of the rotational magnetic moment with the applied magnetic field.

We now show that spin-spin interaction cannot account for the line width of the fluorine resonance spectrum. First of all, we can rule out the electron-coupled part

of the interaction since these coupling constants (6) are only 10 cp/s. In discussing the effects of the direct dipole-dipole interaction, let us be specific and consider the spin-spin interaction between the fluorine and the ortho-protons. The pertinent terms in the Hamiltonian are then

$$\left(\frac{\mu_F}{I_F}\right)\left(\frac{\mu_H}{I_H}\right)\frac{1}{R^3} \times\left(\vec{I}_{H_1}\cdot\vec{I}_F - \frac{3(\vec{I}_{H_1}\cdot\vec{R}_1)(\vec{I}_F\cdot\vec{R}_1)}{R_1^2} + \vec{I}_{H_2}\cdot\vec{I}_F - \frac{3(\vec{I}_{H_2}\cdot\vec{R}_2)(\vec{I}_H\cdot\vec{R}_2)}{R_2^2}\right) \quad (4)$$

where μ_F and μ_H are respectively the magnitude of the fluorine and proton nuclear moments; $\vec{I}_F$ and $\vec{I}_H$ are the fluorine and proton spin operators; and $\vec{R}_i$ denotes the radius vector from the fluorine to the ith proton (i=1,2). By symmetry, $|\vec{R}_1| = |\vec{R}_2| = R$. Since the coupling constant $\left(\frac{\mu_F}{I_F}\right)\left(\frac{\mu_H}{I_H}\right)\frac{1}{R^3}$ is only 6 kc/s, any splittings of the fluorine resonance due to this fluorine-proton spin-spin interaction is confined within the molecular beam resonance line width, which in this study is 12 - 13 kc/s (full width at half-intensity). The coupling constants for the meta- and para-proton coupling are even smaller. On the above basis, we can therefore conclude that spin-spin interaction cannot contribute significantly to the overall width of the fluorine resonance spectrum. This

leaves the fluorine spin-rotational interaction as the only source of broadening for the fluorine spectrum. Actually, the gross difference between the widths of the fluorine and proton spectra is strong evidence that the principal source of broadening in the fluorine resonance is spin-rotational interaction. If spin-spin interaction was important, then by virtue of the similar magnitudes of the fluorine and proton nuclear moments and the symmetrical distribution of these magnetic nuclei, both the fluorine and proton resonance spectra should exhibit somewhat similar widths. On the other hand, large differences in the fluorine and proton spin-rotational interactions within the same molecule are not unknown and are to be expected. For example, in hydrogen fluoride (5), C_F is -305 kc/s and C_H is ±71 kc/s.

In the next section, we shall attempt to analyze the observed fluorine resonance spectrum in terms of the following considerably simplified Hamiltonian

$$\frac{\mathcal{H}^{(F)}}{\hbar} = -\nu_0 \vec{I}_F \cdot \frac{\vec{H}}{H} - \vec{I}_F \cdot \underset{\sim}{C}_F \cdot \vec{J} \qquad (5)$$

$$= -\nu_0 \frac{\vec{I}_F \cdot \vec{H}}{|H|} - \bar{C}_{gg'} C^F_{gg'} I_{Fg} J_{g'}$$

The diagonal elements of $\mathcal{H}^{(F)}/\hbar$ in the uncoupled J,τ,I_F,M_J,M_F scheme are

$$\langle \mathcal{H}^{(F)}/h \rangle = -\nu_0 M_F - \sum_{gg'} C^F_{gg'} \langle J\tau I_F M_J M_F | I_{Fg} J_{g'} | J\tau I_F M_J M_F \rangle$$

$$= -\nu_0 M_F - \sum_{gg'} C^F_{gg'} \sum_{\tau} \langle J\tau I_F M_J M_F | I_{Fg} | J\tau' I_F M_J M_F \rangle \quad (6)$$

$$\times \langle J\tau' I_F M_J M_F | J_{g'} | J\tau I_F M_J M_F \rangle$$

Since 7,8

$$\langle J\tau I_F M_J M_F | I_{Fg} | J\tau' I_F M_J M_F \rangle$$

$$= \frac{1}{J(J+1)} \langle J\tau I_F M_J M_F | J_g | J\tau' I_F M_J M_F \rangle \langle J\tau' I_F M_J M_F | \vec{J}\cdot\vec{I}_F | J\tau' I_F M_J M_F \rangle$$

(7)

$$= \frac{M_F M_J}{J(J+1)} \langle J\tau I_F M_J M_F | J_g | J\tau' I_F M_J M_F \rangle$$

we have from expression (6)

$$\langle \mathcal{H}^{(F)}/h \rangle = -\nu_0 M_F - \frac{M_F M_J}{J(J+1)} \sum_g C^F_{gg} \langle J\tau | J^2_g | J\tau \rangle \quad (8)$$

predicting fluorine nuclear transitions at the following frequencies:

$$\nu(J,\tau,M_J) = \nu_0 + M_J \sum_g C^F_{gg} \frac{\langle J\tau | J^2_g | J\tau \rangle}{J(J+1)} \quad (9)$$

Since well over 100 J levels of the fluorobenzene molecule are populated at room temperature (Figure 2), we see that the full width of the fluorine resonance can be as much as 400 kc/s if the C^F_{gg} 's are approximately 1 - 2 kc/s.

A similar analysis of the observed proton resonance will not be attempted. The proton resonance spectrum is not only a composite spectrum over many rotational states, but also includes contributions from three sets of non-equivalent protons. Thus, three sets of C^H_{gg} 's are involved here, and the extraction of nine constants from the analysis of a simple unresolved spectrum would be an impossible task. Moreover, since the proton resonance spectrum is not much wider than the width of a single resonance transition, the method we have adopted for the analysis of the fluorine resonance spectrum is not applicable.

E. SPECTRAL ANALYSIS.

1. Method of Analysis.

For $^1\Sigma$ linear molecules, where $C_{aa} = C_{\parallel} = 0$ and $C_{bb} = C_{cc} = C_{\perp}$. spin-rotational splittings in the

FIGURE 2. Rotational population distribution for fluorobenzene.

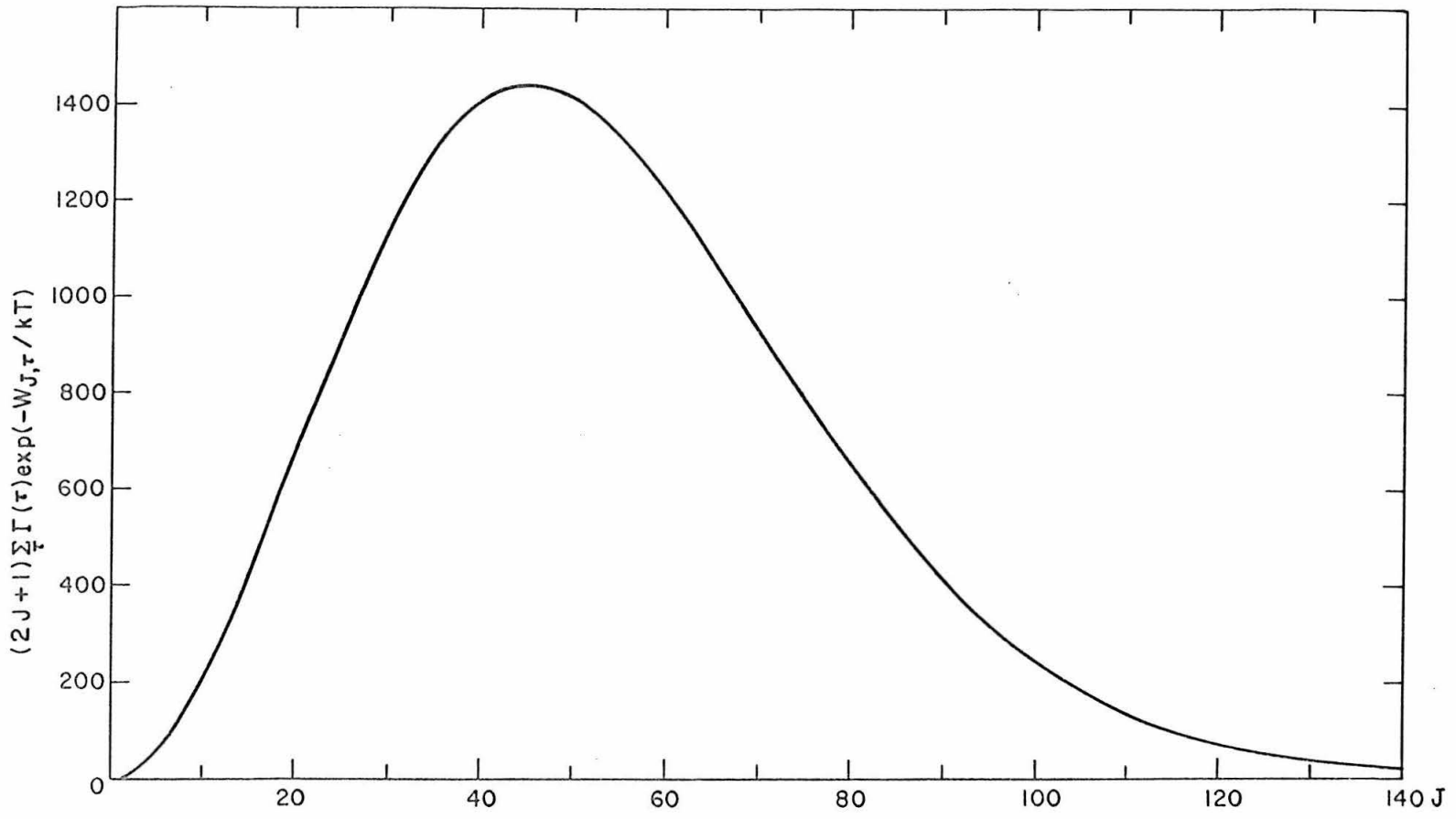
1400
1200
1000
800
600
400
200
0
20
40
60
80
100
120
140 J
$(2J+1)\sum_{\tau}\Gamma(\tau)\exp(-W_{J,\tau}/kT)$

molecular beam nuclear magnetic resonance are often resolved and the coupling constant $C_\perp$ unambiguously determined. However, where the coupling constant becomes of the same order of magnitude as the nuclear resonance line width, for example in heavy diatomic molecules, spherical tops, symmetric and asymmetric top molecules, statistical methods must be employed to extract the coupling constant from the partially resolved or unresolved spectra arising from the superposition of the various $\Delta J=0$, $\Delta M_J=0$, $\Delta M_I=\mp 1$ transitions. Such statistical methods of spectral analysis have indeed been developed (9); however, they are limited to diatomic and spherical top molecules where the spectrum depends or may depend, explicitly on one experimental constant. For symmetric and asymmetric top molecules, where two or three spin-rotational constants are explicitly involved, these statistical methods are clearly not directly applicable.

In this section, we develop a method of moment analysis for extracting spin-rotational constants from unresolved molecular beam magnetic resonances. Even though the method is quite general and is in principle applicable to any molecule, its application cannot be made without some care, since in some incidences, the moments of

the resonance, in particular the higher moments, may be rather poorly defined. Furthermore, as we shall see, the solution of the moment equations in general tends to emphasize one or two of the interaction constants so that the remaining constants are determined with considerably poorer accuracy. Despite these shortcomings, however, the moment technique can be extremely useful in arriving at a preliminary set of constants which can later be refined by iterative syntheses of the composite spectrum.

Let us consider the following n th absolute moment of a resonance spectrum defined by

$$M_n = \int_{-\infty}^{\infty} |\nu-\nu_0|^n I(\nu)\, d\nu \Big/ \int_{-\infty}^{\infty} I(\nu)\, d\nu \qquad (10)$$

$I(\nu)$ is the intensity of the experimental resonance spectrum at frequency ν . We will assume that $I(\nu)$ is symmetric about ν_0 ; that is, the resonance spectrum is symmetric about the nuclear Larmor frequency. This is not a serious assumption, as in the absence of other strong magnetic interactions, first order theory predicts a symmetric spectrum for a resonance broadened by spin-rotation interaction. The normal odd moments of a symmetric resonance vanish identically, thus it is

clear that to take full advantage of the experimental data, we should consider the absolute moments.

The theoretical moments can be predicted as follows.

$$M_n = \frac{\int_0^\infty x^n \sum_{v,J,\tau} \sum_{M_J=-J}^{+J} \Gamma(v,J,\tau) \exp(-W_{vJ\tau}/kT) f(x-x_{vJ\tau M_J})\, dx}{\int_0^\infty \sum_{v,J,\tau} \sum_{M_J=-J}^{+J} \Gamma(v,J,\tau) \exp(-W_{vJ\tau}/kT) f(x-x_{vJ\tau M_J})\, dx}$$

$$= \frac{\sum_{v,J,\tau,M_J} \Gamma(v,J,\tau) \exp(-W_{vJ\tau}/kT) \int_0^\infty x^n f(x-x_{vJ\tau M_J})\, dx}{\sum_{v,J,\tau,M_J} \Gamma(v,J,\tau) \exp(-W_{vJ\tau}/kT) \int_0^\infty f(x-x_{vJ\tau M_J})\, dx} \qquad (11)$$

where, to be as general as possible, we focus our attention on discussing the asymmetric rotor. $x = \nu - \nu_0$, and

$$x_{vJ\tau M_J} = M_J \sum_g C_{gg} \langle vJ\tau | J_g^2 | vJ\tau \rangle / J(J+1)$$

$W_{vJ\tau}$ is the energy of the asymmetric rotor in its vth vibrational state and J, τ th rotational state. $\Gamma(v, J, \tau)$ is the nuclear statistical weight factor for this level. $f(x-x_{vJ\tau M_J})$ represents the line-shape function for each resonance transition. Throughout, we shall ignore the dependence of the C_{gg}'s on the vibrational-rotational state, that is, we ignore vibrational and centrifugal effects. If we further assume that the rotational energy levels are essentially independent of the vibrational

state, and that the temperature is sufficiently high to ignore statistical weights, equation (11) simplifies to

$$M_n = \frac{\sum_{J,\tau} \sum_{M_J=-J}^{J} \exp(-W_{J\tau}/kT) \int_0^\infty x^n f(x - x_{J\tau M_J})\, dx}{\sum_{J,\tau} \sum_{M_J=-J}^{J} \exp(-W_{J\tau}/kT) \int_0^\infty f(x - x_{J\tau M_J})\, dx} \qquad (12)$$

The next obvious approximation is that of replacing the line-shape function $f(x - x_{J\tau M_J})$ by the Dirac delta function $\delta(x - x_{J\tau M_J})$. This approximation leads to great simplifications for the moment equations. It is only rigorously valid in the limit where the width of the resonance spectrum is much greater than the width of the individual resonance transition. This condition is pretty well satisfied by the fluorine resonance in fluorobenzene.

Within this approximation,

$$M_n = \frac{\sum_{J\tau} \sum_{M_J=0}^{J} x^n_{J\tau M_J} \exp(-W_{J\tau}/kT)}{\sum_{J\tau} (J+\tfrac{1}{2}) \exp(-W_{J\tau}/kT)} \qquad (13)$$

The first, second, and third theoretical moments are then given by

$$M_1 = \sum_{\alpha} \sigma_\alpha C_{\alpha\alpha} \tag{13a}$$

$$M_2 = \sum_{\alpha,\beta} \sigma_{\alpha\beta} C_{\alpha\alpha} C_{\beta\beta} \tag{13b}$$

$$= \sum_{\alpha} \sigma_{\alpha\alpha} C_{\alpha\alpha}^2 + 2 \sum_{\alpha>\beta} \sigma_{\alpha\beta} C_{\alpha\alpha} C_{\beta\beta}$$

$$M_3 = \sum_{\alpha,\beta,\gamma} \sigma_{\alpha\beta\gamma} C_{\alpha\alpha} C_{\beta\beta} C_{\gamma\gamma} \tag{13c}$$

$$= \sum_{\alpha} \sigma_{\alpha\alpha\alpha} C_{\alpha\alpha}^3 + 3 \sum_{\alpha\neq\beta} \sigma_{\alpha\alpha\beta} C_{\alpha\alpha}^2 C_{\beta\beta} + 6 \sigma_{\alpha\beta\gamma} C_{\alpha\alpha} C_{\beta\beta} C_{\gamma\gamma}$$

where the indices α, β, and γ all run through a, b, and c, labels for the principal axes of the molecule, and

$$\sigma_\alpha = \frac{\sum_{J,\tau} \langle J\tau | J_\alpha^2 | J\tau \rangle \exp(-W_{J\tau}/kT)}{\sum_{J\tau} (2J+1) \exp(-W_{J\tau}/kT)}$$

$$\sigma_{\alpha\beta} = \frac{\sum_{J,\tau} \langle J\tau | J_\alpha^2 | J\tau \rangle \langle J\tau | J_\beta^2 | J\tau \rangle \frac{2J+1}{J(J+1)} \exp(-W_{J\tau}/kT)}{3 \sum_{J,\tau} (2J+1) \exp(-W_{J\tau}/kT)}$$

$$\sigma_{\alpha\beta\gamma} = \frac{\sum_{J,\tau} \langle J\tau|J_\alpha^2|J\tau\rangle\langle J\tau|J_\beta^2|J\tau\rangle\langle J\tau|J_\gamma^2|J\tau\rangle \frac{1}{J(J+1)} \exp(-W_{J\tau}/kT)}{2\sum_{J\tau}(2J+1)\exp(-W_{J\tau}/kT)}$$

Obviously, $\sigma_{\alpha\beta} = \sigma_{\beta\alpha}$, and $\sigma_{\alpha\beta\gamma} = \sigma_{\alpha\gamma\beta} = \sigma_{\beta\alpha\gamma} = \sigma_{\beta\gamma\alpha} = \sigma_{\gamma\alpha\beta} = \sigma_{\gamma\beta\alpha}$.

Equating equation 13 (a) - (c) to the experimental first, second, and third moments yields three equations from which the three diagonal components of the spin-rotational tensor can be obtained. This system of equations is non-linear and one must resort to numerical or graphical methods for solution. The coefficients in these equations are all infinite sums, but in practice one needs merely to sum over all the significantly occupied rotational levels of the molecule.

2. Comparison of the Method of Moment Analysis with Existing Statistical Methods.

Before applying the method developed in the previous section to the analysis of the fluorine resonance spectrum in fluorobenzene, it is perhaps important to show that the method of moments leads to identical results

when compared with previously developed statistical methods for linear and spherical top molecules. We now demonstrate this equivalence.

(a) Linear Molecules

Consider the superposition molecular beam spectrum corresponding to the magnetic reorientation of a magnetic nucleus in a linear molecule. Assume for simplicity of discussion that there is only one magnetic nucleus in the molecule, and that its spin is $\frac{1}{2}$ to eliminate electric quadrupole effects. For a linear molecule, $\nu = \nu_0 + C_\perp M_J$. Since, except for a small dependence of $C_\perp$ on vibrational-rotational state, these transitions are otherwise independent of v, J and are solely dependent on M_J, the intensity of the molecular beam composite spectrum at frequency ν is given by

$$I(\nu) \propto \sum_{\substack{J=|M_J| \\ =|(\nu-\nu_0)/C_\perp|}}^{\infty} \Gamma(J) \exp\left(-B\,J(J+1)/kT\right) \qquad (14)$$

B is the rotational constant of the molecule. Under the circumstances where nuclear spin statistics may be ignored and where

$$B/kT \ll 1$$

$$I(\nu) \propto \int_{\left|\frac{\nu-\nu_0}{C_\perp}\right|}^{\infty} \exp\left(-BJ(J+1)/kT\right) dJ$$

$$\cong \frac{1}{2}\left(\frac{\pi kT}{B}\right)^{1/2}\left(1-\operatorname{erf}\left(\left(\frac{B}{kT}\right)^{1/2}\left|(\nu-\nu_0/C_\perp\right|\right)\right) \qquad (15)$$

Erf (x) is the error function. This intensity distribution, which has previously been obtained by Nierenberg and Ramsey (9) yields a full width at half height of $1.91\ C_\perp\ /\ (kT/B)^{\frac{1}{2}}$ for the composite spectrum.

To establish the equivalence of the method of moments and the approach just described, it is adequate to show that the intensity distribution given by equation (15) yields the same moments as that predicted by equations 13 (a) - (c). Since only one spin-rotational constant is involved here, we shall merely concern ourselves with the first moment. Upon direct integration of equation (15), we obtain

$$M_1 = \int_0^\infty \chi\left(1-\operatorname{erf}\left(\left(\frac{B}{kT}\right)^{1/2}\frac{|\chi|}{C_\perp}\right)\right) \Big/ \int_0^\infty \left(1-\operatorname{erf}\left(\left(\frac{B}{kT}\right)^{1/2}\frac{|\chi|}{C_\perp}\right)\right) d\chi \qquad (16)$$

$$= \frac{1}{4} C_\perp \left(\frac{\pi kT}{B}\right)^{1/2}$$

From equation 13 (a), the first moment can be approximated by

$$M_1 \simeq C_\perp \int_0^\infty J(J+1)\exp(-BJ(J+1)/kT)\,dJ \Big/ \int_0^\infty (2J+1)\exp(-BJ(J+1)/kT)\,dJ$$

$$= \frac{1}{8} C_\perp \left(\frac{\pi B}{kT}\right)^{1/2} (2kT/B - 1)\exp(B/4kT) \qquad (17)$$

which in the limit B/kT << 1, reduces to the same result given in (16).

(b) Spherical Top Molecules

A spherical top molecule, such as CF_4, SF_6, CH_4, etc., contains in addition to the central atom, a number of equivalent nuclei. For the central atom, if it is magnetic, the coupling of the magnetic moment with overall rotation is still given by (5), and since $\langle J_a^2 \rangle = \langle J_b^2 \rangle = \langle J_c^2 \rangle = J(J+1)/3$, may be rewritten as

$$-\bar{C}\,\vec{I}\cdot\vec{J}$$

where $\bar{C} = 1/3 \sum_\alpha C_{\alpha\alpha}$. For the equivalent nuclei,

$$\mathcal{H}_{SR}/h = -\sum_k \vec{I}_k \cdot \underset{\sim}{C}(k) \cdot \vec{J}$$

Unlike the spin-rotational coupling for equivalent nuclei in a linear molecule, where the C(k) 's are equal so that the spin-rotational Hamiltonian may be simply expressed in terms of the resultant nuclear spin vector $\vec{I} = \sum_k \vec{I}_k$ some of the C(k) tensors for a spherical top molecule are in general different. However, since these various C(k)

tensors are merely related to each other by similarity transformations, it is possible to reexpress the spin-rotational Hamiltonian in terms of an overall scalar coupling term, $\bar{C}\,\vec{I}\cdot\vec{J}$, plus a tensor coupling term involving the anisotropy in the spin-rotational tensor. If $C_{\parallel}$ and $C_{\perp}$ refer to diagonal components of the spin-rotational tensor parallel and perpendicular to one of the bond axes, $\bar{C} = 1/3\ (2C_{\perp} + C_{\parallel})$ and anisotropy $= C_{\parallel} - C_{\perp}$.

In the analysis of unresolved molecular beam resonance spectra for a spherical top molecule, it is generally assumed that the spin-rotational coupling may be adequately represented by the scalar coupling term. As mentioned above, this assumption is not always valid. In any event, if this were an adequate approximation, the shape of the molecular beam magnetic resonance spectrum would be essentially gaussian. Extending the statistical approach of Nierenberg and Ramsey, we find that the intensity of a composite molecular beam spectrum due solely to spin-rotational coupling is given by

$$I(\nu) \propto \sum_{J=|M_J|}^{\infty} \Gamma(J)\,(2J+1)\,\exp\left(-BJ(J+1)/kT\right)$$
$$= |(\nu-\nu_0)/\bar{C}|$$

$$\longrightarrow \int_{\left|\frac{\nu-\nu_0}{\bar{C}}\right|}^{\infty} (2J+1)\, \exp\left(-BJ(J+1)/kT\right) dJ$$

$$= \left(\frac{kT}{B}\right) \exp\left(-\left(\frac{B}{kT}\right)\left|\frac{x}{\bar{C}}\right| / \left(1+\left|\frac{x}{\bar{C}}\right|\right)\right)$$

(18)

The full width at half height of the resonance spectrum would be $\sim 1.66\ \bar{C}\ (kT/B)^{\frac{1}{2}}$. The first moment of this resonance spectrum would be $(\bar{C}kT/B\pi)^{\frac{1}{2}}$. This value is to be compared with a first moment of $(\bar{C}kT/B\pi)^{\frac{1}{2}}$ exp-(B/4kT) obtained from equation 13 (a) after the infinite sum has been replaced by the appropriate integral.

3. Application of Fluorobenzene.

The rotational energy levels of the fluorobenzene molecule and expectation value of the squares of the rotational angular momenta along the principal inertia axes of the molecule for each J, τ rotational level are needed for evaluating σ_α , $\sigma_{\alpha\beta}$, $\sigma_{\alpha\beta\gamma}$. These were obtained by diagonalizing the rotational energy matrix of the molecule constructed in the symmetric rotor

representation and transforming one of the angular momentum matrices in the standard way. $\underset{\sim}{J_a^2}$ was transformed and $\underset{\sim}{J_b^2}$ and $\underset{\sim}{J_c^2}$ were obtained by solving

$$W_{J\tau} = A\langle J_a^2\rangle + B\langle J_b^2\rangle + C\langle J_c^2\rangle$$

and $$J(J+1) = \langle J_a^2\rangle + \langle J_b^2\rangle + \langle J_c^2\rangle$$

The necessary structural parameters were taken from the microwave data of Bak et al (10). The coefficients σ_α, $\sigma_{\alpha\beta}$, $\sigma_{\alpha\beta\gamma}$ are infinite sums over J, τ. However, contributions from the higher J states are slowly damped out by the Boltzmann factor. Figure 3 illustrates the convergence of these coefficients to their limiting asymptotic values given in Table I. As can be seen, the slowest converging coefficient converges essentially at J=140.

All total, four experimental fluorine resonances were obtained. Within experimental error, they were all nearly gaussian with a full width at half-intensity of 155 $\pm$ 10 kc/s. The width of the resonance line was more reproducible from run to run than the details of the resonance. Consequently, the data were averaged prior to the determination of the experimental moments. Data points taken every 10 kc/s interval were then fitted to

FIGURE 3 a,b. Convergence of the coefficients in the moment equations.

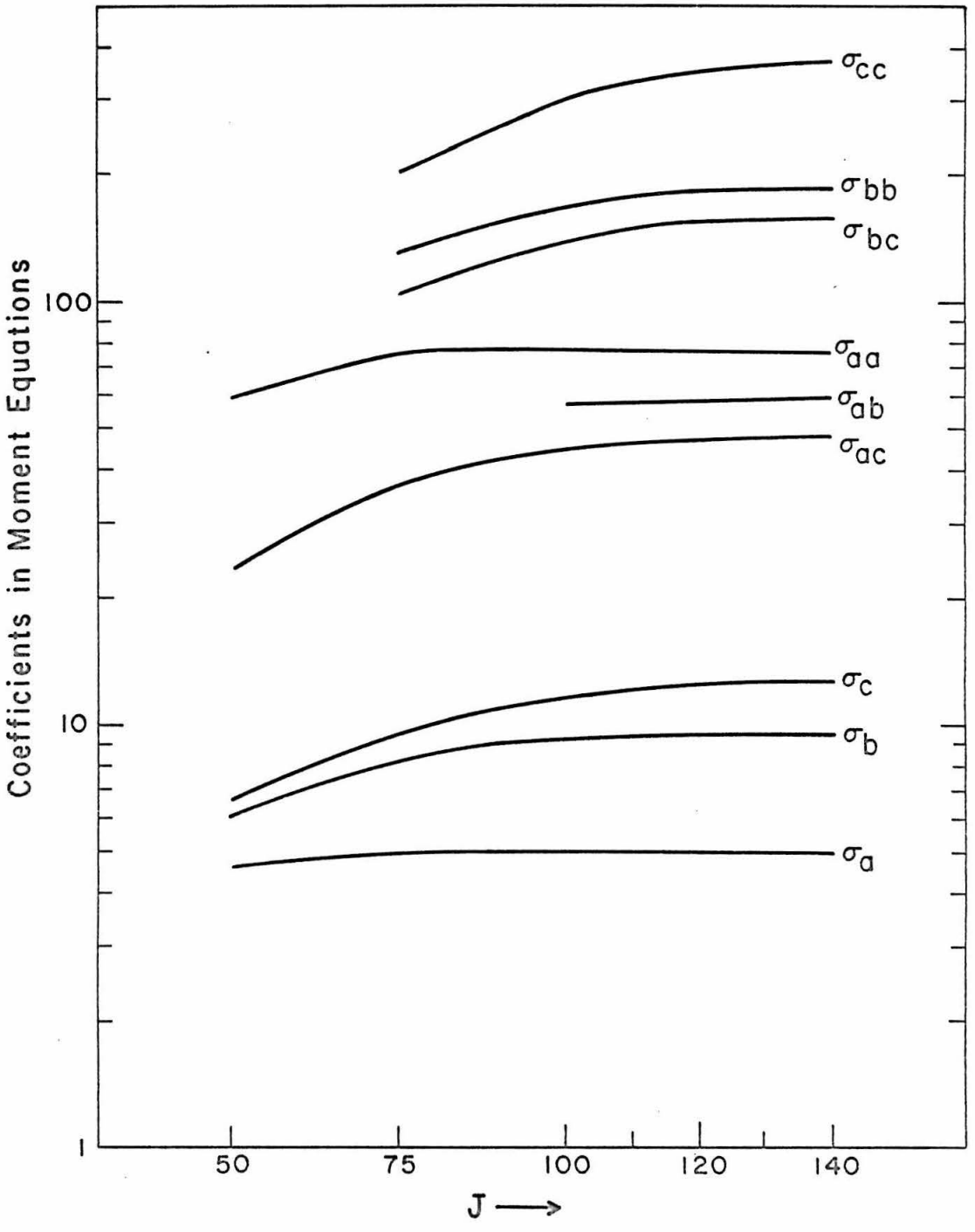
Coefficients in Moment Equations
100
10
1
50
75
100
120
140
J ⟶
σcc
σbb
σbc
σaa
σab
σac
σc
σb
σa

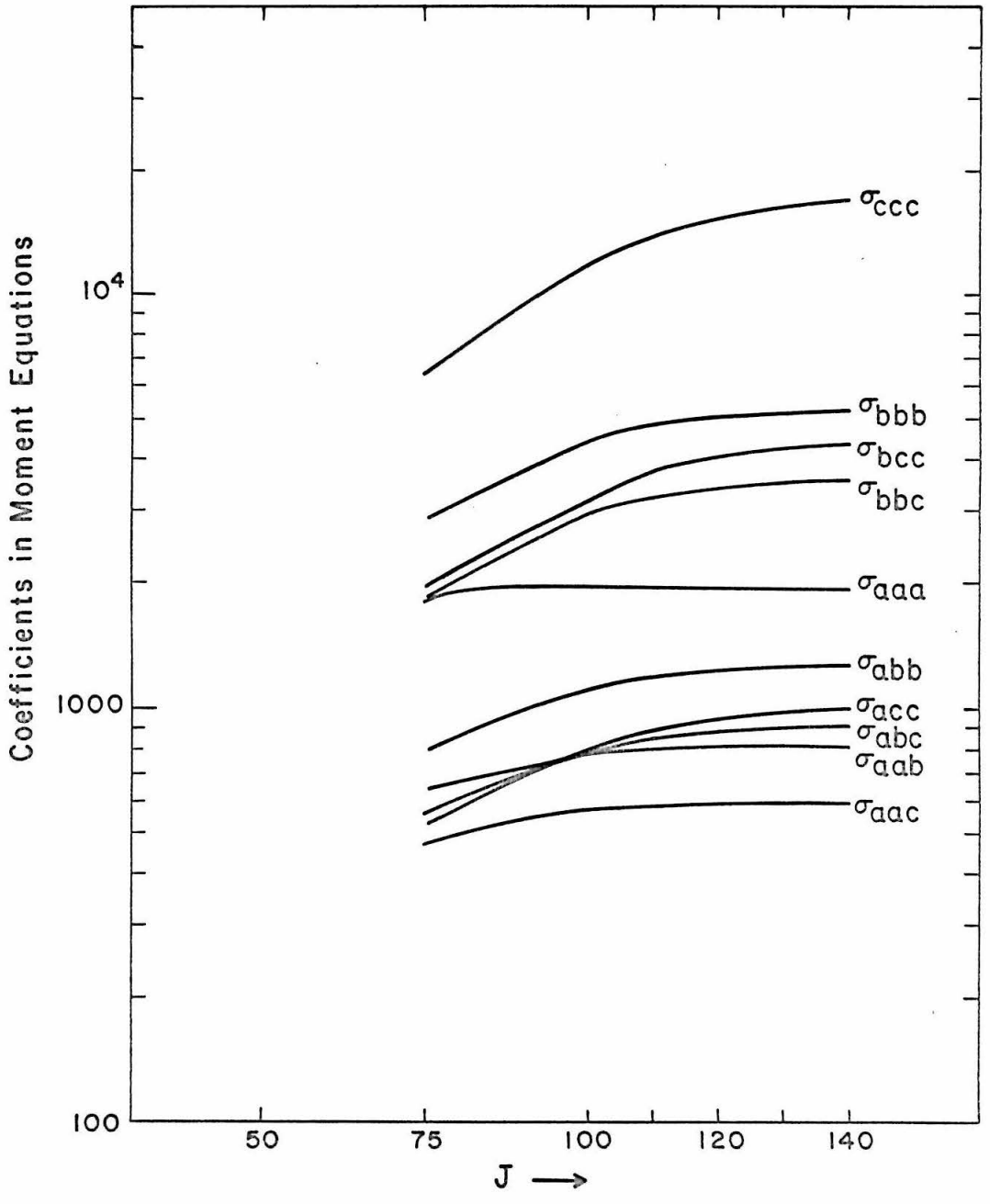
Coefficients in Moment Equations
10^4
1000
100
50
75
100
120
140
J ⟶
σ_{ccc}
σ_{bbb}
σ_{bcc}
σ_{bbc}
σ_{aaa}
σ_{abb}
σ_{acc}
σ_{abc}
σ_{aab}
σ_{aac}

Table I. Coefficients of the Moment Equations

σ_a	4.949
σ_b	9.435
σ_c	12.560
σ_{aa}	75.62
σ_{ab}	58.99
σ_{ac}	47.97
σ_{bb}	184.81
σ_{bc}	156.66
σ_{cc}	370.46
σ_{aaa}	1.902×10^3
σ_{aab}	0.8012×10^3
σ_{aac}	0.5877×10^3
σ_{abb}	1.254×10^3
σ_{abc}	0.9012×10^3
σ_{bbb}	5.222×10^3
σ_{bbc}	3.537×10^3
σ_{bcc}	4.334×10^3
σ_{cac}	0.9872×10^3
σ_{ccc}	1.705×10^4

(a) a single gaussian function, and (b) a sum of two gaussian functions, by the method of least squares. Each half of the resonance spectrum was treated separately and the results compared. On the whole, a better overall fit to the data points was provided by the sum of two gaussian functions, particularly in the regions towards the center of the resonance peak and in the wings (see Figure 4).

The experimental moments were computed on the basis of the analytical functions obtained from least square fits of the experimental data. These results are tabulated in Table II. For either the single gaussian or two gaussian fits, there is little difference in the parameters of the analytical functions or the computed moments for the two halves of the resonance spectrum, a result to be expected if the resonance spectrum is symmetric. On the other hand, the single and two gaussian fits yield significantly different second and third moments. This emphasizes the importance of proper consideration of the wings of the resonance for reliable values of the higher moments. As the sum of two gaussians improved the least square fitting of the experimental data at the tails of the resonance, it is probable that

FIGURE 4. Least-squares fits of the fluorine resonance spectrum. ----, least-squares fit by single gaussian; ——, least-squares fit by two gaussians; •, experiment.

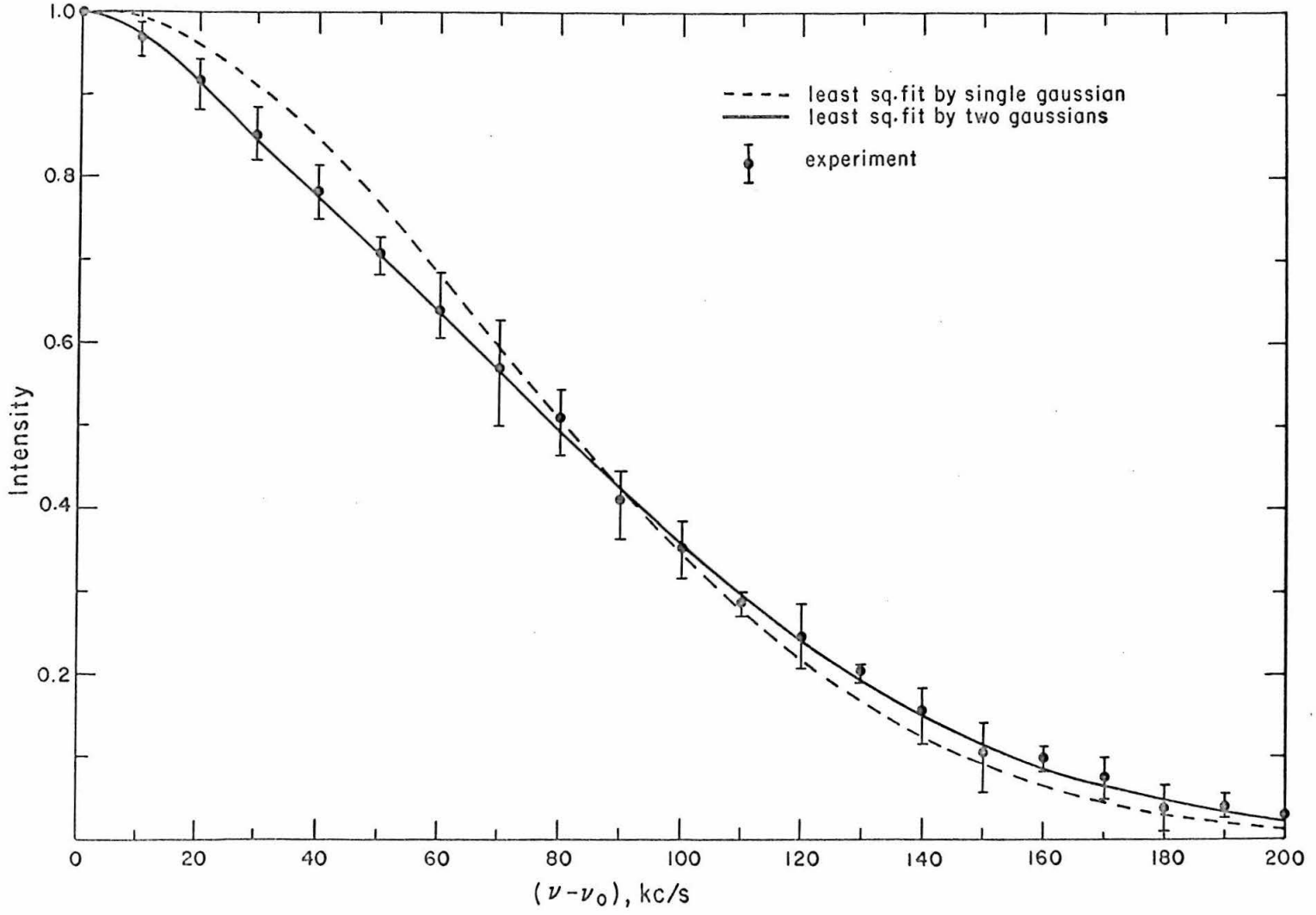
least sq.fit by single gaussian
least sq.fit by two gaussians
experiment
Intensity
1.0
0.8
0.6
0.4
0.2
0
20
40
60
80
100
120
140
160
180
200
(ν-ν0), kc/s

Table II. Results of least Square Fits of the Fluorine Resonance and Experimental Moments.

	Low Frequency Half of Spectrum	High Frequency Half of Spectrum
Single Gaussian Fits		
Half-width of gaussian	78.07 kc/s	80.70 kc/s
M_1	52.91 kc/s	54.69 kc/s
M_2	$43.97 \times 10^2 (kc/s)^2$	$46.98 \times 10^2 (kc/s)^2$
M_3	$46.52 \times 10^4 (kc/s)^3$	$51.38 \times 10^4 (kc/s)^3$
Two Gaussian Fits		
Gaussian 1		
Half-width	86.89 kc/s	87.61 kc/s
	85.72	88.40
Gaussian 2		
Half-width	19.02 kc/s	22.12 kc/s
	14.28	11.60
M_1	57.26 kc/s	57.95 kc/s
M_2	$52.64 \times 10^2 (kc/s)^2$	$53.71 \times 10^2 (kc/s)^2$
M_3	$61.90 \times 10^4 (kc/s)^3$	$63.67 \times 10^4 (kc/s)^3$

the moments obtained from the two gaussian fit are closer to their true values. The spin-rotational constants extracted from these moments are therefore expected to be more reliable.

The Newton-Raphson iterative method (11) was used to extract the $C^F_{\alpha\alpha}$'s from equations 13 (a)-(c). Even though the moments computed from the two gaussian fits were considered to be more reliable, the moments predicted from the single gaussian fits were also subjected to the same treatment to provide some estimates of the uncertainties in the extracted spin-rotational constants. A summary of the extracted $C^F_{\alpha\alpha}$'s is presented in Table III. As expected, both halves of the resonance spectrum yielded pretty much identical results. Although the sign of these interaction constants are not determined in these experiments, their relative signs are given by our treatment. However, their absolute signs are most certainly all negative. Of the three spin-rotational constants, it is clear from Table III that C^F_{cc} is the most precisely determined and C^F_{aa} is the least reliable. Naturally, the origin of this predicament lies in the fact that C^F_{cc} is associated with the largest coeffients in the moment equations while C^F_{aa} is associated with the smallest

Table III. Extracted Fluorine Spin-Rotational Constants

	Low Frequency Half of Spectrum	High Frequency Half of Spectrum
Single Gaussian Fits		
C^F_{aa}	$\pm$ 2.80 kc/s	$\pm$ 2.84 kc/s
C^F_{bb}	$\pm$ 1.70 kc/s	$\pm$ 1.79 kc/s
C^F_{cc}	$\pm$ 1.83 kc/s	$\pm$ 1.89 kc/s
Two Gaussian Fits		
C^F_{aa}	$\pm$ 1.90 kc/s	$\pm$ 2.01 kc/s
C^F_{bb}	$\pm$ 2.51 kc/s	$\pm$ 2.50 kc/s
C^F_{cc}	$\pm$ 1.93 kc/s	$\pm$ 1.95 kc/s

coefficients. Judging from the differences in the two sets of interaction constants, that set extracted from the moments of the single gaussian function and that extracted from the more reliable moments of the two gaussian function, we feel that our determined C_{cc}^{F} has a probable uncertainty of ± 0.1 kc/s while the uncertainty in both C_{aa}^{F} and C_{bb}^{F} is probably $\pm$ 1 kc/s. Our preferred values of the spin-rotational constants for the fluorine nucleus in fluorobenzene are

$$C_{aa}^{F} = -2 \pm 1 \text{ kHz}$$

$$C_{bb}^{F} = -2.5 \pm 0.8 \text{ kHz}$$

$$C_{cc}^{F} = -1.9 \pm 0.1 \text{ kHz}$$

(a-axis along C-F bond axis; c-axis $\perp$ plane of ring).

4. Synthesis of Composite Spectrum: Refinement of Spin-Rotational Constants.

There are definite shortcomings with the method of moment analysis. As mentioned earlier, the higher moments are usually rather poorly defined. The solution of the moment equations for the spin-rotational constants in general also tend to emphasize one or two of the interaction constants so that the remaining

constants are determined with considerably poorer accuracy. This is evidently the case here in fluorobenzene. Consequently, whenever possible, the spin-rotational constants obtained by the method of moment analysis should be checked by direct computation of the shape of the composite resonance spectrum.

Two methods are known for the direct computation of the band-shape of molecular beam nuclear resonance broadened by spin-rotational interaction. Gordon (12) has recently developed a semiclassical approach and has indeed applied it to the fluorine resonance reported here in this work. The computation time for a spectrum is extremely short so that iterative work is economically feasible on most computers. The other approach merely involves direct brute force summing of contributions from all the significantly occupied rotational states to the nuclear resonance spectrum. This fully quantum mechanical method must certainly lead to the correct spectral shape. However, such calculations are generally exceedingly lengthy even on a digital computer. For our present problem, for instance, 3.7 million transitions are involved through $J = 140$. Thus, the determination of spin-rotational constants by iterative

syntheses of the resonance shape to the extent possible with the semi-classical procedure is pretty much out of the question here. We have nevertheless chosen to synthesize the molecular beam composite spectrum by the brute force method. First of all, a preliminary set of spin-rotational constants has been obtained by the method of moment analysis. Synthesis of the band shape would therefore only serve to check the accuracy of these constants and to provide, if necessary, a basis for further refinements. The number of iterations necessary to attain convergence is not expected to be large so that the amount of computer time can still be kept within reason. Finally, since the brute force method must lead to the correct line shape, these calculations will also serve to check the validity and the usefulness of the semi-classical approach.

The intensity of the resonance at frequency ν_0 is proportional to

$$\sum_{J,\tau} \sum_{M_J=-J}^{+J} f(\chi-\chi_{J\tau M_J}) \exp(-W_{J\tau}/kT) \qquad (19)$$

The line shape function, $f(\chi-\chi_{J\tau M_J})$, is known for a given r.f. coil length, r.f. power, temperature, and

under our experimental conditions, is approximately a Lorentzian function with a half width at half-height of $\sim$ 13 kc/s.

Three fluorine resonance spectra synthesized in accordance with expression (20) are given in Figure (5). All transitions up through J = 105 have been included, and in one case the sum was also taken up through J = 140 to show that the band shape of the synthesized spectrum has converged at J =105. The band shape also remained essentially unchanged when the half width at half-height of the individual resonances was varied from 4 to 20 kc/s.

One of the calculated spectra (curve A) in Figure 5 was compiled using the spin-rotational constants obtained in the previous section by the method of moment analysis. Even though the overall agreement between the calculated and the experimental spectra is only fair, the wings of the calculated resonance are in excellent agreement with experiment. This result is not unexpected, since $|C^F_{cc}|$ was accurately determined by the moment method and the same rotational states which contribute heavily to the coefficients σ_c , σ_{cc} , σ_{ccc} in the moment equations also contribute heavily to the tails of the spectrum. The center of the resonance should be sensitive to the

FIGURE 5. Synthesized band shapes for the fluorine resonance spectrum. •, experiment. Curve A, C^F_{aa} = 2.0kHz, C^F_{bb} = 2.5 kHz, C^F_{cc} = 1.9 kHz. Curve B, C^F_{aa} = 1.0 kHz, C^F_{bb} = 2.5 kHz, C^F_{cc} = 1.9 kHz. Curve C, C^F_{aa} = 1.0 kHz, C^F_{bb} = 2.8 kHz, C^F_{cc} = 1.9 kHz.

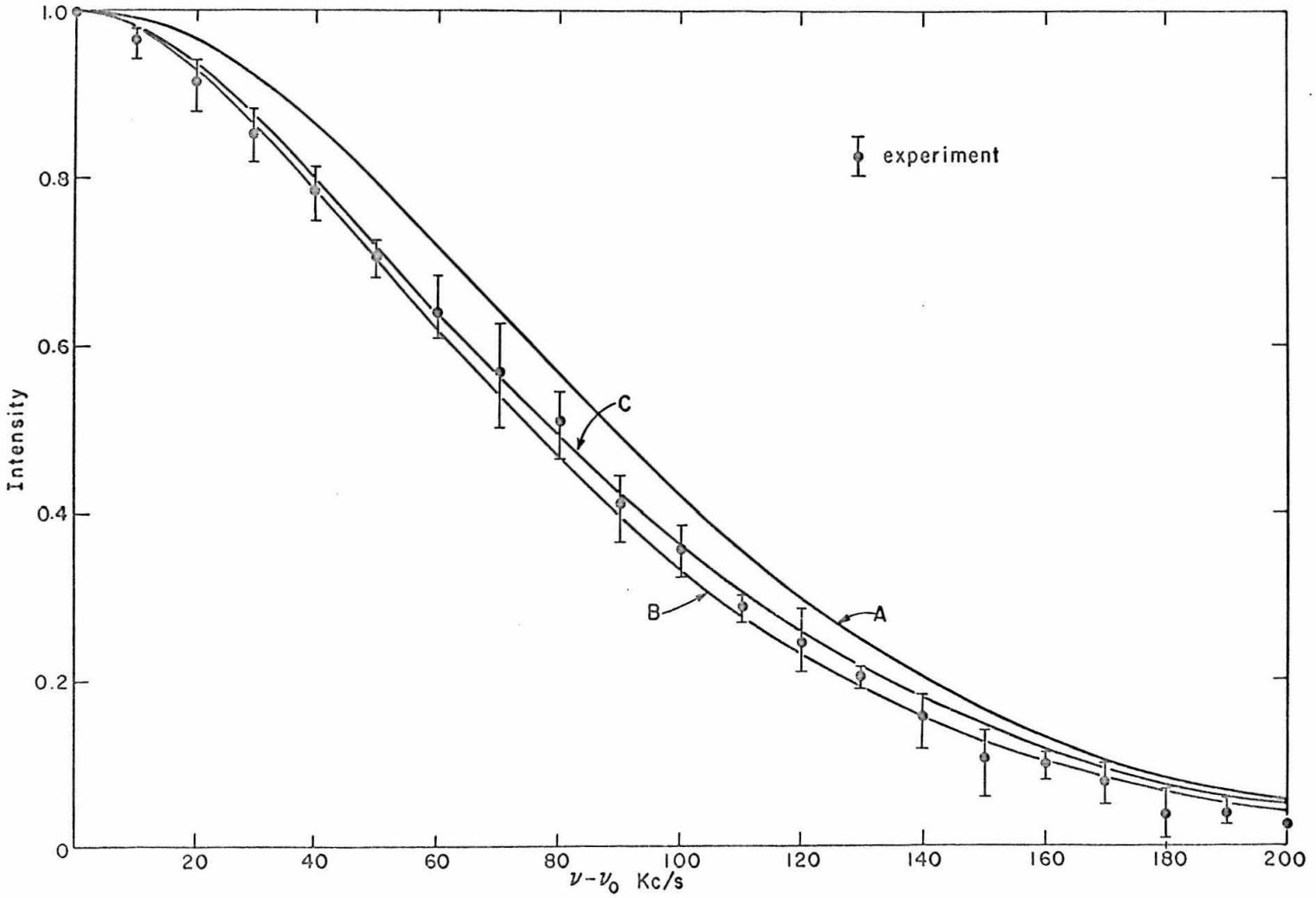
1.0
0.8
0.6
0.4
0.2
0
Intensity
20
40
60
80
100
120
140
160
180
200
$\nu-\nu_0$ Kc/s
experiment
A
B
C

value of $|C^F_{aa}|$, the least accurately determined of the three interaction constants. A comparison of curve A with the experimental points suggests that the value of 2 kc/s for $|C^F_{aa}|$ is probably too large. When $|C^F_{aa}|$, was reduced to 1.0 kc/s, without altering $|C^F_{bb}|$ and $|C^F_{cc}|$, curve B was obtained, which is in essential agreement with experiment. Further improvement was obtained near the half-width when $|C^F_{bb}|$ was raised from 2.5 to 2.8 kc/s (curve C). In view of the quality of the experimental data, we feel that further refinement is not warranted.

Thus, by analysis of the first three moments of the fluorine resonance and by direct computation of the line shape, we have determined the spin-rotational constants for the fluorine nucleus in fluorobenzene to be

$$C^F_{aa} = -1.0 \pm 0.5 \text{ kHz}$$

$$C^F_{bb} = -2.7 \pm 0.2 \text{ kHz}$$

$$C^F_{cc} = -1.9 \pm 0.1 \text{ kHz}$$

This set of interaction constants is in disagreement with the set obtained by Gordon via his semi-classical computation of the line shape, namely

$|c^F_{aa}|$ = 1.0 kc/s, $|c^F_{bb}|$ = 3.8 kc/s, and $|c^F_{cc}|$ = 2.4 kc/s. As expected, when this set of interaction constants was used to synthesize the composite spectrum with our program, we obtained a resonance shape which is considerably wider than the experimental curve.

All the numerical computations outlined in this and the previous section were carried out on the IBM 7094 computer at the California Institute of Technology. The calculations of the rotational energies and the expectation values of J_a^2 , J_b^2 , and J_c^2 required 2-3 minutes per J for J's $\sim$ 100. The evaluation of the σ 's from the calculated $W_{J\tau}$'s and $\langle J_\alpha^2 \rangle$'s upon summing from J=0 to 140 took 3-4 minutes. The solution of the non-linear simultaneous algebraic equations took 5 seconds. The folding of the complete fluorine spectrum required 30 minutes.

F. DISCUSSION.

Spin-rotational interaction is one of the principal mechanisms responsible for the rapid spin-lattice relaxation of the fluorine nucleus in liquid and gaseous fluorine compounds. A study of the temperature dependence

of the F^{19} spin-lattice relaxation time in fluorobenzene has recently been reported by Powles and Green (13). These investigators placed a lower limit of 1.1 kc/s for $|\bar{C}|$, some undefined average spin-rotational constant. They suggested, however, that $|\bar{C}|$ is probably close to 2.1 kc/s. In any case, the spin-rotational constants obtained from our present molecular beam study are not in serious disagreement with the spin-lattice relaxation results.

With our present spin-rotational constants, we obtain a value of -284 ± 10 ppm for the paramagnetic contribution to the fluorine nuclear shielding. Of this -284 ppm, -136 ppm is accounted for by the third term in equation (2), that is, the term involving the sum of the $C^F_{\alpha\alpha} I_{\alpha\alpha}$'s, products of the spin-rotational constants and the principal moments of inertia of the molecule. The sum of the first two terms in equation (2) is proportional to the total electrostatic potential at the nucleus under investigation. This potential energy is not expected to be too sensitive to the chemical environment in which the nucleus is placed, particularly for heavy nuclei, where there is a large number of electrons around the nucleus. Consequently, when the chemical shifts of a

nucleus in different chemical enviroments are plotted versus $\bar{\zeta}_{\alpha} C_{\alpha\alpha} I_{\alpha\alpha}$, a straight line with slope $(e^2/3mc^2)$ $(h/4Mg_I\mu_N^2)$ should be obtained. Such a linear correlation between chemical shift and $\bar{\zeta}_{\alpha} C_{\alpha\alpha} \times I_{\alpha\alpha}$ was first shown for fluorine by Ramsey and coworkers (14) and has since also been demonstrated for nitrogen chemical shifts (15). In Figure 6, we have reproduced the plot of Ramsey et al for fluorine chemical shifts and have included our new result for fluorobenzene and the recent results (16) on F_2 and SiF_4. It is gratifying that our present result for fluorobenzene also falls on the same line determined by the remaining five fluorine compounds. Since here the chemical shift is plotted versus the last term in expression (2), the theoretical correlation should be a straight line with unit slope, as it is.

The above agreement between our measured σ^P as determined from our spin-rotational constants and that predicted from the chemical shifts and spin-rotational constants of other fluorine compounds confirms our choice of signs (all negative) for our spin-rotational constants. The excellent agreement also suggests that the individual spin-rotational constants themselves are quite accurate.

FIGURE 6. σ_{AV}^{CI} versus F^{19} chemical shift for several fluorine compounds.

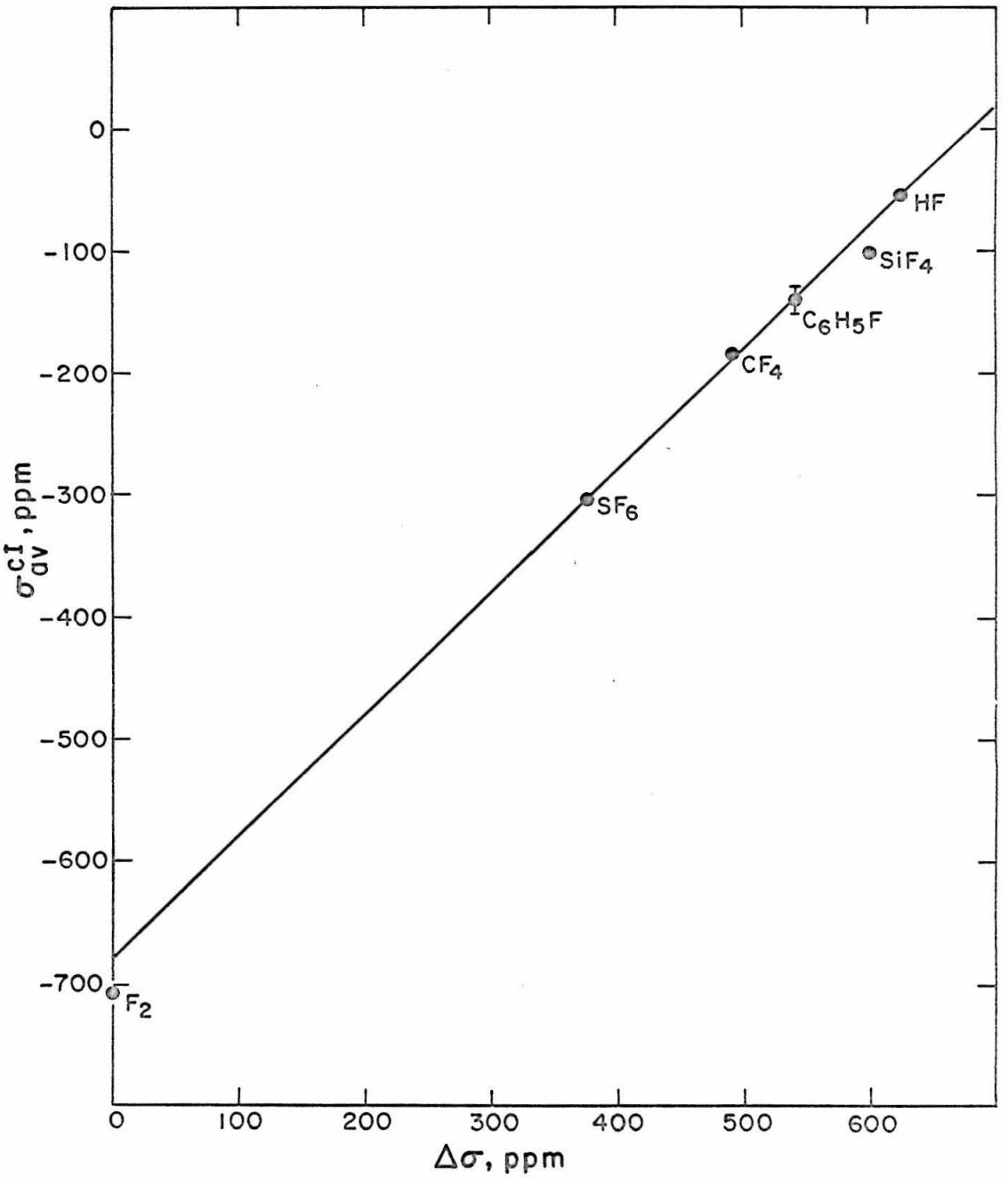
0
-100
-200
-300
-400
-500
-600
-700
σ_{av}^{Cl}, ppm
HF
SiF_4
C_6H_5F
CF_4
SF_6
F_2
0
100
200
300
400
500
600
$\Delta\sigma$, ppm

A calculation of the diamagnetic part of the fluorine shielding (Lamb term) in fluorobenzene has not been reported in the literature. However, it is possible to make an extremely good estimate of the total fluorine shielding in fluorobenzene in the following manner. As mentioned above, the total electrostatic potential at the fluorine is principally determined by the core electrons and the non-bonded valence electrons and is therefore fairly insensitive to the chemical environment in which the atom is placed. This constancy of the total electrostatic potential at the fluorine is substantiated by the linear correlation depicted in Figure 6. The sum of the first two terms in the shielding expression for fluorobenzene can then be calculated with reasonable certainty if the diamagnetic screening of the isolated F atom or F^- ion is known, or if the Lamb term in the fluorine shielding is known for some molecule. The diamagnetic shielding of the fluorine atom as calculated by Dickinson (17) using a Hartree-type SCF wave function is 464 ppm. More recent calculations by Sidwell and Hurst (18) using Hartree-Fock wave functions yield 478.3 ppm for the diamagnetic screening of the fluorine atom and 480.3 ppm for the fluoride ion. Lipscomb and

coworkers (3) have also recently reported diamagnetic screening constants (Lamb term) for HF and F_2. Employing molecular Hartree-Fock functions of Nesbet, they obtained σ^D's of 481.6 ppm for HF and 529.5 ppm for molecular fluorine. When these σ^D's are combined with the second term in the shielding expression for these molecules, one obtains a total of 470.5 ppm and 471.4 ppm for F_2 and HF respectively. The constancy of the sum of the first two terms of the shielding expression (the second term vanishes for the fluorine atom and the fluoride ion) is certainly convincing, at least for fluorine shielding. To be as conservative as possible, we shall assign a value of +470 $\pm$10 ppm to the sum of the first two terms in the shielding expression for fluorine in fluorobenzene. The Lamb term for fluorine in fluorobenzene is then (470 + 148) or 618 $\pm$10 ppm, and the net shielding of the fluorine nucleus is (470 − 136) or +334 $\pm$10 ppm.

It is interesting to note that, for fluorine shielding, changes in the Lamb term are not as negligible as they are often assumed to be. For example, σ^D increases by 136 ppm in going from HF to fluorobenzene and the corresponding change in σ^P is −227 ppm. There is no

physical reason why changes in the diamagnetic term should necessarily be negligible or small. After all, the operator $1/r_{Nk}$ falls off quite slowly with distance and in a molecule with many other heavy atoms, the contribution of the core electrons in these other atoms and the bonding electrons localized in other bonds to the Lamb term may mount up to about 100 ppm. However, these electrons should not contribute significantly to the diamagnetic screening of the nucleus under investigation as their dimagnetic circulation about the nucleus in question is strongly hindered by the electrostatic forces of the nuclei to which these electrons are principally bound. In fact, the second term in the shielding expression for molecules corrects for the ineffective screening of these electrons which are principally localized at other atoms. For heavy nuclei, therefore, only the diamagnetic screening of the core electrons and the non-bonded valence electrons is effective, and this, of course, is insensitive to the chemical environment in which the atom is located. The chemical shift of heavy atoms such as F, N, etc. is thus given by changes in the last term in the shielding expression, which accounts for the local paramagnetic electron currents arising

from the partial unquenching of the orbital angular momentum of the valence electrons in the presence of a magnetic field. This partial unquenching of the orbital angular momentum of the valence electrons is, of course, hindered by the anisotropic electrostatic fields produced by neighboring atoms, thus accounting for the strong variation of the effect with chemical environment. It is pertinent that even though the last term in the shielding expression involves both the nuclear and electronic contributions to the rotational magnetic field at the nucleus of interest, the nuclear contribution from the remaining heavy atoms in the molecule is largely offset by that part of the electronic contribution which has its origin in electrons principally localized at these atoms. This is reasonable since these electrons generally follow the motion of the nuclear framework and do not slip appreciably upon molecular rotation. These statements, of course, do not apply to light atoms, such as the hydrogen atoms in the molecule; however, their contribution to the rotational magnetic field is generally small compared to the actual rotational field seen by the nucleus in question. We therefore see that the principal contribution to the rotational field at a heavy nucleus, and

hence to the spin-rotational constants, arises from local paramagnetic currents induced by end-over-end rotation of nuclear framework.

We now turn our attention to the discussion of the anisotropy of the fluorine shielding in fluorobenzene. The various diagonal components of the shielding tensor are given by

$$(\sigma_N)_{\alpha\alpha} = \frac{e^2}{2mc^2}\left(\langle\psi_0|\sum_k \frac{r_{Nk}^2 - (r_{Nk})_\alpha^2}{r_{Nk}^3}|\psi_0\rangle - \sum_{N'\neq N}\frac{R_{NN'}^2 - (R_{NN'})_\alpha^2}{R_{NN'}^5}\right) + \frac{e^2}{mc^2}\frac{h}{4M\mu_N^2 g_N} C_{\alpha\alpha} I_{\alpha\alpha} \qquad (20)$$

In general, neither the first nor the second term in the above expression is isotropic. However, to a good approximation, their sum is isotropic. We can justify this point mathematically or reason it out using the same argument we used earlier to justify the constancy of this sum. Thus, just as the chemical shift between various fluorine compounds is given by differences in the CI term in equation (2), similarly the anisotrophy of the fluorine shielding is given by differences in the last term in expression (20) along the various directions; that is, $\sigma_{\alpha\alpha} - \sigma_{\beta\beta} = \sigma_{\alpha\alpha}^{CI} - \sigma_{\beta\beta}^{CI}$, where σ^{CI} donotes the CI term of the paramagnetic shielding. As mentioned above, this term arises from partial unquenching of the orbital

angular momentum of the valence electrons of the nucleus under investigation in the presence of the magnetic field. Therefore, it is primarily a property of the bond in which the nucleus is a part. If the charge cloud along the bond has approximate local axial symmetry, then we might expect $\sigma_{\alpha\alpha}^{CI} \simeq \sigma_{\beta\beta}^{CI} \simeq \sigma_{\perp}^{CI}$ and $\sigma_{\gamma\gamma}^{CI} \simeq \sigma_{\parallel}^{CI} \simeq 0$. The C-F bond in fluorobenzene is not axially symmetric due to the conjugation of one of the fluorine lone pairs into the pi-system of the ring and the interaction of the in-plane lone pair with the σ-skeleton. Neither of these effects are, however, expected to be large, so that one might expect σ_{aa}^{CI} to be small, at least smaller than σ_{bb}^{CI}, σ_{cc}^{CI}. This is close to what we find from our measured spin-rotational constants. $\sigma_{aa}^{CI} = -31$ ppm, $\sigma_{bb}^{CI} = -184$ ppm, and $\sigma_{cc}^{CI} = -193$ ppm. Thus the fluorine nucleus in fluorobenzene is most shielded when the applied field is along the C-F bond. This result is in agreement with the findings of Andrew and Turnstall (19) for 1,2,4-trifluorobenzene. From a moment analysis of the asymmetric nuclear resonance line in polycrystalline samples of the trifluorobenzene, they concluded that $\sigma_{\parallel} - \sigma_{\perp}$ was about +250 ppm. Using the theory of Karplus and Das (4) one can calculate an anisotropy in the shielding of $\sim$ 230 ppm,

in apparent agreement with the nuclear resonance results of Andrew and Turnstall. However, we obtained quite a different value for the magnitude of the anisotropy of the shielding from our measured spin-rotational constants. If we assume approximate axial symmetry and define

$$\sigma_{\parallel} - \sigma_{\perp} \simeq \sigma_{aa} - \tfrac{1}{2}(\sigma_{bb} + \sigma_{cc}) \simeq \sigma_{aa}^{CI} - \tfrac{1}{2}(\sigma_{bb}^{CI} + \sigma_{cc}^{CI})$$

we obtain an anisotrophy of only +160 ppm for the fluorine shielding in fluorobenzene. The uncertainty in this number is about 30 ppm, and it is more probable for this value of the anisotrophy to be high than low by this amount. To further elucidate the discrepancy between theory and experiment, we have tabulated in Table IV the $\sigma_{gg}^{(2)}$'s predicted on the basis of the Karplus and Das theory. Here $\sigma_{gg}^{(2)}$ is to be distinguished from σ_{gg}^{P}, since it is the genuine second order paramagnetic shielding, that is, that part of the nuclear shielding arising from the unquenching of the orbital angular momenta of the bonding valence electrons in the presence of the magnetic field. In contrast, the conventional σ_{gg}^{P} includes, in addition to $\sigma_{gg}^{(2)}$, the nuclear term which offsets the ineffective diamagnetic screening

of those electrons localized on other atoms. The $\sigma_{gg}^{(2)}$'s predicted on the basis of the localized theory should therefore be compared with our determined σ_{gg}^{CI}'s rather than the total σ_{gg}^{P}'s . From Table IV, it is seen that our determined σ_{gg}^{CI}'s are all approximately half the theoretical $\sigma_{gg}^{(2)}$'s . (The fact that our determined σ_{gg}^{P}'s appear to be in agreement with the theoretical $\sigma_{gg}^{(2)}$'s is merely coincidental, since in fluorobenzene, $\sigma_{gg}^{CI} \simeq \sigma_{gg}$ nuclear). Since the anisotrophy in the magnetic shielding as well as the individual σ_{gg}^{CI}'s are all roughly half the theoretically predicted values, this suggests that one of the empirical constants in Karplus and Das semi-empirical theory may be too high by a factor of 2. To examine this possibility, we recall that in the localized theory of Karplus and Das,

$$\sigma_{xx}^{(2)} = \frac{3}{2}\sigma_0 \left(1-S-I+IS+\rho_y(S+I)\right)$$

$$\sigma_{yy}^{(2)} = \frac{3}{2}\sigma_0 \left(1-S-I+IS+\rho_x(S+I)\right)$$

$$\sigma_{zz}^{(2)} = \frac{3}{2}\sigma_0 \left(\rho_x+\rho_y-\rho_x\rho_y\right) \qquad (21)$$

Here, s denotes the extent of sp hybridization of the fluorine σ -bonding orbital in the C-F bond and I is its

Table IV. Comparison Between Theory and Experiment

g	$\sigma_{gg}^{nuclear}$	σ_{gg}^{CI}	σ_{gg}^{P}	$\sigma_{gg}^{(2)}$
			Karplus-Das	
a	-33ppm	-33ppm	-64ppm	-130ppm
b	-189	-184	-373	-410
c	-222	-193	-415	-310

ionic character. ρ_x and ρ_y denote the double-bond characters of the C-F bond in the directions orthogonal to the bond axis (z-axis). σ_0 which is the empirical constant referred to above, is

$$-\frac{2}{3}\frac{e^2\hbar^2}{m^2\Delta}\langle r^{-3}\rangle$$

$\langle r^{-3}\rangle$ is the expectation value of the operator $1/r_{NK}$ for the normalized p-orbital radial function and Δ, the usual mean excitation energy. In their treatment, Karplus and Das attempted to obtain σ_0 empirically from the chemical shift between fluorobenzene and molecular fluorine. For fluorobenzene, they selected the following bond parameters: s=0.05, I=0.75, ρ_x=0.126, and ρ_y=0; for F_2, s=0.02, I=0, and $\rho_x=\rho_y$=0. However, there is every reason to expect that the average excitation energy, Δ, is quite different for these two molecules. Since $\sigma_{av}^{(2)}$ is much smaller in magnitude for fluorobenzene than for F_2, −141 ppm versus −709 ppm, the procedure of Karplus and Das would tend to yield a value of σ_0 which is more representative of the F_2 molecule. A value of σ_0 may be obtained for each molecule by setting $\sigma_{av}^{CI}=\sigma_{av}^{(2)}$. If this latter method is applied to the F_2 molecule, we obtain a σ_0 of −720 ppm, in

reasonable agreement with the value of −863 ppm obtained and employed by Karplus and Das. However, when this same procedure is applied to HF, we obtained a σ_0 of −400 ppm for this molecule. To estimate $\sigma_{av}^{(2)}$ for HF, we assumed $\rho_x = \rho_y = 0$, $s \cong 0$, and an ionic character I of 0.86 obtained from the ionic character versus electronegativity curve of Dailey and Townes (20). The F^{19} chemical shifts of C_6H_5F and HF are not grossly different; C_6H_5F is only 84 ppm downfield from HF. Thus, we might expect the value of σ_0 to be not grossly different for these two molecules. If this is the case, the discrepancy between theory and experiment would be satisfactorily accounted for.

G. REFERENCES

1. R. Schwartz, Ph.D. Thesis, Harvard University, 1953 (unpublished).

2. H. J. Kolker and M. Karplus, J. Chem. Phys. 41, 1259 (1964).

3. R. M. Stevens, R. M. Pitzer, and W. N. Lipscomb, J. Chem. Phys., 38, 550 (1963); R. M. Stevens and W. N. Lipscomb, J. Chem. Phys. 40, 2238 (1964); R. M. Stevens and W. N. Lipscomb, J. Chem. Phys. 41, 184, 3710 (1964).

4. M. Karplus and T. P. Das, J. Chem. Phys. 34, 1683 (1961).

5. M. R. Baker, H. M. Nelson, J. A. Leavitt, and N. F. Ramsey, Phys. Rev. 121, 807 (1961); ibid., 122,856 (1961); ibid., 124, 1482 (1961).

6. H. S. Gutowsky, C. H. Holm, A. Saika, and G. A. Williams, J. Am. Chem. Soc. 79, 4596 (1957).

7. E. U. Condon and G. H. Shortley, The Theory of Atomic Spectra, (Cambridge University Press, London, England, 1963), p.64.

8. D. W. Posener, Aust. J. Phys. 11, 1 (1958).

9. W. A. Nierenberg and N. F. Ramsey, Phys. Rev., 72, 1075 (1947).

10. B. Bak, D. Christensen, Lise Hansen-Nygaard, and E. Tannenbaum, J. Chem. Phys., 26, 134 (1957).

11. H. Margenau and G. M. Murphy, The Mathematics of Chemistry and Physics, (D. Van Nostrand Company, Inc., Princeton, New Jersey, 1956), p. 493.

12. R. G. Gordon, J. Chem. Phys. 44, 1184 (1966).

13. J. G. Powles, and O. K. Green, Physics Letters 3, 134 (1962).

14. N. F. Ramsey, Am. Scientist, 49, 509 (1961).

15. S. I. Chan, M. R. Baker, and N. F. Ramsey, Phys. Rev., 136, 1224 (1964).

16. I. Ozier, L. M. Crapo, J. W. Cederberg, and N. F. Ramsey, Phys. Rev. Letters, 13, 482 (1964); L. Crapo, Ph.D. Thesis, Harvard University, 1964 (unpublished).

17. W. C. Dickinson, Phys. Rev. 80, 563 (1950).

18. T. W. Sidwell and R. P. Hurst, J. Chem. Phys., 37, 203 (1962).

19. E. R. Andrew and D. P. turnstall, Proc. Phys. Soc. (london), 81, 986 (1963).

20. B. P. Dailey and C. H. Townes, J. Chem. Phys. 23, 118 (1955).